İSTANBUL TECHNICAL UNIVERSITY ★ GRADUATE SCHOOL OF SCIENCE ENGINEERING AND TECHNOLOGY

MATHEMATICAL MODELING OF NOx AND SOOT EMISSIONS FOR DIESEL ENGINES

M.Sc. THESIS

Rüştü Taylan YARAR

Department of Mechancal Engineering

Heat Transfer – Fluid Mechanics Programme

DECEMBER 2017

İSTANBUL TECHNICAL UNIVERSITY ★ GRADUATE SCHOOL OF SCIENCE ENGINEERING AND TECHNOLOGY

MATHEMATICAL MODELING OF NOx AND SOOT EMISSIONS FOR DIESEL ENGINES

M.Sc. THESIS

Rüştü Taylan YARAR
(503141128)

Department of Mechanical Engineering

Heat Transfer – Fluid Mechanics Programme

Thesis Advisor: Prof. Dr. Cem SORUŞBAY

DECEMBER 2017

İSTANBUL TEKNİK ÜNİVERSİTESİ ★ FEN BİLİMLERİ ENSTİTÜSÜ

DİZEL MOTORLARDA NOx VE İS EMİSYONLARININ MATEMATİKSEL MODELLENMESİ

YÜKSEK LİSANS TEZİ

Rüştü Taylan YARAR
(503141128)

Makine Mühendisliği Anabilim Dalı

Isı-Akışkan Yüksek Lisans Programı

Tez Danışmanı: Prof. Dr. Cem SORUŞBAY

ARALIK 2017

Rüştü Taylan Yarar, a M.Sc. student of İTU Graduate School of Science Engineering and Technology student ID 503141128, successfully defended the thesis entitled "MATHEMATICAL MODELING OF NOx AND SOOT EMISSIONS FOR DIESEL ENGINES", which he prepared after fulfilling the requirements specified in the associated legislations, before the jury whose signatures are below.

Thesis Advisor :	**Prof. Dr. Cem SORUŞBAY** İstanbul Technical University	.....
Jury Members :	**Prof. Dr. Muammer ÖZKAN** Yıldız Technical University	.....
	Asst. Prof. Dr. Hikmet ARSLAN İstanbul Technical University	.....

Date of Submission : 9 November 2017
Date of Defense : 14 December 2017

To my beloved family,

FOREWORD

Firstly, I would like to express my gratitude to Prof. Dr. Cem SORUŞBAY for giving me the opportunity to conduct this work under his guidance and valuable instructions. I also appreciate all instructors in the Department of Mechanical Engineering for contributions to the advancement of my education.

My special thanks go to Ford Otosan for its funding and supplying experimental section of this thesis.

My greatest thank goes to my beloved family for their continuous support, encouragement and understanding.

December 2017

Rüştü Taylan YARAR
(Mechanical Engineer)

TABLE OF CONTENTS

Page

ABBREVIATIONS

DI : Direct Injection
SI : Spark Ignition
HC : Hydrocarbon
IC : Internal Combustion
0D : 0 Dimensional
1D : 1 Dimensional
3D : 3 Dimensional
CFD : Computational Fluid Dynamics
DPF : Diesel Particle Filter
LNT : Lean NOx Trap
ECU : Electronic Control Unit
NSC : Nagle and Stickland-Constable
MLP : Multilayer Perceptron
EGR : Exhaust Gas Recirculation
RPM : Revolutions Per Minute
PM : Particulate Matter
GPR : Gaussian Process Regression
ANN : Artificial Neural Network
NN : Neural Network
DoE : Design of Experiment
WHTC : World Harnonized Transient Cycle
TQ : Torque
MAF : Mass Air Flow
MCP : Maximum Cylinder Pressure
TFQ : Total Fuel Quantity
IMT : Intake Manifold Temperature
IMP : Intake Manifold Pressure
TIT : Turbine Inlet Temperature
TIP : Turbine Inlet Pressure
ES : Engine Speed
RFP : Rail Fuel Pressure
SOMI : Start of Main Injection
PIQ : Pilot Injection Quantity
SOPI : Start of Pilot Injection
SOI : Start of Injection
BD : Burn Duration
MCT : Maximum Cylinder Temperature

SYMBOLS

K_p	: Pressure Loss Coefficient
Δx	: Delta displacement
Δt	: Delta time
V	: Volume
K_f	: Formation Coefficient
T	: Temperature
M_{sf}	: Soot Mass Formation Rate
M_{so}	: Soot Mass Oxidation Rate
M_c	: Carbon Molecular Weight
σ_d	: Horizontal Scale Parameter
ρ	: Density
ρ_s	: Soot Density
∂	: Partial derivative
P	: Pressure
m	: Mass flowrate
C_f	: Fanning Friction Factor
H	: Total Specific Enthalpy
e	: Total Specific Internal Energy
A	: Cross-sectional Flow Area
A_s	: Heat Transfer Surface Area
D	: Equivalent Diameter
R	: Specific Gas Constant
u	: Velocity of Boundary
A_f, A_o	: Pre-exponential Factors
E_f, E_o	: Activation Energies

LIST OF TABLES

Page

LIST OF FIGURES

Page

MATHEMATICAL MODELING OF NOx AND SOOT EMISSIONS FOR DIESEL ENGINES

SUMMARY

The diesel engine is a type of internal combustion engines in which the fuel that is injected into combustion chamber is ignited by high temperature due to greatly compression of air. Only the air is compressed for diesel engines work. This causes the air to reach high temperatures inside the cylinder and atomized diesel fuel which is injected into the combustion chamber is ignited.

Since 19th century, researchers have focused on diesel engines and they came into use with ships and submarines in early years of the 20th century. Then, diesel engines were seen for trucks, locomotives and heavy equipment. After a first quarter of the 20th century, they slowly began to be used in a few automobiles and the diesel engines play an important role in today's automotive world.

Diesel engines have many advantages and plenty of drawbacks. When diesel engines and gasoline engines are compared, diesel engines burn less fuel than gasoline engines due to the engine's higher temperature of combustion and greater expansion ratio. Diesel engines have higher thermal efficiency than gasoline engines due to property of compression ignition. Due to this fact, diesel engines can convert over 45% of the chemical energy into mechanical energy while gasoline engines are typically 30% efficient. However, the most important disadvantage of diesel engines is that they emit more hazardous compounds for environment and human health than gasoline engines. Since the fuel in diesel engine is ignited by the heat of compressed air, the fuel had no time to be fully mixed with the air and it produces unburned HC, NOx and soot during the combustion process. Due to NOx and soot emissions, legislation concerning the pollutant gas emissions of diesel cars is becoming increasingly restrictive. Then, it requires many tests to reach the desired limits of the pollutant emissions.

Testing with an engine results in long, expensive and inaccurate works. Therefore, it has needed to find a solution for reducing cost and time, also increasing test efficiency. Computer-aided engineering programs have been widely used with the developing computer technology and many engineering problems have been solved by using the computer-aided engineering programs. Some of these programs are developed by engineers to simulate the engine in the system order. Thus, computer aided engineering programs, which are referred as one-dimensional simulation programs in literature provide solution in the system order of an engine.

Today, engineers are able to get through to detailed investigations of production engines from early studies of model engine by using one dimensional engine simulation programs. They provide very quick solutions when compared to three dimensional computational fluid dynamics programs. Also, they shorten test duration of engine dynamometer and provide further investigations for multi-parameter effects of engine performance parameters. One dimensional engine simulation programs are widely used by many automotive manufacturers due to the significant advantages described above.

In one dimensional engine simulation programs, it is accepted that the axial velocity of the fluid is higher than the fluid velocity in other directions. Due to this reason, three dimensional conservation equations are reduced to one dimension. Continuity, momentum and energy equations are solved simultaneously by the model. All equations are solved in one dimension and all quantities are averaged across flow direction. The system is discretized into smaller volumes and volumes are connected by boundaries. Also, the scalar variables are calculated at the center of the volume and vector variables are calculated for each boundary. This type of discretization is referred as staggered grid.

In literature, combustion of diesel engines are modeled with high accuracy by using one dimensional engine simulation. On the other hand, the emission modeling of diesel engines have been very challenging for researchers due to irregular chemistry of the exhaust gases.

Apart from physical modeling, mathematical modeling is also commonly used. Mathematical modeling is very beneficial especially for the problems which cannot be explained by physical modeling. Therefore, mathematical modeling which is constructed according to measured data, could be very helpful to analyzed unknown systems. In accordance with this purpose, mathematical model can be used for prediction of exhaust gases.

In this thesis study, mathematical model of NOx and soot emissions based on Gaussian Regression method is used for fast and accurate predictions. It is proved that NOx and soot emissions can be modeled mathematically with high accuracy for diesel engine. Experimental design is generated to collect training data for mathematical models. Instead of using conventional DoE methods, spacing filling DoE method is utilized. The results show that it's good enough to describe complex behaviors of the engine.

Results are subdivided according to steady state and transient conditions. Firstly, steady state modeling is handled. Models using combustion input parameters are created to predict soot and NOx emissions. These parameters is directly or indirectly controlled by ECU. Optimization of the input parameters are performed to obtain highest results, and the model comprising of eight parameters are sufficient to predict soot and NOx emissions. Suggested model includes the parameters: engine speed, fuel rail pressure, total fuel quantity, start of main injection, start of pilot injection, mass air flow, intake manifold temperature and intake manifold pressure. Due to dependency of EGR rate to other model parameters, it is not required to add EGR rate parameter into the models. Controlling of pilot injection quantity have high errors, and thus its effect on modeling quality could not be observed.

The models include combustion input and output parameters. However, some parameters cannot be measured directly on a dynamometer, and therefore 1D model of the engine is created. The values of these parameters are obtained by using 1D engine model.

Effects of some combustion output parameters are also investigated in this thesis. Modeling improvement is aimed by using these parameters. Studies show that adding turbine inlet temperature into the models increases modeling quality of soot emissions. Also, it is obtained that using maximum cylinder pressure in the models increases the accuracy of validation data for steady state conditions, but it requires to use other combustion parameters such as turbine inlet pressure, burn duration 0-50%, burn duration 0-90% and burn duration 10-90%.

In this thesis, it is also aimed to model emissions mathematically by using only outputs of the 1D engine model and to show its feasibility. Thus, optimum design of an engine can be obtained by using a coupled model of 1D engine model with a mathematical emission model. However, the results show that NOx emissions can be assessed during design optimization process but the same thing cannot be stated for soot emissions.

The models including combustion input and output parameters are run in MATLAB to evaluate the model quality for transient conditions. World harmonized transient cycle (WHTC) is used for comparison of model and test data. The results show that mathematical emission models are capable of predicting transient results of emissions. The same model suggested for steady state conditions can be also used for transient conditions. However, there are some problems observed during analysis of transient results of the models. These problems are overestimation of soot emissions and time delay between model and test results. One of transient cycle points is out of range for training data of the models, and it results in overshooting of soot emissions. Setpoints of combustion variables are specified at the beginning of combustion by ECU, however, soot and NOx emissions are measured at engine outlet. This situation causes a delay between test and model results.

DİZEL MOTORLARDA NOx VE İS EMİSYONLARININ MATEMATİKSEL MODELLENMESİ

ÖZET

Dizel motor büyük sıkıştırılma oranından ötürü yüksek sıcaklığa sahip olan havanın yanma odasında yakıt püskürtülerek ateşlenmesi sağlanan içten yanmalı bir motor türüdür. Dizel motorlar yalnızca sıkıştırılmış hava ile çalışır. Bu durum havanın silindir içerisinde yüksek sıcaklıklara sahip olmasına ve yanma odasına püskürtülen dizel yakıtın atomize edilmesine olanak sağlar.

19. yüzyıldan beri araştırmacılar dizel motorlar üzerine odaklanmıştır ve 20. Yüzyılın başlarında gemi ve denizaltı araçlarında kullanılmaya başlanmıştır. Daha sonra dizel kamyon, lokomotif ve ağır araçlarda kullanışmıştır. Dizel motorlar 20. Yüzyılın ilk çeyreğinden sonra yavaş yavaş bazı otomobillerde kullanılmaya başlanmış ve günümüzde otomotiv dünyasında önemli rol oynamaktadır.

Dizel motorlar birçok avantaj ve dezavantaja sahiptir. Dizel motorlar, benzinli motorlar ile karşılaştırıldığında; yüksek sıkıştırma oranları ve yanma sıcaklıklarından ötürü dizel motorlar daha az yakıt tüketmektedir. Dizel motorlar sıkıştırılmalı ateşleme özelliğinden ötürü benzinli motorlardan daha yüksek termal verime sahiptir. Bu sebepten ötürü; benzinli motorlar genellikle %30 verimle çalışırken, dizel motorlar kimyasal enerjinin %45'den fazlasını mekanik enerjiye çevirebilmektedir. Ancak, dizel motorların en önemli dezavantjı benzinli motorlardan daha fazla oranda çevreye ve insan sağlığına zararlı birçok bileşiği yaymasıdır. Dizel motorlarda yakıt sıkıştırılan havanın ısısıyla ateşlendiğinden ötürü, havanın yakıtla tamamı ile karışması için gerekli zaman yoktur ve bu durum yanma sürecinde yanmamış HC, NOx ve is oluşmasına neden olmaktadır. NOx ve is emisyonundan dolayı, dizel motorların çevreye zararlı gaz emisyonlarını ilgilendiren kanunlar giderek katılaşmaktadır. İstenilen limitlerde çevreye kirliliğine sebep olan emisyon seviyesinin elde edilmesi için bir çok test yapmasını gerekmektedir.

Motor ile yapılan testler uzun süre, yüksek maliyet ve hatalı çalışamayla sonuçlanabilmektedir. Bu sebep ile, maliyeti ve zamanı azaltacak, test verimini artıracak bir çözüm yolu bulunmasına ihtiyaç duyulmuştur. Bilgisayar destekli mühendislik programları bu ihtiyaçlara fazlasıyla karşılık verebilmektedir.

Günümüzde, mühendisler bir boyutlu motor simülasyon programlarını kullanarak model motorun ilk çalışmalarından itibaren üretilecek motor ile ilgili detaylı araştırmaya ulaşabilmektedirler. Bu programlar üç boyutlu hesaplamalı akışkanlar dinamiği programları ile karşılaştırıldığında çok daha hızlı çözüm sunabilmektedir. Ayrıca, bu programlar motor dinamometresinin test sürelerini kısaltmak ile birlikte motor performans parametrelerinin çok boyutlu etkisi üzerinde daha fazla araştırma yapma olanağı sağlamaktadır. Yukarıda açıklanan önemli avantajlarından öürü, bir boyutlu motor simülasyon programları birçok otomotiv üreticisi firma tarafından yaygın bir şekilde kullanılmaktadır.

Bir boyutlu motor simülasyon programlarında, akışkanın eksenel hızının diğer doğrultulardaki akışkan hızından daha yüksek olduğu kabul edilmektedir. Bu sebepten dolayı, üç boyutlu korunum denklemleri tek boyuta indirgenmektedir. Süreklilik, momentum ve enerji denklemleri model tarafından anlık olarak çözülmektedir. Tüm niceliklerin akış doğrultusunda ortalaması alınıp tüm denklemler bir boyutta çözülmektedir. Sistem küçük hacimlere ayrıştırılmaktadır ve bu hacim alanları sınırlarından birbirine bağlıdır. 1 boyutlu modellerde Skaler büyüklükler hacim alanının orta noktasına indirgenerek, vektörel büyüklükler ise her sınır için hesaplanır.

Literatüre baktığımızda dizel motorlarda yanmanın bir boyutlu mühendislik programları kullanılarak yüksek doğruluk ile modellenebildiği görülmektedir. Diğer bir taraftan, egzoz gazlarının düzensiz kimyasından ötürü araştırmacılar tarafından dizel motorlarda emisyonların modellenmesi oldukça zordur.

Fiziksel modellerin dışında matematiksel modellerde günümüzde yaygın olarak kullanılmaktadır. Özellikle fiziksel olarak açıklanamayan problemlerin çözümü için matematiksel modeller oldukça faydalı olmaktadır. Bu sebep ile, ölçüm verilerine göre oluşturulan matematiksel modeller bilinmeyen sistemlerin analiz edilmesinde yardımcı olabilmektedir. Matematiksel modeller bu amaç doğrultusunda egzoz gazlarının tahmini için kullanılabilmektedir.

Bu tez çalışmasında, NOx ve is emisyonlarının matematiksel modeli hızlı ve doğru tahminler elde edilebilmek için kullanılmıştır. Literatürde farklı ampirik model yöntemleri bulunmasına rağmen, bu tez kapsamında Gaussian regresyon metodu kullanılmıştır. Dizel motorlar için NOx ve is emisyonlarının bu metod ile yüksek doğrulukta modellenebileceği ispatlanmıştır. Matematiksel modellere beslenecek verinin toplanması için klasik DoE yöntemleri yerine boşluk doldurma DoE yöntemi tercih edilmiştir. Elde edilen sonuçlar, motorun karmaşık davranışlarını açıklamak için bu metodun yeterli düzeyde olduğu göstermektedir.

Sonuçlar durağan ve değişken durumlar için ayrı ayrı incelenmiştir. Öncelikle motorun durağan koşullardaki emisyonları matematiksel olarak modellenmiştir. Sadece yanma giriş parametreleri kullanılarak modeller oluşturulmuştur. Oluşturulan modellerin sonuçları incelenerek parametre optimizasyonu yapılmıştır. Motor hızı, yakıt ray basıncı, hava debisi, toplam yakıt miktarı, ön püskürtme avansı, ana püskürtme avansı, emme manifoldu sıcaklığı ve emme manifoldu basıncını kullanarak oluşturulan modelin is ve NOx emisyonlarının tahmin edilmesinde yüksek kabiliyete sahip olduğu ortaya konmuştur. Emisyon model parametresi olarak EGR oranının kullanılmasına gerek duyulmadığı gösterilmiştir. EGR oranının diğer model parametrelerine bağımlılığından ötürü model kalitesinde bir iyileştirme sağlayamamaktadır. Ayrıca, ön püskürtme miktarının kontrolü ve ölçümündeki hatalardan ötürü bu parametrenin de modelleme hatasını azaltmak konusunda etkisi görülememiştir.

Oluşturulan modeller yanma giriş ve çıkış parametrelerini içermektedir. Fakat, bu parametrelerin hepsi direk olarak dinamometrede ölçülememektedir. Bu sebeple, motorun bir boyutlu modeli oluşturulmuştur. Oluşturulan model ile gerekli parametrelerin değerleri elde edilmiştir.

Yanma giriş parametrelerine ek olarak çıkış parametrelerinin de modelleme kalitesine etkisi incelenmiştir. İlk aşamada elde edilen modelin parametrelerine farklı yanma çıkış parametreleri eklenerek model iyileştirmesi amaçlanmıştır. Çalışmalar türbin giriş sıcaklığının kullanılmasının is emisyonlarının modellenme kalitesini arttırdığını ortaya koymuştur.

Bu tez kapsamında, yalnızca bir boyutlu modelden elde edilen parametreler kullanılarak da emisyonların matematiksel olarak modellebilmesi amaçlanmıştır. Bu sayede; motorun ilk tasarım aşamalarında, emisyonlar da göz önünde bulundurularak optimum sistem tasarımı elde edilebilecektir. Fakat, sonuçlar bunun NOx emisyonları için belirli bir düzeyde olabileceğini gösterirken, soot emisyonlarının ise modellenemediğini göstermektedir.

Motorun farklı noktalarda, durağan haldeki parametre değerlerini kullanarak oluşturulan modeller ayrıca değişken koşullar için de değerlendirilmiştir. Bu amaçla, modeller MATLAB ve Simulink formatlarına uygun şekilde tekrar elde edilmiştir. WHTC çevrimine göre dinamometrede koşulan testin girdileri ve çıktıları kullanılarak bu modellere beslenmiştir. Elde edilen emisyon sonuçları dinamometrede elde edilen sonuçlar ile karşılaştırılmıştır. Hem is hem de NOx emisyonlarının değişken koşullar için de yüksek doğrulukta modellenebileceği ortaya konmuştur.

1. INTRODUCTION

1.1 Overview and History of Diesel Engine

Rudolph Diesel invented the diesel engine in 1983, and its patent was taken by R. Diesel for the design of a greatly efficient compression ignition of internal combustion engine. After the invention of the diesel engine, a new competition was started for energy conversion systems because of its significant superiority to the coal and steam industry. The diesel engine produces much more mechanical energy from a specific amount of fuel as compared to other energy conversion systems due to the engine's higher temperature of combustion and greater expansion ratio. Due to air compression before fuel injection, diesel engines can have perfect fuel economy and satisfying performance even with a small amount of fuel. Thus, high temperatures are obtained in combustion chambers, and atomized fuel droplets are mixed with surrounding air in these regions. Self-ignition of the mixture occurs by means of high temperatures and chemical energy inside the fuel converted to mechanical energy. There are two types of diesel engines in terms of cylinder and piston arrangement: two-stroke and four-stroke engines. A combustion cycle is completed in two strokes for two-stroke engines, whereas it's completed in four strokes for four-stroke engines. Also, four-stroke diesel engines are categorized in two parts with regard to its design: direct-injection and indirect-injection engines. Fuel is directly injected into the main combustion chamber in direct-injection diesel engines, whereas fuel is injected into a pre-chamber before main combustion chamber in indirect-injection diesel engines. Indirect-injection engines have increased pumping losses due to passage between pre and main combustion chambers although it improves noise characteristics of the engine. Accordingly, direct-injection engines have higher fuel economy than indirect-injection diesel engines about 10%.

Fuel safety characteristics, high efficiency, lower friction losses, durability and reliability are shown as advantages of diesel engines as compared to other energy conversion systems [21]. Since 19th century, researchers have focused on diesel

engines, and they came into use with ships and submarines in early years of the 20th century. Then, diesel engines were seen for trucks, locomotives and heavy equipment. The first light duty vehicle were introduced in the 1970's [37].

The most important disadvantage of diesel engines is that diesels emit too much hazardous compounds for environment and human health and legislation concerning the pollutant gas emissions of diesel cars is becoming restrictive more and more. Despite everything, light duty truck sales are growing at the rate of 4% per year in the U.S. [21].

1.2 Characterization of Diesel Emissions

Diesel engine primarily produces CO_2, H_2O, O_2, N_2 and SO_2 during combustion process. In addition to these products, a variety of pollutants which can have negative health and environmental effects are produced. The combustion process, which produces of all these pollutants, includes reactions between mixture components under high pressure and temperature, combustion of non-hydrocarbon components of diesel fuel and incomplete combustion of fuel [31].

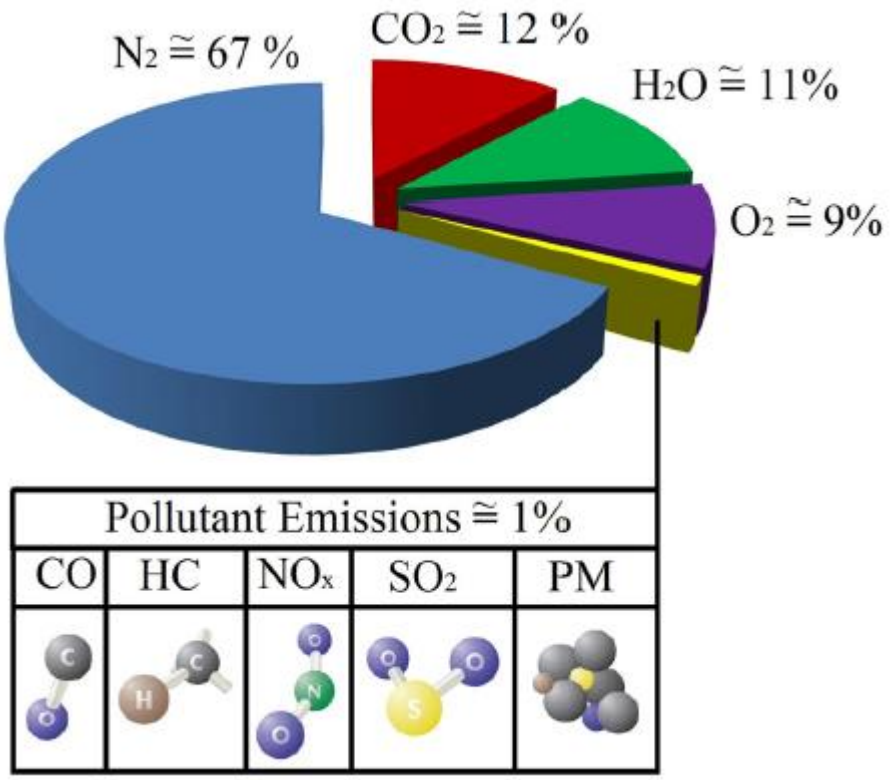

Figure 1.1: The compositions of diesel exhaust gas [31].

Many countries have applied pollutant restrictions and regulations because of environmental and health impacts of diesel emissions. Regulations include Nitrogen Oxides (NOx), Hydrocarbons (HC), Carbon Monoxide (CO) and particulate matter (PM) (Figure 1.1)[34].

Spark-ignition engines and compression-ignition engines produces different types of pollutants during combustion processes. In general, SI engines produce more CO, NOx and HC while CI engines produce greater concentrations of PM emissions. The raw emissions of diesel engines are low as compared to gasoline engines. For example, the CO emissions are 90% lower and the NOx emissions are 70% lower for diesel engines. However, a conventional three-way catalytic converter, which reduces emissions substantially in gasoline engines couldn't be adapted for diesel engines due to an exess of oxygen. Today's diesel pollutant control technologies primarily focus on reducing NOx and PM [1].

1.3 Motivation

Due to more stringent emissions legislation, pollutant emissions from automobiles, power plants and industrial processes have become a challenging area of researches for many years. Controlling of these pollutants has played a part in the design of combustion systems. Detailed investigations have been needed to understand formation processes of these pollutants. Empirical models, semi-physical models, thermodynamic models and CFD models have been used to analyze these processes.

In opposition to gasoline engines, where a three-way catalyst solves many aftertreatment problems, there is no aftertreatment system found for diesel engines, which has same efficiency of a three-way catalyst. A diesel particle filter (DPF) tackles reduction of particulate matters with a high fuel economy because of regenerations of the filter. Lean NOx trap (LNT) and a selective catalytic reduction (SCR) catalysts are used to reduce nitrogen oxides (NOx) emissions, however, these catalysts have limited conversion rates. For this reason, the optimal control of the whole engine system is required to reduce these pollutants.

The structure of a modern diesel engine system with its components and actuators in is shown in Figure 1.2. New technology advancements such as intake charge cooling, injection pressure control, injection timing control, air path management and variable

valve technology are used to optimize pollutants. The calibration of the electronic control unit (ECU) provides the optimization of pollutants besides controls of combustion processes. Currently, the control of diesel engines is mostly based on two-dimensional maps [32]. Input parameters of these maps can be used to control and predict pollutants. Also, in addition input parameters, combustion and output parameters can be variables of pollutant emissions.

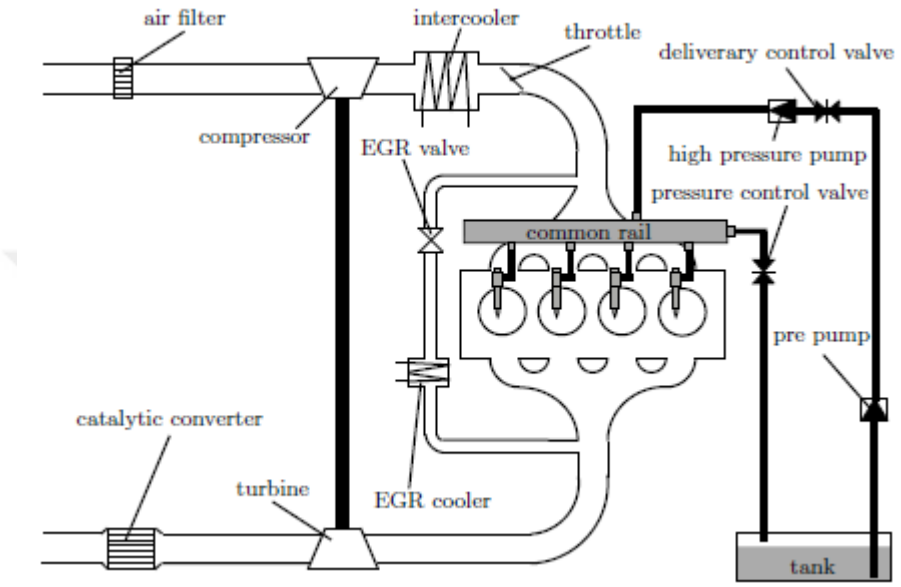

Figure 1.2: Schematic representation of diesel engine and its components [5].

1.4 Objectives of This Study

Due to time and cost issues, mathematical models are very useful tools to optimize engine system operations by taking account of limited test bench availability. The main objective of this study is to build an emissions model of diesel engines which shows good predictability across a wide variety of operating conditions.

The main focus is on predictions of PM and NOx emissions. Effects of combustion input parameters, controlled by ECU, affecting NOx and PM emissions are investigated by considering variable dependency and modeling error.

This study also investigates effects of combustion and output parameters on NOx and PM emissions. However, all combustion parameters would not be measured due to hardware problems and 1D engine model is used to obtain these parameters.

1D engine models are widely used to get through to detailed investigations of production engines from early studies of model engine. On the basis of advantages of

1D engine models, results of a coupling of 1D engine model with mathematical emissions model are observed.

1.5 Structure of the Thesis

The thesis is organized as follows. Firstly, a brief literature review focused on diesel combustion, combustion modeling, soot and NOx formation processes is given. Chapter 3 presents overview to empirical modeling whereas Chapter 4 presents experimental design followed for this thesis. Results have been subdivided according to steady state and transient conditions in Chapter 6. For steady state conditions, emission models that have been created by using Gaussian Regression Method are evaluated. The models include some combustion input and output parameters. However, all of these parameters cannot be measured directly on a dynamometer, and thus 1D model of the engine was created. The values of these parameters are obtained by using the 1D engine model. The theory of 1D engine modeling and correlation results of the model are shared in Chapter 5. For transient conditions, world harmonized transient cycle (WHTC) is used to compare model and test results. Models created based on steady state data are also evaluated with this cycle. Finally, Chapter 7 briefly summarizes the main conclusions of the study, and suggestions for future work are provided.

2. LITERATURE REVIEW

2.1 Combustion Process

The combustion process of diesel engines is an unsteady, heterogeneous, three-dimensional process due to its complex nature. For diesel engines, only air is sent into the combustion chamber during the intake stroke. This air is compressed into high pressures during the compression stroke. Combustion process begins with the start of injection towards the end of compression stroke. The fuel is injected through the injectors, and it atomizes into small droplets due to its high pressure and velocity. The fuel droplets penetrates into the combustion chamber, and vaporized fuel is mixed with high-temperature and high-pressure cylinder air. Due to the air above the fuel's ignition point and the temperature of this mixture of air and fuel, ignition after a delay period of a few crank angle degrees starts spontaneously. The cylinder pressure increases as combustion of the air-fuel mixture occurs. Atomization, vaporization, air-fuel mixing and combustion processes continue once all the fuel pass through each process essentially. Then, burned and unburned gasses in the cylinder proceed to the expansion stroke. To summarize overall combustion process of diesel engine can be shown with respect to the heat release rate in four stages: ignition delay, premixed combustion phase, mixing controlled combustion phase and late combustion phase. All the phases with respect to the heat release rate can be seen in Figure 2.1.

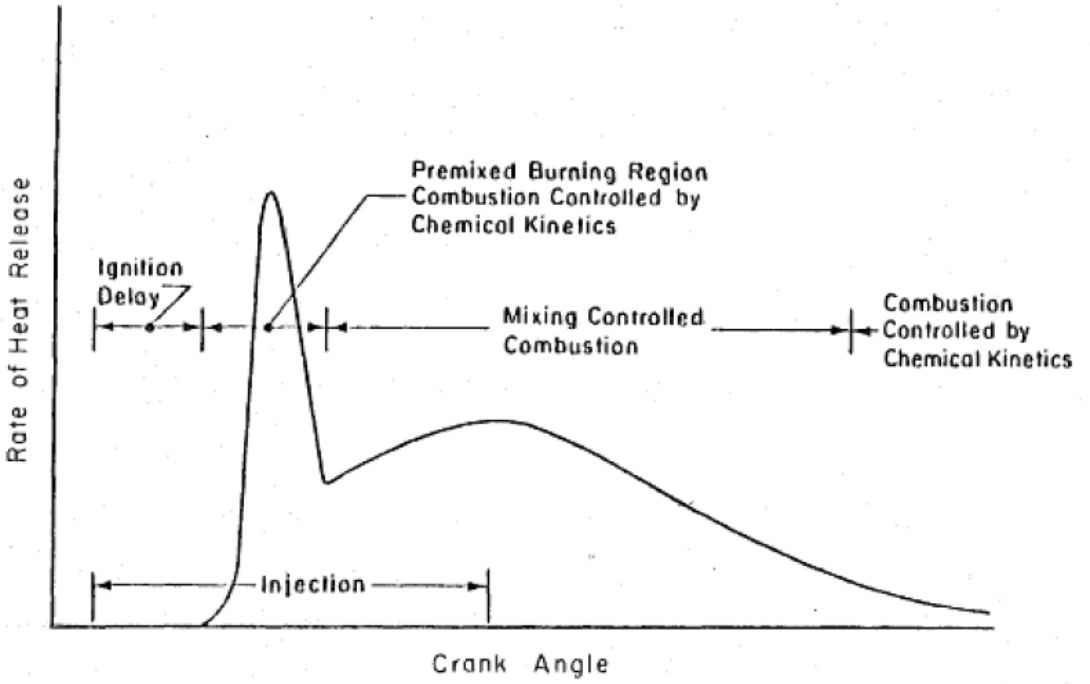

Figure 2.1: Diesel combustion phases with respect to the heat release rate [15].

The ignition delay period indicates the time between the start of injection and the start of combustion. Engine noise and exhaust emissions are highly affected by the ignition delay period. The best identification of ignition delay is made from the change in slope of of the heat release rate, which is specified from the cylinder pressure data. The ignition delay period includes both physical and chemical processes. Premixed combustion phase is the combustion of the fuel which has mixed with air within flammability limits during ignition delay period. In this phase, the combustion occurs at a very high rate due to high heat release rate characteristics. After the premixed phase, the remaining combustion is controlled by the rate at which mixture becomes available for burning in the mixing-controlled combustion phase. The rate of burning is also controlled by means of atomization, vaporization and the mixing of fuel vapor and air. The last phase, late combustion phase, is the combustion at which a lower rate of heat release is obtained, and it continues into the expansion stroke [15].

2.2 Pollutant Emissions of Diesel Engines

On the basis of ideal thermodynamic equilibrium, the entire combustion process of diesel combustion process would only produce CO_2 and H_2O in combustion chambers [27]. Nevertheless, the diesel engine generates a variety of harmful products during combustion process due to many reasons such as the air-fuel ratio, ignition timing,

combustion temperature, turbulence in the combustion chamber, etc. The most important products are NOx, PM, CO and HC.

Pollutant emissions have a rate of less than 1% in the diesel exhaust gas. CO and HC have lower proportion in pollutant emissions since diesel engines are operated at lean mixtures. On the other hand, concentration of NOx in pollutant emissions is maximal with a rate of more than 50%. After NOx emissions, PM has the second highest proportion [31]. In this thesis, the two main pollutant emissions (NOx and PM) from diesel engine are investigated.

Table 2.1: Euro standards of European Union for heavy-duty vehicles [10].

	CO	**HC**	**NOx**	**PM**
	(g/kWh)	(g/kWh)	(g/kWh)	(g/kWh)
Euro I	4.5	1.1	8	0.61
Euro II	4	1.1	7	0.15
Euro III	2.1	0.66	5	0.13
Euro IV	1.5	0.46	3.5	0.02
Euro V	1.5	0.46	2	0.02
Euro VI	1.5	0.13	0.4	0.01

Due to adverse effects of diesel emissions on health and environment, Europe has developed European emission standards. Table 2.1 shows that Euro standards have been more stringent more and more. Compared to Euro I standard, Euro VI standard for CO, HC, NOx, and PM emissions was decreased 66%, 76%, 95% and 98% respectively. Euro VI standard was implemented for heavy-duty vehicles on 1st September 2014 [10].

2.3 Combustion Modeling

In literature, there have been many types of models of internal combustion engines used by researchers for the purpose of analysis and prediction of engine performance and emission related characteristics. Current models reported can be divided into four main categories:

- Empirical models
- Semi-physical models
- Thermodynamic models (0D)
- CFD models (3D)

There are three criteria considered while classifying these models: sampling period, the kind of input variables and the mathematical model form [28]. The classification is also summarized in Table 2.2.

Table 2.2: Classification of the models [28].

Type	Sampling Period	Input Variables	Model
Empirical model	Quasi-static	-Injection settings -Air system variables -In-cylinder variables	-Static 2D map -Polynomial Static ANN
	Cycle resolved		-Dynamic ANN
Semi-physical model	Cycle resolved	-Air system variables -In-cylinder variables	-Algebraic relations inspired by physico-chemical phenomena
	Crank angle resolved		
Thermodynamic model (0D)	Crank angle resolved	-In-cylinder species concentrations -In-cylinder variables	-Ordinary differential equations
CFD	Crank angle resolved		-Partial differential equations

2.3.1 Empirical models

The phenomenological and the CFD models are basically crank-angle-based and explain extensively in-cylinder processes. Because of the overpriced computational of these models, such approaches are not suitable for transient simulations, which must run faster than real-time. Hence, event- or- time-dependent empirical models are computationally more influential. Therefore, these models can be applicable for real-time simulations. The well-known examples of these models are black-box models. Due to lack of knowledge of internal structure of the system, the input/output behavior can be modeled either with an artificial neural network (ANN) algorithm or with a polynomial approach [7], [2]. The thorough knowledge of physicochemical

phenomena occurring in the cylinder is not needed for empirical models. Additionally, these models show a low complexity, and finite number of the calculation power and time are required. Moreover, the basic ones among these empirical models are 2D static maps, which depend on engine speed and torque.

2.3.2 Semi-physical models

Semi-empirical - or grey box - models are stated as algebraic relations originated by the physico-chemical phenomena which takes place in the cylinder. These models are basically used input combustion related variables, calculated from the in-cylinder pressure signal, instead of control variables. Additionally, discrete in-cylinder variables, for example maximum in-cylinder temperature or combustion phasing angles, should be used ([33], [38]).

2.3.3 Thermodynamic models (0D)

In principle, the 0D combustion models are fundamental models used to study basic engine performance features depend on conservation laws as described former. On the other hand, there is complex structure in diesel engines, therefore numerous input parameters for example; injection timing, number of pulses, EGR etc., affect their performance and emissions. Consequently, 0D models have difficulties for predictions [3].

Correspond to the leading law of thermodynamic analysis, a homogenous thermodynamic state and composition is supposed to exist through the control volume that is invariant with according to infinitesimal time steps over which the whole process is clarified by solutions. These models are generally attached to simplifications; therefore, those are used for analysis of heat release, burn rate and fuel consumption. They have finite prediction ability from the point of emission due to lack of spatial resolution [26].

2.3.4 CFD models (3D)

The in-cylinder flow field tremendously affects the combustion characteristics i.e. ignition delay, pressure rise and pollutant formation. Owing to the introduction of progressive injection and after-treatment techniques, new combustion chamber designs, the importance of defining mixture formation and its following effect on combustion features is even more increasing. Despite the phenomenological models

are attractive to predict fundamental combustion parameters, most particularly for homogenous mixtures, it could not be applied for key engine systems development such as piston bowl, combustion chamber design, and injector spray profile [8].

Physical models have insufficient ability to detailed description of the combustion process, from fuel injection to pollutant formation, during fuel atomization, fuel evaporation, air-fuel mixing, and combustion. Because of the principle of combustion in diesel engine, it is highly complicated and nonuniform. Hence, 3D CFD models are required to explain precisely this phenomenon [29].

Consequently, numerous methods are used for study on the flow fields inside an engine, all variations in computation time and prediction accuracy. It is depending on the engine designers to select the appropriate method for strike a rational balance between computational time and prediction accuracy.

2.4 NOx Phenomenology

Combustion in diesel engines is obtained by using highly compressed hot air to ignite the fuel. Air fundamentally consists of oxygen and nitrogen compounds. Normally, the nitrogen in the air does not react with oxygen, and it is emitted out of the combustion chamber. However, high temperatures above 1600 °C lead to reaction of the nitrogen with oxygen, and it generates NOx emissions [31].

Nitrogen oxides (NOx) emissions in diesel engines include both NO and NO2. Approximately 90% of nitrogen oxides (NOx) is composed of NO. It is also slowly converted to NO2 in the atmospheric air. Although NO and NO2 are identified as NOx, these two pollutants have distinguishable differences. NO is a odorless and colorless gas which results from the oxidation of atmospheric nitrogen at high pressure and temperature, whereas NO2 is a toxic reddish brown gas characterized by pungent odor [20]. Some characteristics of these pollutants are shown in Table 2.3.

Table 2.3: Characteristics of NO and NO_2.

	Nitric Oxide	**Nitrogen Dioxide**
Formula	NO	NO2
Formula Weight	30.01 g/mole	46.01 g/mole
Appearance	Colorless Gas	Red-Brown Gas
Density	1.0367	-
Melting Point	-161 °C	-9.3 °C
Boiling Point	-151 °C	21.3 °C

The formation of NOx in diesel engines is highly affected by some parameters: gas temperature in the cylinder, the cylinder pressure, oxygen concentration, as well as the residence time of air-fuel mixture with suitable temperatures [15].

Nitrogen oxides (NOx) emissions emitted from the vehicles result in a large amount of health and environmental danger. NOx emissions make contribution to formation of ozone, formation of smog and acidization, which most cities in the world struggle against at the present time [13].

2.5 NOx Mechanisms

Various mechanisms for the formation process of NOx in IC engines have been asserted in the literature. The following section present a review of these different mechanisms.

2.5.1 The thermal mechanism

This mechanism is also known as the Zeldovich mechanism of the formation by a set of highly temperature-dependent chemical reactions. The principal reactions of the Zeldovich mechanism governing the formation of NO from molecular nitrogen are as follows:

$$O + N_2 \leftrightarrow N + NO \tag{2.1}$$

$$N + O_2 \leftrightarrow O + NO \tag{2.2}$$

A third reaction contributing to the thermal formation, especially in rich mixtures and at near stoichiometric conditions, is given below:

$$N + OH \leftrightarrow H + NO \tag{2.3}$$

The Zeldovich mechanism describes the reaction of nitrogen, N_2, with oxygen, O_2, in the combustion air to produce NOx. Very high temperatures are required to complete these reactions, and it shows that the formation process is highly dependent on the temperature. In addition, the forward and reverse reaction rates have been investigated comprehensively by numerous studies on various temperatures and equivalence ratios [15].

2.5.2 The prompt mechanism

The prompt mechanism, also known as the Fenimore mechamism, is originally suggested as a possible route of NO formation by C.P. Fenimore [12]. The thermal mechanism describes the growth of NO in the post-flame well but it is not capable of a faster transient formation of NO in the primary reaction zone. Radical hydrocarbons are generated through the combustion of the fuel. Reaction of these hydrocarbons with the nitrogen, N2, in the combustion air occurs very quickly in order to from transition substances that then oxidize to NO. The most significant equation of this process is given:

$$CH + N_2 \leftrightarrow HCN + N \tag{2.4}$$

where the transition substance, HCN, decomposed into atomic nitrogen through the below equations:

$$HCN + O \leftrightarrow NCO + H \tag{2.5}$$

$$NCO + H \leftrightarrow NH + CO \tag{2.6}$$

$$NH + H \leftrightarrow N + H_2 \tag{2.7}$$

The reaction below also contributes to the breaking of the N_2 bond at higher temperature.

$$C + N_2 \leftrightarrow CN + N \tag{2.8}$$

Then, the nitrogen atoms are oxidized to NO through the equation:

$$N + OH \leftrightarrow NO + H \tag{2.9}$$

This process usually occurs at slightly low temperatures in the beginning of the combustion. Moreover, a path diagram of prompt NO formation showing major steps can be seen in the Figure 2.2.

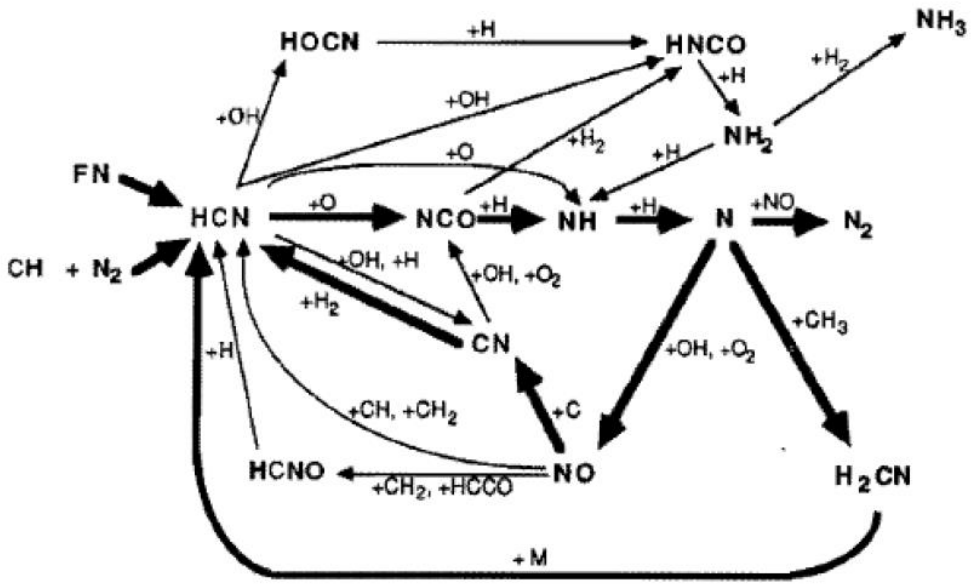

Figure 2.2: Pathways of prompt NO formation [22].

2.5.3 The NO_2 mechanism

Diesel engines emit substantial fractions of total nitrogen oxides (NOx) as NO_2. The following equations define the process during combustion:

$$NO + HO_2 \leftrightarrow NO_2 + OH \tag{2.10}$$

$$NO_2 + H \leftrightarrow NO + OH \tag{2.11}$$

$$NO_2 + O \leftrightarrow O_2 + NO \tag{2.12}$$

HO_2 compounds react with NO which is generated in high temperature regions and move into the low temperate regions by diffusion. Decomposition reactions of NO_2 take place rapidly, and NO_2 is converted back to NO. It is clearly seen that the formation of NO_2 is dependent on the presence of HO_2. The concentration of HO_2 specifies the production rate of NO_2 [22]. Relative concentrations of NO and NO_2 in diesel engines can be seen in the Figure 2.3.

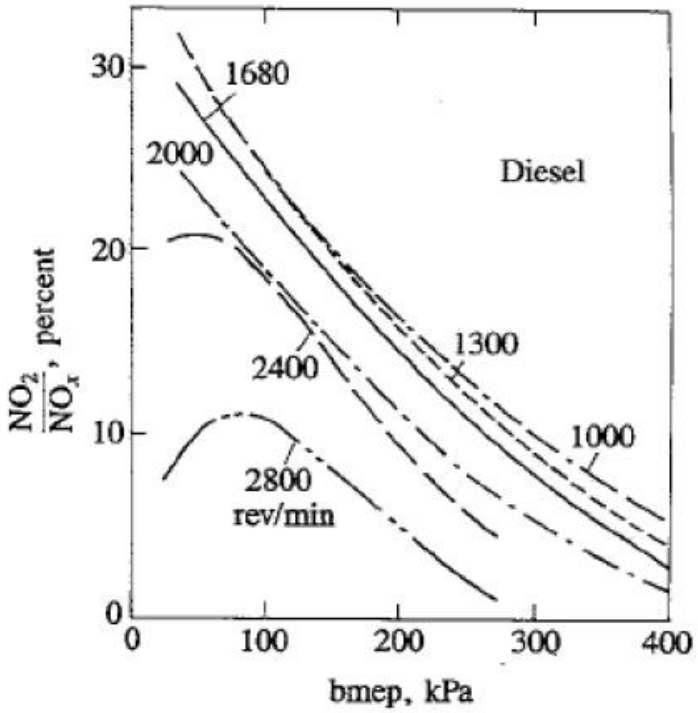

Figure 2.3: Relative concentrations of NO and NO_2 in diesel engines [15].

2.5.4 Fuel NOx mechanism

The reaction of nitrogen in the fuel with the oxygen in the combustion air is defined as fuel NOx formation. Conversion of fuel nitrogen to NO is dependent on nitrogen concentration in the fuel-air mixture. Typically, gaseous fuels contain relatively low amount of bound nitrogen. Due to low nitrogen fraction in diesel fuel, 0.5 – 2.0% by weight, the contribution of fuel bound nitrogen to NOx formation is negligible [22]. In addition, the reaction mechanism from fuel NOx is modeled by the following two equations:

$$N_{Complex} + OH \leftrightarrow NO + Y \tag{2.13}$$

$$N_{Complex} + NO \leftrightarrow N_2 + Y \tag{2.14}$$

where $N_{complex}$ symbolizes fuel bound nitrogen, and Y symbolizes other products [17].

2.6 Soot Phenomenology

Many researchers have been focused on the formation of PM for many years. PM emissions in exhaust gas are resulted from combustion process. PM mainly consists of

soot, and the generation process of soot comprises of two events fundamentally: formation and oxidation. These processes occurs in the cylinder at the same time. A schematic representation of processes is shown in Figure 2.4. In the literature, processes are commonly defined as pyrolysis, inception, surface growth, coagulation, agglomeration and oxidation [18].

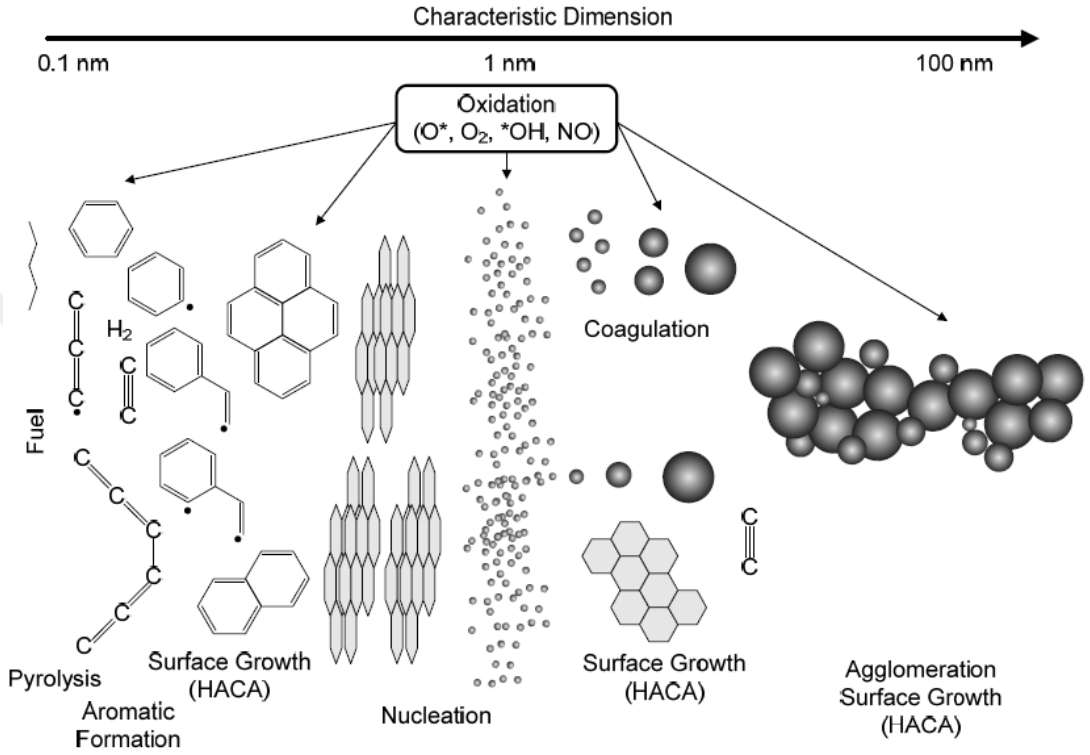

Figure 2.4: Schematic representation of the fundamental soot formation mechanisms [18].

Soot mainly has a solid graphite-like structure consisting of carbon with a small part of hydrogen. The density of soot is measured as 1.84 ± 0.1 g/cm^3 [6]. Soot generation roughly occurs at temperature between 1600 K and 1800 K, pressure between 50 bar and 100 bar and rich mixtures due to oxygen availability [36]. Accordingly, it can be asserted that the availability of oxygen and combustion temperatures are key factors which affect the production of PM.

Environmental and heath effects of PM emissions have been also studied by many researchers. These studies show that inhaling of particulate matters might result in significant health problems such as premature death, asthma, lung cancer, and other cardiovascular issues [11].

2.7 Soot Mechanisms

Soot is caused by incomplete combustion of fuel hydrocarbons. Due to the heterogeneous combustion in diesel engines, fuel accumulates in a pocket, in which complete combustion cannot be obtained, and it results in the formation of soot [15]. The process in a diffusion flame can be seen in Figure 2.5. Some of soot particles are burnt towards to the ends of combustion by the help of high temperatures prior to exhaust of emissions gases to the environment. Despite the fact that the details of mechanism resulting in soot formation are not clear, it is known that some parameters such as pressure, temperature and air-fuel ratio affect soot formation rates.

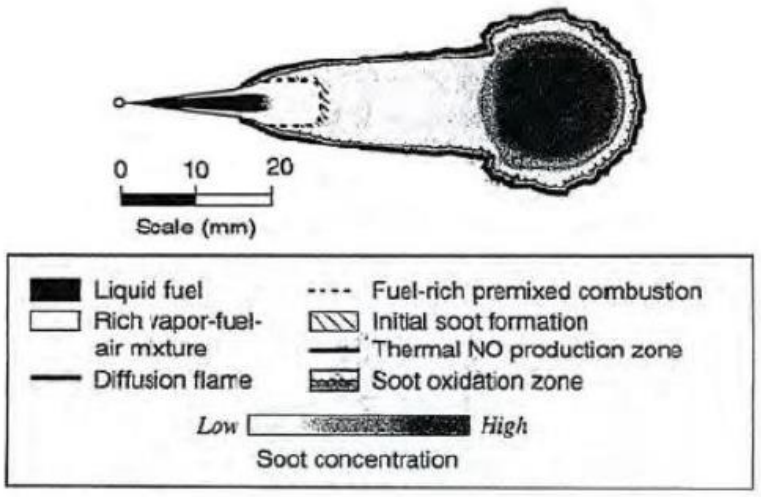

Figure 2.5: Concentration of soot in a diffusion flame [9].

In literature, soot generation has been described by means of phenomenological or semi-empirical models. These models calculate the soot within two steps: formation and oxidation.

A simple soot model was developed at first by Hiroyasu. The soot model, which is single-step and two-process, is shown schematically below [16].

$$Fuel \cdots K_f \rightarrow Soot \cdots K_o \rightarrow CO \tag{2.15}$$

where K_f is a formation coefficient, and K_o is a oxidation coefficient of soot. Then, the model was applied to multidimensional diesel combustion by Belardini et al. [4]. The model predicts the production of soot mass, which is formulated as below:

$$\frac{d(M_s)}{dt} = \dot{M}_{sf} - \dot{M}_{so} \tag{2.16}$$

where $\dot{\mathbf{M}}_{sf}$ is soot mass formation rate, and $\dot{\mathbf{M}}_{so}$ is soot mass oxidation rate. The soot mass formation and oxidation rates are given by:

$$\frac{d(M_{sf})}{dt} = K_f M_f \tag{2.17}$$

$$\frac{d(M_{so})}{dt} = K_o M_S Z_{O2} \tag{2.18}$$

The formation and oxidation rates can be defined in Arrhenius form as below:

$$K_f = A_f P^{0.5} \exp(-E_f/RT) \tag{2.19}$$

$$K_o = A_{O2} P^{1.8} \exp(-E_o/RT) \tag{2.20}$$

where A_f and A_o are the pre-exponential factors; E_f and E_o are the activation energies; Z_{O2} is oxygen molar fraction; R is the spesific gas constant; T is the gas temperature. The activation energies and Arrhenius pre-exponential constants are modifed from Belardini et al. in order to match the experimental and model data [4].

- E_f = 12500 cal/mole and A_f = 100
- E_o = 14000 cal/mole and A_o = 30

However, this model is found to give relatively low peak in-cylinder soot concentrations. A more realistic model is obtained by placing Nagle and Strickland-Constable (NSC) oxidation model into general equation [23]. In this model, carbon oxidation occurs by two mechanisms whose rates depend on surface chemistry including more reactive A sites and less reactive B sites. The chemical reactions are shown below:

$$A + O_2 \leftrightarrow A + 2CO \tag{2.21}$$

$$B + O_2 \leftrightarrow B + 2CO \tag{2.22}$$

$$A \leftrightarrow B \tag{2.23}$$

The NSC soot oxidation rate is formulated as:

$$\frac{dm_{so}}{dt} = \frac{M_c}{\rho d_s} m_s w \tag{2.24}$$

where M_c is the carbon molecular weight, ρ_s is the soot density, and d_s is the soot diameter. The term 'w' in equation is the net reaction rate of chemical reactions.

$$w = \left(\frac{K_A p_{ox}}{1 + K_s p_{ox}}\right) x + K_B p_{ox}(1 - x) \tag{2.25}$$

where ρ_{ox} is the oxygen partial pressure in atm. The proportion, x is given by**:**

$$x = \frac{p_{ox}}{p_{ox} + \left(\frac{K_T}{K_B}\right)} \tag{2.26}$$

The rate constants used in NSC oxidation model are given in Table 2.4.

Table 2.4: Rate constants of NSC oxidation model

Rate Constant	**Units**
K_A=20 exp(-15100/T)	g-C/cm^2.s.atm
K_B=4.46x10^{-3} exp(-7640/T)	g-C/cm^2.s.atm
K_T=1.51x10^5 exp(-48800/T)	g-C/cm^2.s
K_Z=20 exp(-15100/T)	atm^{-1}

3. COMPARISON OF EMPIRICAL MODELS

3.1 Polynomial Models

The polynomial model is fundamental and basic model, and in order to optimize its parameters rapidly the Least Squares method should be used. Although, the quantity of parameters increases immediately in accordance with advancing input dimensional quantities, therefore, polynomial models are not fitted for high dimensional problems. Moreover, the explication of this model is depressed, and so the integration of former knowledge has low probability. The most important problem of polynomial models is the optimization of the structure for high dimensional problems because of the great quantity of the potential regressors [25].Therefore, denominated subset selection techniques are suitable for to apply. In order to solve complex problems, high order polynomials incline to overfit are not useful. Additionally, the universal modelling approach inclines to a very rigid modelling chain. The polynomial model is capable of sustain a model supply a model uncertainty by using the input data applicable for training into account. It is named errorbars. In general aspect, it was estimated from data can be anticipated to be better in regions where the data was intense and to be worse in regions where the data few [25]. On the other hand, polynomial models are capable of performed as an ECU function, because of limitation of multiplications of mathematical operations, summations. Moreover, the ECU memory have to store only the parameters.

3.2 Neural Networks

The artificial neural networks (NN) are inspired by the biological networks in the human and animal brains [25]. The fundamental of NN is to use basic units in a large number and link these units to a network. The two classes of NN have great importance in artificial neural networks which called multilayer neural networks and recurrent

neural networks [24]. Figure 3.1 demonstrates the fundamental structure of these networks.

The network simply includes an input layer, one or many hidden layers and one output layer. The hidden layer comprises of hidden layer neurons that generally consist of a weighted sum and a nonlinear function. In general, the output of neuron is a linear conjunction of the hidden layer basis functions with an extra offset that is occasionally named Bias [25]. The extensively known structure of a multilayer NN is called Multilayer Perceptron (MLP).

Figure 3.1 demonstrates the static and dynamical structure. The design of perceptrons in MPL structure including of weighted summation of the inputs and the bias associated with a nonlinear activation function. In order to activate function, the sigmoid function is a general option [25].

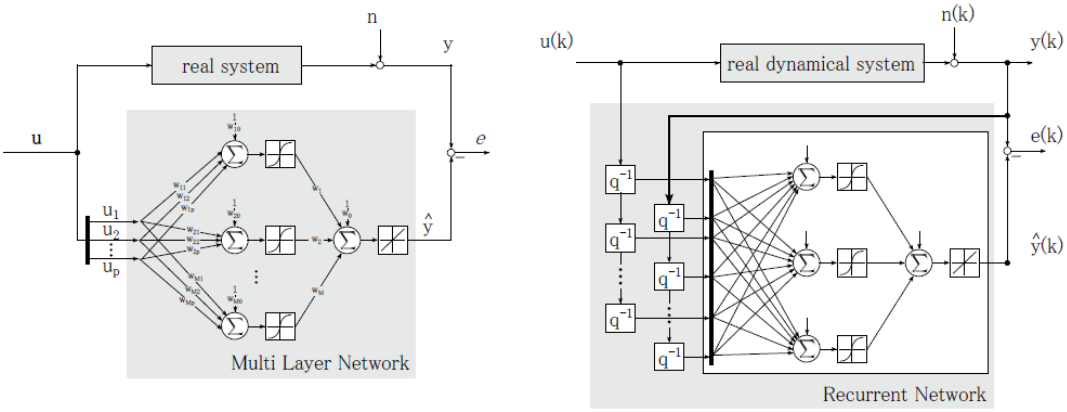

Figure 3.1: Structure of a MLP network [35].

3.3 Gaussian Process Regression

It is accepted that the parametric model is a deterministic mean function for Gaussian Process of the inverse model error. (Gaussian Process: *"A Gaussian process is a collection of random variables, any finite number of which has a joint Gaussian distribution."* [30]). Assuming the additive independence and identical distribution of the noise, and y is the error of the parametric model. The relationship between inputs (x) and the output (y) can be written as:

$$y = f(x) + \varepsilon, \varepsilon \approx N(O, {\sigma_n}^2) \tag{3.1}$$

Former covariance on the noisy observations y_i and y_j is given as:

$$cov(y_i, y_j) = k(x_i, x_j) + {\sigma_n}^2 \delta_{ij} \tag{3.2}$$

$k(x_i,x_j)$ is a covariance function explained with input samples x_i and x_j, and δ_{ij} is the Kronecker delta function. $k(x_i,x_j)$ is established as:

$$k(x_i, x_j) = \sigma_d e^{-0.5{x_{jl}}^T x_{jl}} \tag{3.3}$$

Here, σ_d is the horizontal scale parameter and x_{ij} is a scaled input sample given by:

$$x_{jl} = \left[\frac{x_{j1}}{l_1} \frac{x_{j2}}{l_2} \cdots \frac{x_{jn}}{l_n}\right]^T \tag{3.4}$$

In the given formula, l_j is the length scale parameter. If it is assumed that n samples of training inputs, it can be written the given covariance matrix that can be used in following analysis:

$$K(X,X) = \begin{bmatrix} k(x_1,x_1) & k(x_1,x_2) & \cdots & k(x_1,x_n) \\ \vdots & \vdots & \vdots & \vdots \\ \cdots & \cdots & k(x_i,x_j) & \cdots \\ \cdots & \cdots & \cdots & k(x_n,x_n) \end{bmatrix} \tag{3.5}$$

where "l" is length scale and "σ_d" is horizontal scale which named hyper parameters. These parameters optimized with model training. There are two "x" values (namely "training and test values") for Gaussian process modeling. In order to calculate hyper parameters, training values are used, and also they turn into a model itself. Test inputs written as x_*. The covariance vector between simulation point and the training points defined as below:

$$k_* = [k(x_*,x_1) \quad k(x_*,x_2) \quad \cdots \quad k(x_*,x_n)]^T \tag{3.6}$$

Consequently, the predictor equation written as below:

$$f_* = {k_*}^T (K + {\sigma_n}^2 I)^{-1} y \tag{3.7}$$

For all that, accuracy and simplicity of Gaussian Process Model are favorable, and the price of its computation is expensive for commercial engine control units. Hence, this is the important disadvantage of the method for the industry. Considering present

commercial engine electronic control unit principles, a comparatively easy model is reformed while the necessary profits of the Gaussian Process Regression (GPR) sustain.

The parametric models on engines are basically physical models that based on empirical models. Although, they are generally applicable under established assumptions. It is clear that real physical system is more complex than simplified parametric models. Moreover, the actual physical system models comprise of differential equations that cannot be figure out quicker than real time in the inserted controller. Although simplified parametric models are capable to adjustment of fixed training data, and model accuracy values from the point of errors can be suitable for average of test data, it should be essential to have superior accuracy at given operation conditions. Readjustment of the entire model should necessitate repeated validation in the entire space, and this should be very expensive in both time and money in a contemporarily automotive model advancement cycle. On the other hand, this correction of the parametric model functionality is natural for GPR if distance parameters adjusted according to GPR does not differ output values of the initial parametric model where the beginning performance is good enough.

3.4 Summary of Model Comparison

A polynomial model, neural network and GPR were presented in previous sections. The following table summarizes the properties of the different model types according to the requirements (Table 3.1).

Table 3.1: Comparison of different types of empirical models [35].

Properties	**Polynominal**	**Neural Network**	**GPR**
Accuracy	-	+	++
Parameter estimation	++	--	--
Structure optimization	-	-	++
Sensitivity to noise	+	++	++
Interpretation	0	--	++
Integration of prior knowledge	-	--	0
High dimensional mapping	--	+	++
Large data sets	++	0	--
Training speed	+	--	-
Uneven data distribution	--	++	0
Statement of uncertainty	-	--	++
Weakening extrapolation	--	0	++
Iterative modelling	--	--	--
Model recalibration	--	--	--
Noise variations	--	--	--
Adaptation of local complexity	--	++	--
Adaptation of local changing dynamics	--	--	--
Simulation speed	0	+	-
Requirement of memory	++	+	-
Online adaptation	-	--	--
Effort for ECU implementation	++	+	-
Usability	0	-	++

It is obvious in given above table that, polynomial models, and neural networks have many drawbacks benchmarked with GPR. If the model accuracy taken into account, structure optimization and high dimensional mapping, GPR indicates excellent properties according to the regression difficulty of dynamic nonlinear systems.

4. EXPERIMENTAL DESIGN

A heavy-duty diesel engine, which has been developed by Ford Otosan for Ford Cargo Trucks, was used during the tests. The engine is 12.7 liters, 6-cylinder in line, with common rail fuel injection system. The main specifications of the engine is shown in Table 4.1.

Table 4.1: Main specification of the heavy-duty engine

Parameter	Unit	Value
No of cylinders	-	6
Engine Volume	L	12.7
Bore	mm	130
Stroke	mm	160
Compression Ratio	-	17 ± 0.5:1
Max Power	PS	480
Max Torque	Nm	2500

The engine can produce torque of 2500 Nm between 1000-1200 pm and power of 480 PS at 1800 rpm. Also, torque versus engine speed and power versus engine speed curves can be seen in Figure 4.1.

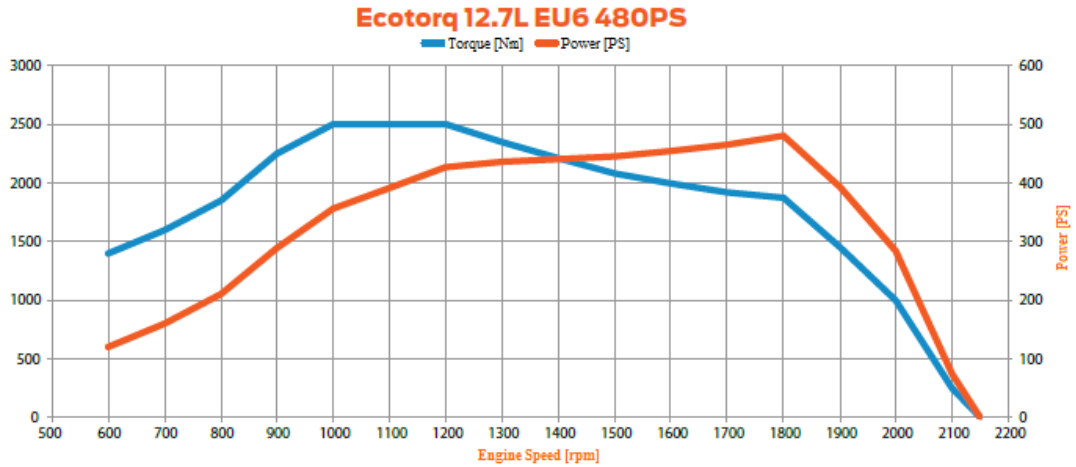

Figure 4.1: Torque and power curves of the engine.

4.1 Experimental Setup

Schematic of the experimental setup is shown in Figure 4.2. The experiments and measurements were performed on the heavy-duty diesel engine by using this setup.

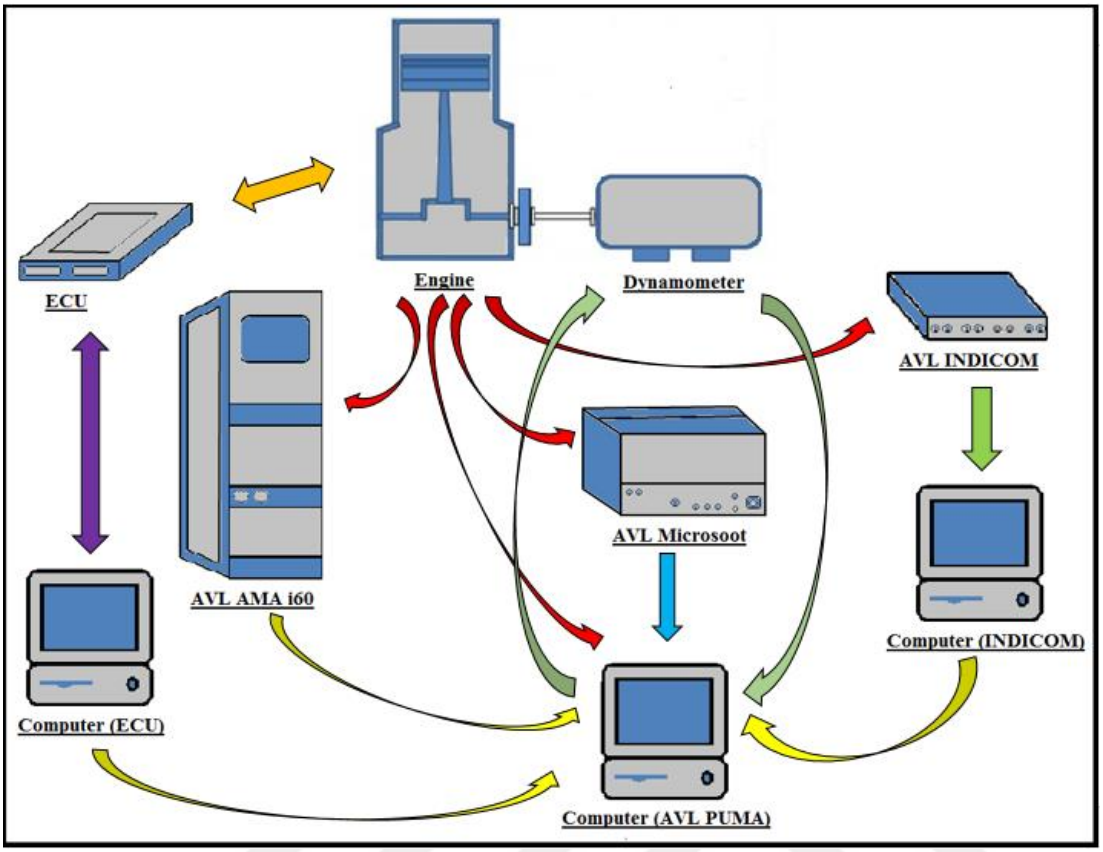

Figure 4.2: Schematic of the experimental setup.

Combustion input parameters such as rail pressure, boost pressure, injection quantity, start of injection, mass air flow, EGR rate, etc., were controlled by engine control unit. A computer that has ETAS INCA tool was utilized for controlling these parameters and also data acquisition from the engine equipped with its own sensors. Dynamometer, coupled with the engine, was used to control load and speed of the engine. AVL IndiCom tool and a computer, which has its own software, were used to measure in-cylinder pressures. The pressure values are calculated based on crank angle and time. The tool provides high-speed data acquisition from the engine. Maximum pressures in cylinders were obtained by using it. HC, CO, CO_2, NOx emissions in the exhaust were measured by an exhaust gas emission analyzer named AVL AMA i60. However, separate measurement device is needed to measure soot emissions, and AVL Microsoot tool was used to measure soot emissions. Finally, all the data is collected in a special computer named AVL Puma. ECU, emission and in-cylinder signals were transiently measured and recorded via AVL Puma. Oil conditioning, coolant conditioning and environment conditioning systems were also used although these systems cannot be seen in schematic of experimental setup. Moreover, instrumentation

chart of the engine that shows positions of mass air flow, temperature and pressure sensors is explained detailedly in the next section.

4.2 Instrumentation

Some temperature and pressure measurements from certain points on the engine were taken through external sensors during the tests besides its own measurements. Instrumentation chart of the engine is shown in Figure 4.3.

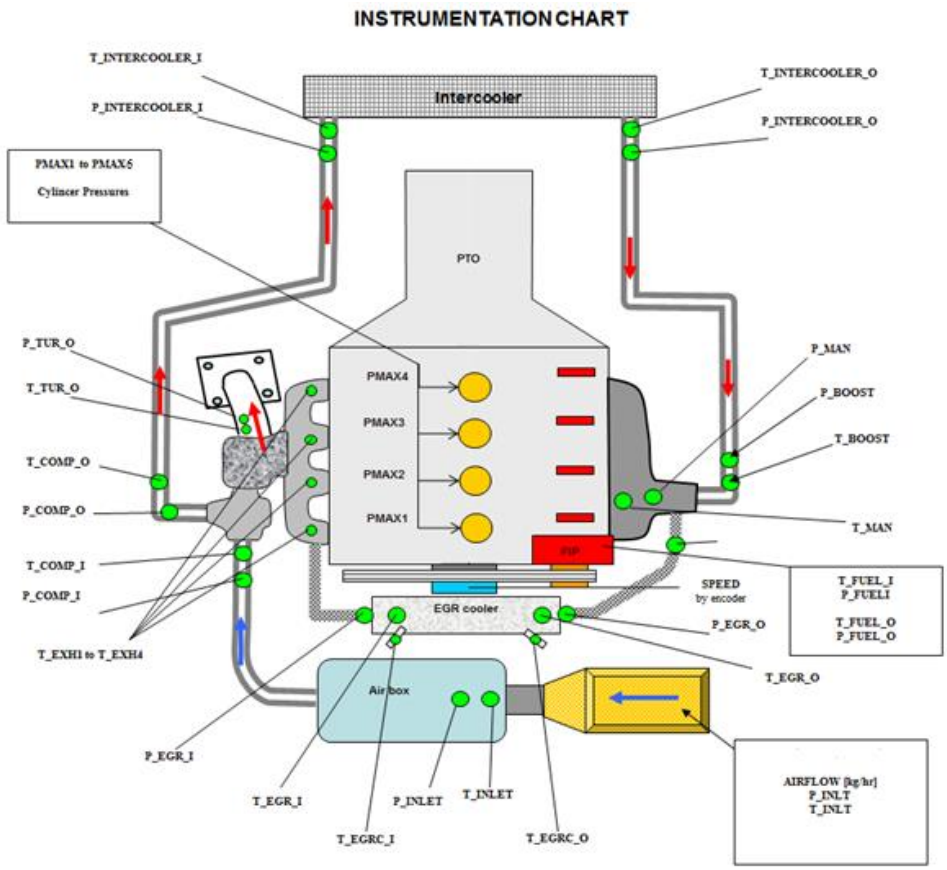

Figure 4.3: Instrumentation chart of the engine.

The engine has own airflow sensor in the airbox, however, external mass air flow sensor named AVL FLOWSONIX Air was used to obtain robust measurements. For measuring maximum cylinder pressures, external pressure sensor was fitted on the engine. AVL IndiCom tool was used to obtain crank based in-cylinder pressures. In addition, descriptions of temperature and pressure sensors can be seen in Table 4.2.

Table 4.2: Descriptions of measurement points on the engine.

Parameter	**Unit**	**Abbreviation**
Air Inlet Temperature	°C	T_INLT
Air Inlet Pressure	hPa	P_INLT
Mass Air Flow	Kg/h	AIRFLOW
Compressor Inlet Temperature	°C	T_COMP_I
Compressor Inlet Pressure	hPa	P_COMP_I
Compressor Outlet Temperature	°C	T_COMP_O
Compressor Outlet Pressure	hPa	P_COMP_O
Intercooler Inlet Temperature	°C	T_INTERCOOLER_I
Intercooler Inlet Pressure	hPa	P_INTERCOOLER_I
Intercooler Outlet Temperature	°C	T_INTERCOOLER_O
Intercooler Outlet Pressure	hPa	P_INTERCOOLER_O
Boost Temperature	°C	T_BOOST
Boost Pressure	hPa	P_BOOST
Intake Manifold Temperature	°C	T_MAN
Intake Manifold Pressure	hPa	P_MAN
Fuel Inlet Temperature	°C	T_FUEL_I
Fuel Inlet Pressure	hPa	P_FUEL_I
Fuel Outlet Temperature	°C	T_FUEL_O
Fuel Outlet Pressure	hPa	P_FUEL_O
Engine Speed	Rpm	SPEED
Maximum Cylinder Pressure	Bar	PMAX
EGR Outlet Temperature	°C	T_EGR_O
EGR Outlet Pressure	hPa	P_EGR_O
EGR Cooler Outlet Temperature	°C	T_EGRC_O
EGR Inlet Temperature	°C	T_EGR_I
EGR Inlet Pressure	hPa	P_EGR_I
EGR Cooler Inlet Temperature	°C	T_EGRC_I
Exhaust Manifold Temperature	°C	T_EXH
Turbine Outlet Temperature	°C	T_TUR_O
Turbine Outlet Pressure	hPa	P_TUR_O

All temperature and pressure sensors except cylinder pressure sensor are connected to same module, and all the data is transmitted to AVL PUMA computer simultaneously. The output setup of the sensors can be seen in Figure 4.4.

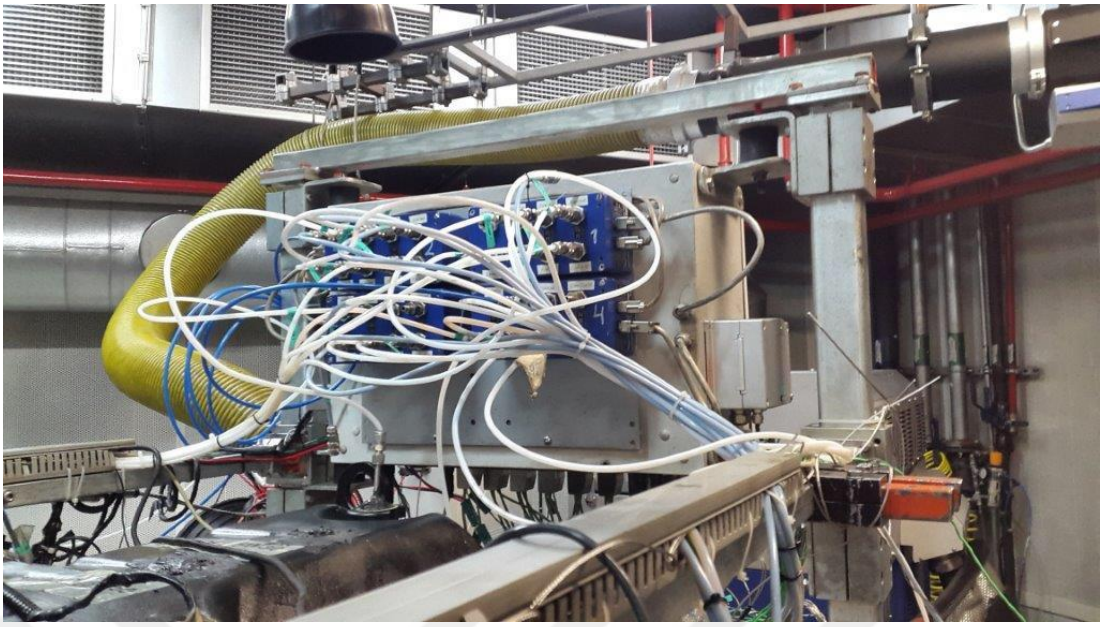

Figure 4.4: The output setup of temperature and pressure sensors.

4.3 Emission Analyzers

4.3.1 NOx emissions

As mentioned in section 4.1, AVL AMA i60 device was used to measure NOx emissions. The measurement device measures NOx emissions with the chemiluminescence method, and this method can measure NO molecules.

$$NO - O_3 \rightarrow NO_2{}^* + O_2 \tag{4.1}$$

Formed NO_2 molecules that have high energy are unstable, and these unstable molecules release their energy as luminous energy. Thus, unstable NO_2 are converted to NO_2 molecules in neutral state.

$$NO_2{}^* \rightarrow NO_2 + luminous\ energy \tag{4.2}$$

This released luminous energy is proportional to available NO concentration. NOx concentration is calculated by measuring the diffusion of light at the end of the reaction. The device used for measuring NOx emissions can be seen in Figure 4.5.

Figure 4.5: The measurement device for NOx emissions.

The device calculates the value of measured NOx emissions in unit of part per million (ppm). The values are converted into unit of g/h by using the following equation [14].

$$(NO_x)_{ppm} * m_{exh} * 0.0011586 = (NO_x)_{g/h} \quad (4.3)$$

where $(NOx)_{ppm}$ denotes NOx emission value in ppm unit, $\dot{m}_{exh}$ is exhaust flow rate, $(NOx)_{g/h}$ denotes NOx emission value in g/h unit.

4.3.2 Soot emissions

As mentioned in section 4.1, AVL MicroSoot device was used to measure soot emissions. The measurement device measures soot emissions with the photoacoustic measurement method. The exhaust gas including soot particles is exposed to adjusted light. With this measurement method, the cyclic warming, cooling, expansion and

contraction of the exhaust gas can be acceptable as a sound wave and detected through microphones. The device used for measuring soot emissions can be seen in Figure 4.6.

Figure 4.6: The measurement device for soot emissions.

The device calculates the value of measured soot emissions in unit of mg/m3. The values are converted into unit of g/h by using the following equation.

$$(Soot)_{g/m^3} * m_{exh}/(1000 * \rho_{air@25°C}) = (Soot)_{g/h} \quad (4.4)$$

where $(Soot)_{g/m3}$ denotes soot emission value in g/m3 unit, $\dot{m}_{exh}$ is exhaust flow rate, $\rho_{air@25°C}$ is the density of air at 25°C, (Soot)g/h denotes soot emission value in g/h unit.

4.4 Design of Experiment (DoE) Methodology

The main purpose of the design of experiments (DoE) is to describe unknown systems by means of measurement data. The methodology of the DoE consists of creation of

the experiment plan based on statistical conditions, the generation of models and the optimization of modeled systems. For automotive systems, test benches or chassis dynamometers causing expensive measuring costs are used for the measurements. Thus, gathering as much information as possible about input-output behavior with minimum test requirement is the key concept of the DoE. Also, the other important goal for the DoE is minimization of measuring effort during the experiment planning [14]. Mathematical approximation methods are commonly used for data-based models.

Classical experiment methods are mostly based on a grid-shaped or star-shaped measurement of the experimental space. The examples for grid measurement and star-shaped measurement of the experimental space can be seen in Figure 4.7.

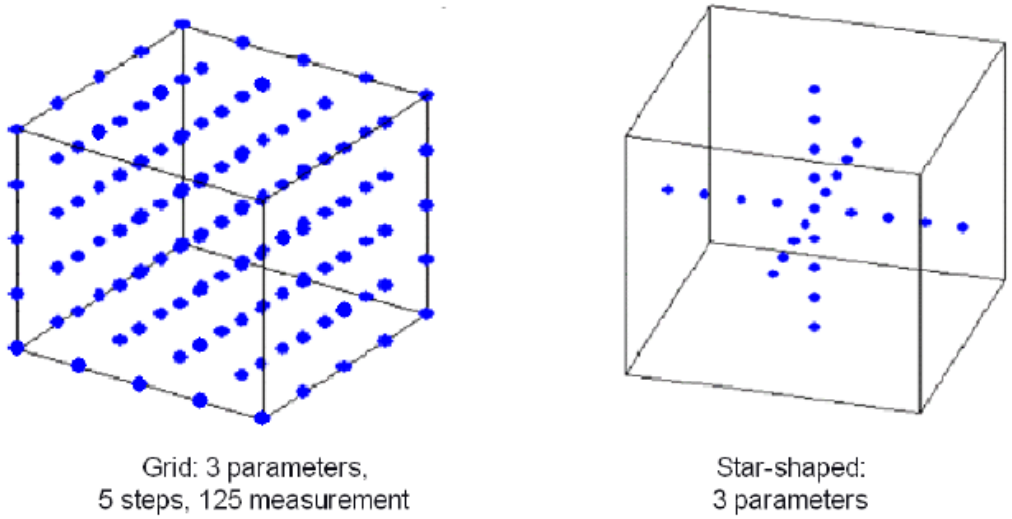

Figure 4.7: Grid measurement and star-shaped measurement of the experimental space [39].

In principle, the grid measurement is suitable for all model types but the exponential increase in required measurements is dramatic with increasing the number of parameters. For the star-shaped measurement, only one parameter is being varied at a time, and this method has a reduced measuring effort as compared to the grid measurement. Nevertheless, interactions between the parameters are neglected in this process, and the process is not capable of describing complex systems [39].

Space-filling plans are characterized by a uniform distribution of the measuring points in the parameter space and an optimal coverage of all parameter levels. Sobol sequence is a good example of space-filling plans. Empirical experiments proved that a distribution of the input parameters based on Sobol sequences is most convenient [19]. The property of a Sobol sequence is to maximize the distance between sampling points

and to make certain that each sampling value of one dimension occurs only once within the design (Figure 4.8). The space filling design provides a more homogenous coverage of the whole input space because of the distance maximization criterion [14].

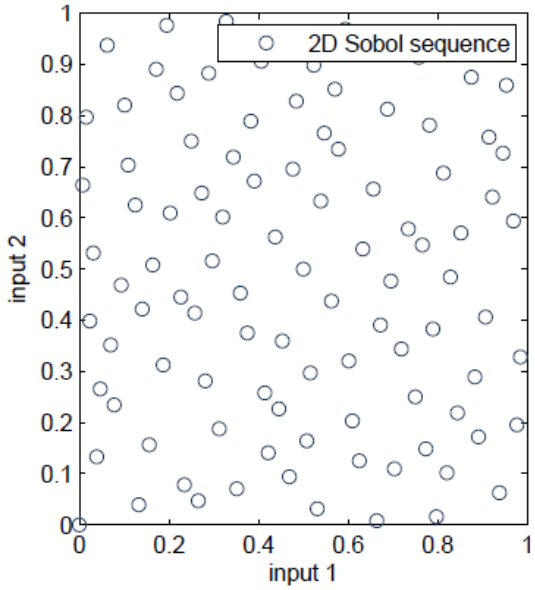

Figure 4.8: Sobol sequence in 2D [35].

For steady-state applications, space filling DoE are successfully implemented in the commercial tools like ASCMO by ETAS. Space filling DoE was applied for this thesis, and a DoE plan that has 1000 measurement points were obtained by using the method. In this thesis, all parameters were converted to unitless values by using the equation below:

$$X_{unitless} = \frac{X_i}{X_{max,meas}} \tag{4.5}$$

where $X_{unitless}$ is a unitless value of parameter, X_i is a value of a parameter, $X_{max,meas}$ is a maximum value of the parameter.

The distributions of some parameters are shown in Figure 4.9.

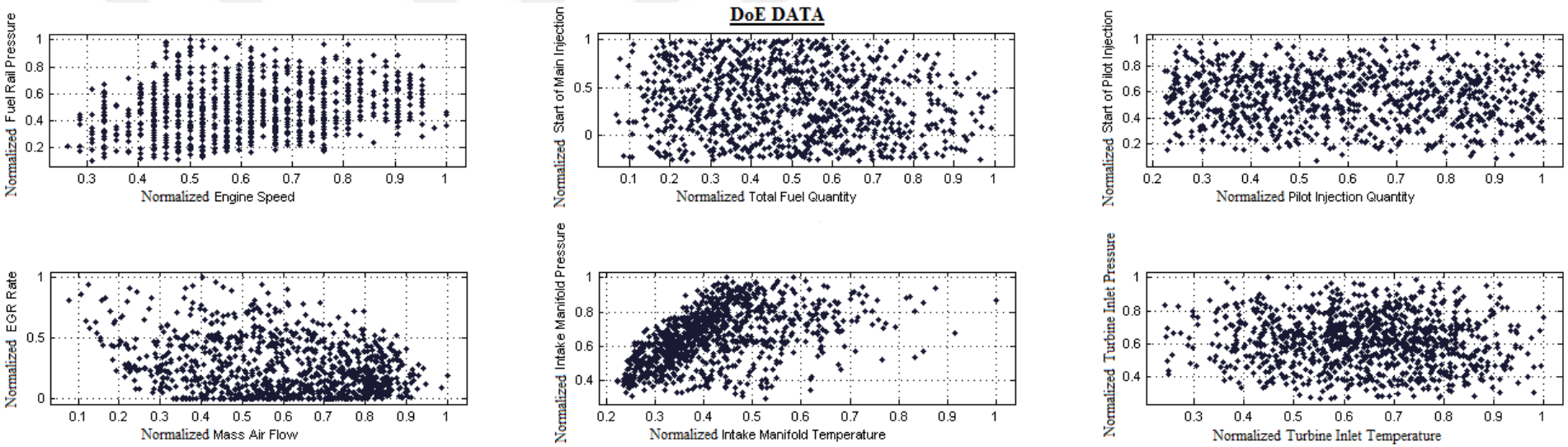

Figure 4.9: Distributions of some parameters obtained from DoE.

The parameters were converted to normalized values, and normalized values of the parameters are shown in all figures for this thesis.

5. 1D ENGINE MODELING

Today, many engineering problems are solved by advancing technology in computer science and computer aided simulation programs parallel to this. Accordingly, some tools are used to simulate an engine with order of the system. These tools are helpful to solve dynamics of pressure wave, mass flow and energy loss equations for pipes, big volumes, manifolds, etc. The tools use equations of 1D gas dynamics fundamentally. In addition, the equations of heat and flow transfer are solved for air induction systems, in-cylinder flow, exhaust systems, etc. For this thesis, one of these tools, GT Suite, was utilized.

Outstanding advantages of 1D engine modeling are listed below:

- Modeling of an engine by considering order of the system
- Providing more rapid solutions compared to 3D computational fluid dynamics.
- Reducing testing time of an engine in a dynamometer and its cost
- Clarification of effects of many parameters on engine performance

Due to the reasons above, 1D engine modeling tools are commonly used by many automotive manufacturers. Especially, in early development phases of an engine, the tools explain the effects of different parameters in system order of the engine.

Usage areas of 1D engine modeling are basically listed below:

- Engine performance analysis
- Design of intake and exhaust manifolds
- Studies on valve timing and valve control
- Fuel consumption analysis
- Analyses regarding EGR
- Acoustic analyses
- Combustion and emission analyses

- Thermal analyses
- Development of dynamic system control

5.1 The Theory of 1D Engine Modeling

It is accepted for 1D engine models that axial velocity of fluids at cross sectional areas is greater than other directions. For this reason, governing equations used for 3D computational fluid dynamics are reduced to one dimension.

The flow model contains the solution of continuity, momentum and energy equations also known as Navier-Stokes equations. These equations are solved in one dimension by using averaged quantities across the flow direction. Two integration methods affecting solution variables and limits on time steps are available. The time integration methods consist of an implicit and an explicit integrator. The main solution variables are mass flow, pressure and total enthalpy for the implicit method whereas mass flow, density and internal energy for the explicit method. In this thesis, explicit method was used to solve the equations of the 1D engine model. Details of the explicit method are explained below.

The entire system is discretized into volumes, which are collected by boundaries. Each split-flow is represented by a single volume, and every pipe is divided into one or more volumes. This type of discretization is named staggered grid method. The vector variables such as mass flux, velocity, mass fraction fluxes, etc. are calculated for each boundary. The scalar variables such as temperature, pressure, internal energy, etc. are accepted to be uniform over each volume (Figure 5.1).

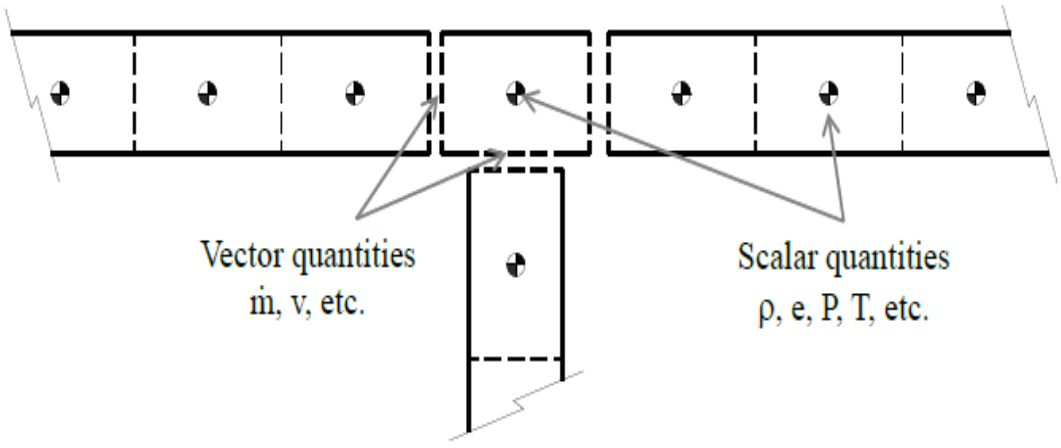

Figure 5.1: Schematic of staggered grid approach [40].

The conservation equations solved by GT Suite are shown below. The left hand side represents the derivatives of the primary variables.

$$Continuity: \frac{dm}{dt} = \sum_{boundaries} \dot{m} \tag{5.1}$$

$$Energy: \frac{d(me)}{dt} = -p\frac{dV}{dt} + \sum_{boundaries} (\dot{m}H) - hA_s(T_{fluid} - T_{wall}) \tag{5.2}$$

$$Momentum: \frac{dm}{dt} = \frac{dpA + \sum_{boundaries}(\dot{m}u - 4C_f \frac{\rho u|u|}{2}\frac{dxA}{D} - K_p\left(\frac{1}{2}\rho u|u|\right)A}{dx} \tag{5.3}$$

where ṁ is boundary mass flux into volume which defined with $\dot{m} = \rho Au$. m is mass of the volume; V, volume; P, pressure; ρ, density; A, cross-sectional flow area; A_s, heat transfer surface area; e, total specific internal energy; H, total specific enthalpy which is explained with $H = e + p/\rho$; h, heat transfer coefficient; T_{fluid}, fluid temperature; T_{wall}, wall temperature; u, velocity at the boundary; C_f, fanning friction factor; K_p, pressure loss coefficient; D, equivalent diameter; d_x, length of mass element in the flow direction (discretization length) ; d_p, pressure differential acting cross d_x, respectively.

The mass conservation equation states that mass flow rates in and out are equal to rate of velocity change at boundaries. The energy conservation equation means that energy change rate is equal to sum of energy in, energy out, work done and heat released. Also, the momentum conservation equation states that total momentum change is equal to sum of pressure forces and wall shear stress applied to a subsystem.

As mentioned above, the primary solution variables in the explicit method are mass flow rate, density, and internal energy. The values of mass flow, density and internal energy at the new time are calculated based on the conservation equations. In the explicit method, the right-hand side of the equations is calculated using values from the previous time step. This yields the derivative of the primary variables and allows the value at the new time to be calculated by integration of that derivative over the time step.

The time step used for calculations is restricted to satisfy the Courant condition. For consistent results, the right-hand side of equation 5.4 must be lower than 1. The Courant condition is formulated as below:

$$\text{Courant Condition} \geq \frac{\Delta t}{\Delta x}(|u| + c) \tag{5.4}$$

where Δt is time step, Δx is length specified for discretization, u is fluid velocity, c is speed of sound.

At each time step, the pressure and temperature are calculated in the following way:

I. Continuity and energy equations yield the mass and energy in the volume.

II. With the volume and mass known, the density is calculated yielding density and energy

III. The equations of state for each species define density and energy as a function of pressure and temperature. The solver will iterate on pressure and temperature until they satisfy the density and energy already calculated for this time step.

5.2 1D Model of the Heavy-Duty Engine

The heavy-duty engine developed by Ford Otosan was modeled in one dimension with GT Suite. The model consists of three parts: air induction system, exhaust system and base engine. For the model design, model geometry representing real engine geometry was used. Also, it is assumed that all the components have their own thermal and material properties.

Pressure drop of the air induction system measured in the dynamometer was correlated by changing a diameter of an orifice in air induction system of the model. For boost pressure control, there is a PID controller, and boost pressure was controlled by changing blade angle of the turbocharger. The temperature values of charge air cooler were directly implemented into the model, and its heat transfer multiplier was set to too high value to obtain the values. GT Suite composes pressure profile of combustion based on in-cylinder pressure data measured in a dynamometer. The data was imported into the tool, and heat release rates were calculated backwardly. Also, injection timing was controlled to correlate maximum in-cylinder pressures against dyno data. The EGR position was controlled based on the amount of air entering the engine. It changes according to mass air flow setpoints. Total injection quantities were directly implemented into the model. EGR cooler temperatures are also implemented into the

model, in the meantime, heat transfer multiplier of the EGR cooler was set to too high value to obtain the values. There is also a PID controller for exhaust system, and a pipe diameter of the exhaust system was changed for each step to correlate turbine outlet pressures. Thus, it provides that a compressor works at correct pressure and shaft speed. 1D model of the heavy duty engine is shown in Figure 5.2.

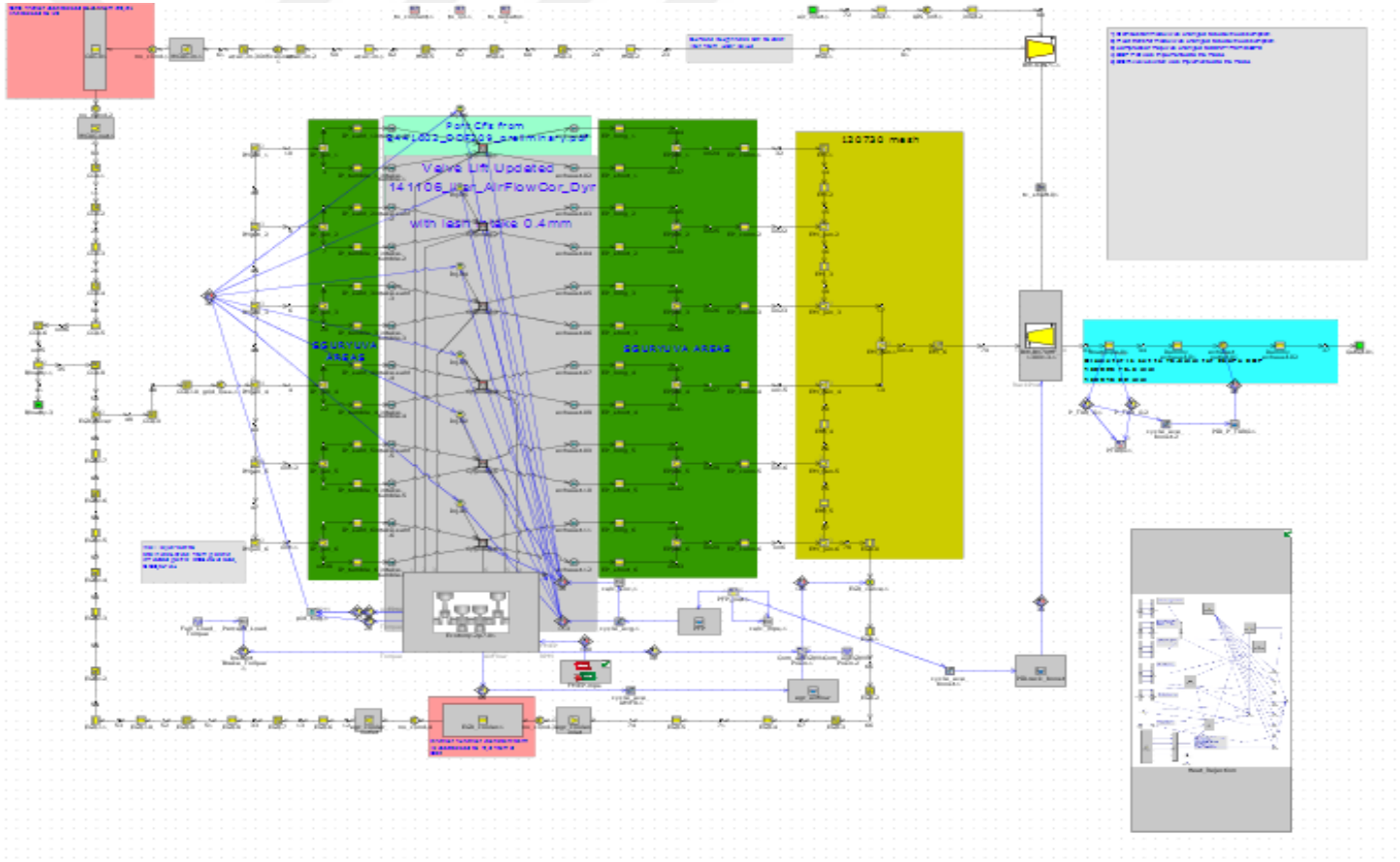

Figure 5.2: 1D model of the heavy-duty engine.

The details of calibration process of air induction system, exhaust system, and base engine are not explained comprehensively in this thesis as it' s not the scope of the thesis. More details can be found in user guide of GT Suite [40].

5.3 Application Results

For model calibration, 186 points including part and full load conditions were selected from the current engine calibration. The points are determined by sweeping engine speed range at 100 rpm steps and torque range at 100 and 200 Nm. Moreover, R^2 values are used to identify quality of the 1D engine model.

R^2 is a relative measure for evaluating the model error-it indicates which portion of the total variance of the measuring data is described by the model. The coefficient of determination R^2 is derived from the comparison of the variance that remains after the model training (SSR) with the variance concerning the mean value of all measuring data (SST).

$$R^2 = 1 - \frac{SSR}{SST} \tag{5.5}$$

Regression sum of squares (SSR) is calculated by given equation below.

$$\mathrm{SSR} = \sum_{\mathrm{i}=1}^{\mathrm{n}} \left(\mathrm{X_{i,pred}} - \mathrm{X_{i,meas}}\right)^2 \tag{5.6}$$

Calculation of total sum of squares (SST) is calculated is shown at equation 5.7.

$$SST = \sum_{i=1}^{n} \left(X_{i,meas} - \overline{X}_{meas}\right)^2 \tag{5.7}$$

Correlation results of the 1D engine model with measured data can be seen in Table 5.1. Also, point to point comparisons of parameters is shown in Figure 5.3.

Table 5.1: Correlation of the model with measured data.

Parameter	**TQ**	**MAF**	**MCP**	**TFQ**	**IMT**	**IMP**	**TIT**	**TIP**
R^2 Value	99.9%	99.6%	100%	100%	93.5%	100%	99.6%	98.6%

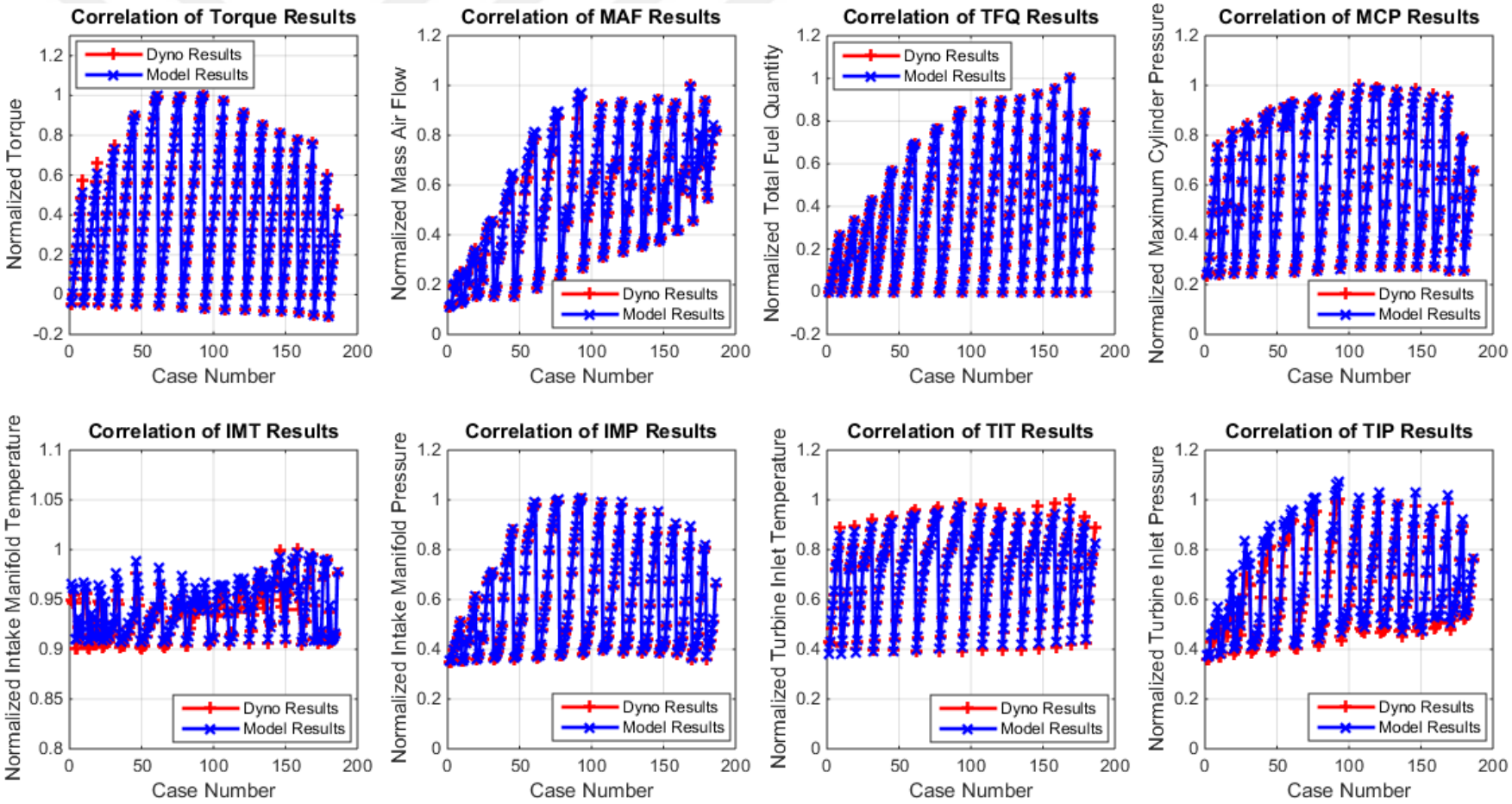

Figure 5.3: Correlation between 1D engine model and mesaured data.

6. MODELING APPROACH FOR NOx AND SOOT EMISSIONS

Advantages of Gaussian Process Regression method are told in section 3.3. There are some industrial tools solving the equations and creating models in industry. ASCMO by ETAS is a mathematical modeling tool which uses Gaussian Process Regression method. For this thesis, ASCMO tool is used to create mathematical model of soot and NOx emissions. Output behaviors of the engine system are modeled based on measured data by using Gaussian Process Regression method (Figure 6.1).

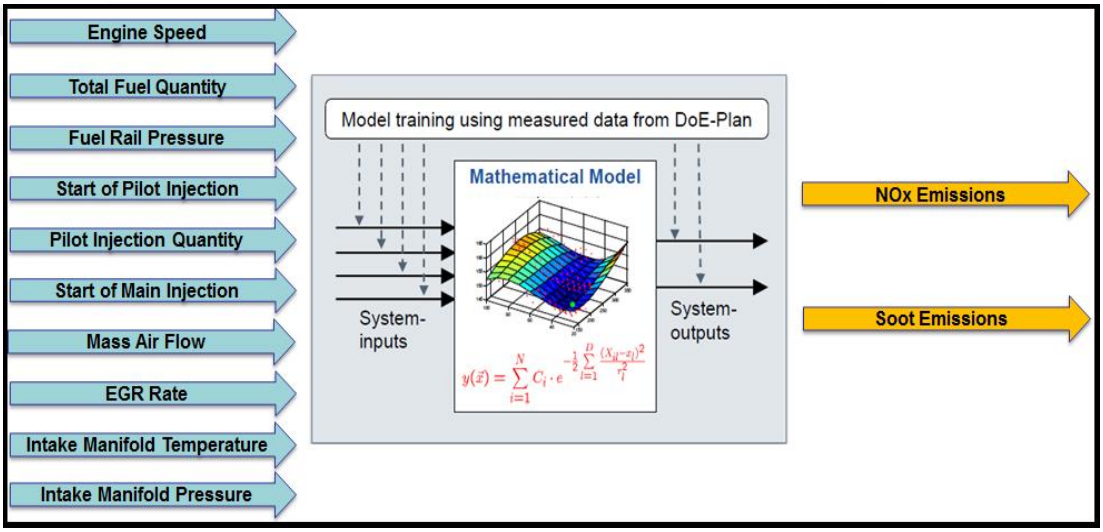

Figure 6.1: Schematic presentation of the model training

R-squared is a statistical measure of how close the data are to the fitted regression line. It is also known as the coefficient of determination, or the coefficient of multiple determination for multiple regression. R-squared values are considered to define steady-state modeling quality. R^2 measure results in the following evaluations [40]:

- $0< R^2<0.5$ The model is not appropriate for predictions
- $0.6< R^2<0.8$ The model is appropriate for predictions
- $0.9< R^2<1.0$ The model is well-defined and hence suitable for quantitative predictions

6.1 Steady State Conditions

In section 4.4, it is told that results of 1000 measurement points were obtained from engine dynamometer. These results explain the steady state behavior of the engine system as input parameters are constant during measurements. Thus, the results of mathematical models created for this section can be compared with measured output data.

10% of measurement points are selected to validate a model and prevent curve fitting errors. The distributions of soot and NOx emissions for model and validation data are shown in Figure 6.2.

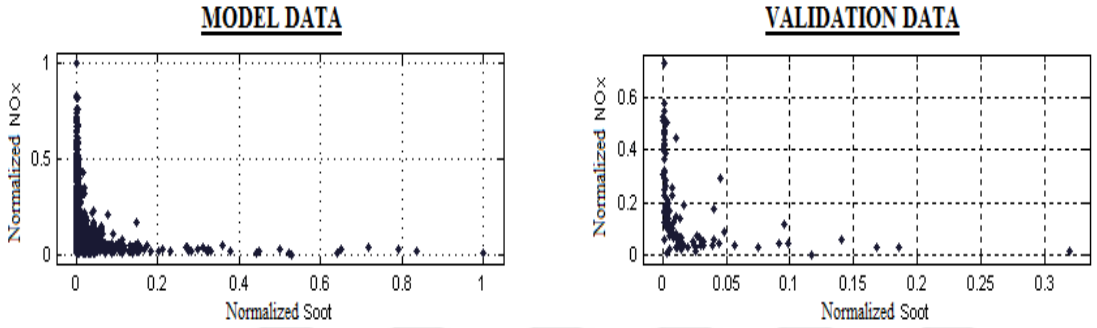

Figure 6.2: The distributions of soot and NOx emissions for model and validation data.

The distribution of model and validation data can be seen in Figure 6.3 and Figure 6.4.

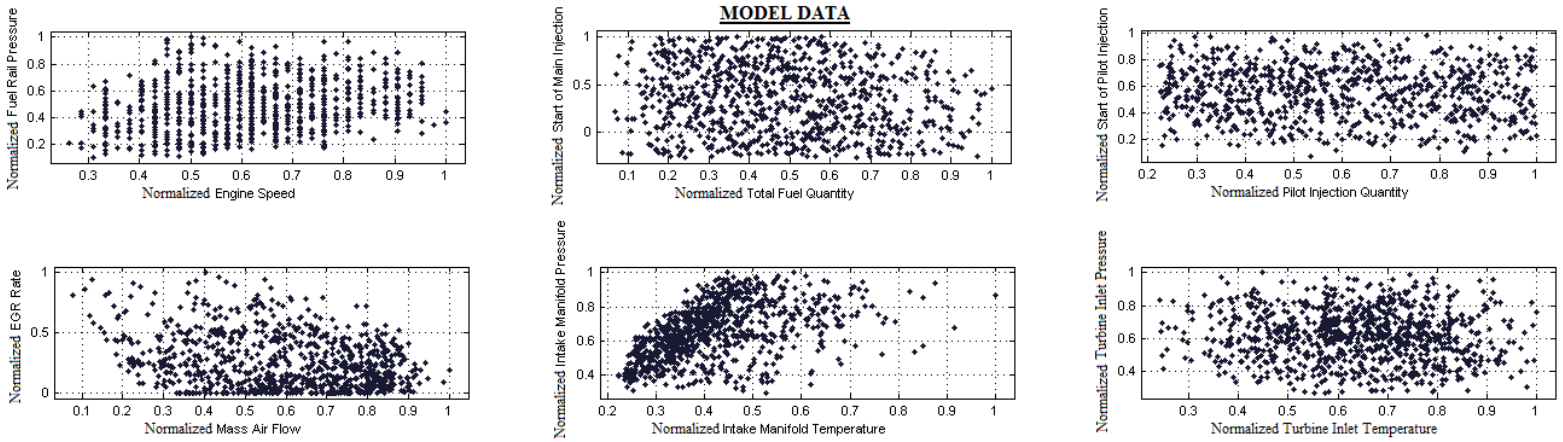

Figure 6.3: Model data after data selection

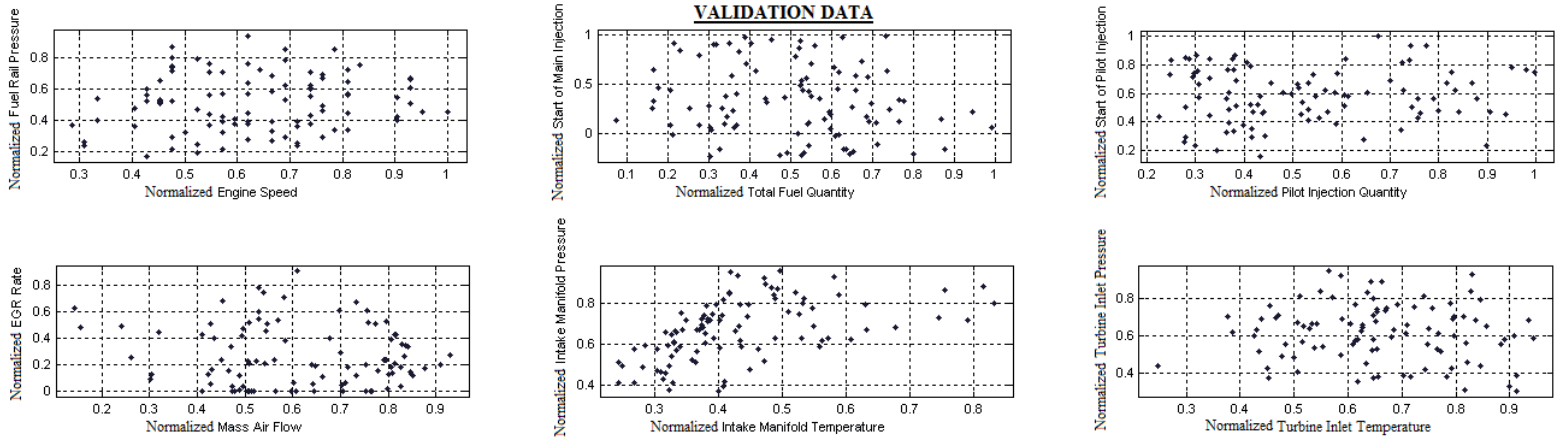

Figure 6.4: Validation data after data selection.

6.1.1 Optimization of combustion input parameters for emission modeling

Some input parameters, which affect combustion characteristics, are directly or indirectly controlled by ECU of the engine. Due to dependency of emissions and combustion, it also means that soot and NOx emissions can be controlled and minimized by selecting optimum operation points of the engine.

In this section, only combustion input parameters were used to predict soot and NOx emissions. It was also aimed to observe the effects of these parameters on NOx and soot emissions. The combustion input parameters used for models are listed below:

- Engine speed
- Fuel rail pressure
- Total fuel quantity
- Start of main injection
- Pilot quantity
- Start of pilot injection
- Mass air flow
- EGR rate
- Intake manifold temperature
- Intake manifold pressure

Full factorial input sets were used to find a model which gives sufficient results: R^2 of 80% for soot prediction and R^2 of 90% for NOx prediction. Models that have 10, 9, 8, 7 input parameters respectively were created and investigated by considering soot and NOx predictions. Totally, 176 models were created for this section.

$$\binom{10}{10} + \binom{10}{9} + \binom{10}{8} + \binom{10}{7} = 176 \tag{6.1}$$

Then, the results were analyzed and models that have less than R^2 of 80% for soot prediction and R^2 of 90% for NOx prediction were filtered out. The highest results obtained from the models are shown in Table 6.1. Also, all results can be seen in Appendix A.

Table 6.1: Highest results obtained from the models (1st step).

Model No	No of Param.	ES	RFP	TFQ	SOMI	PIQ	SOPI	MAF	EGR Rate	IMT	IMP	R2 of Soot Model Data	R2 of Soot Valid. Data	R2 of NOx Model Data	R2 of NOx Valid. Data
1	10	+	+	+	+	+	+	+	+	+	+	87.37%	75.33%	98.91%	95.78%
4	9	+	+	+	+	+	+	+	-	+	+	83.00%	81.40%	98.62%	94.93%
31	8	+	+	+	+	-	+	+	-	+	+	82.89%	87.54%	98.79%	94.56%
35	8	-	+	+	+	+	+	+	-	+	+	82.94%	84.91%	91.56%	93.28%
135	7	-	+	+	+	-	+	+	-	+	+	83.66%	84.87%	91.42%	93.21%

1st model has the highest R^2 value with soot model data but it also has lower than R^2 value of 80% with soot validation data. Measurement errors of dependent parameters can be shown as possible root cause of this problem. On the other hand, 35th and 135th models show almost same results in terms of soot and NOx predictions, however, removal of engine speed parameter from the models results in decrease of NOx prediction capability. Accordingly, these parameters were also filtered out, and 31st model was selected as the best model since it uses less parameters than 4th model. The results of 31st model can be seen in Figure 6.5.

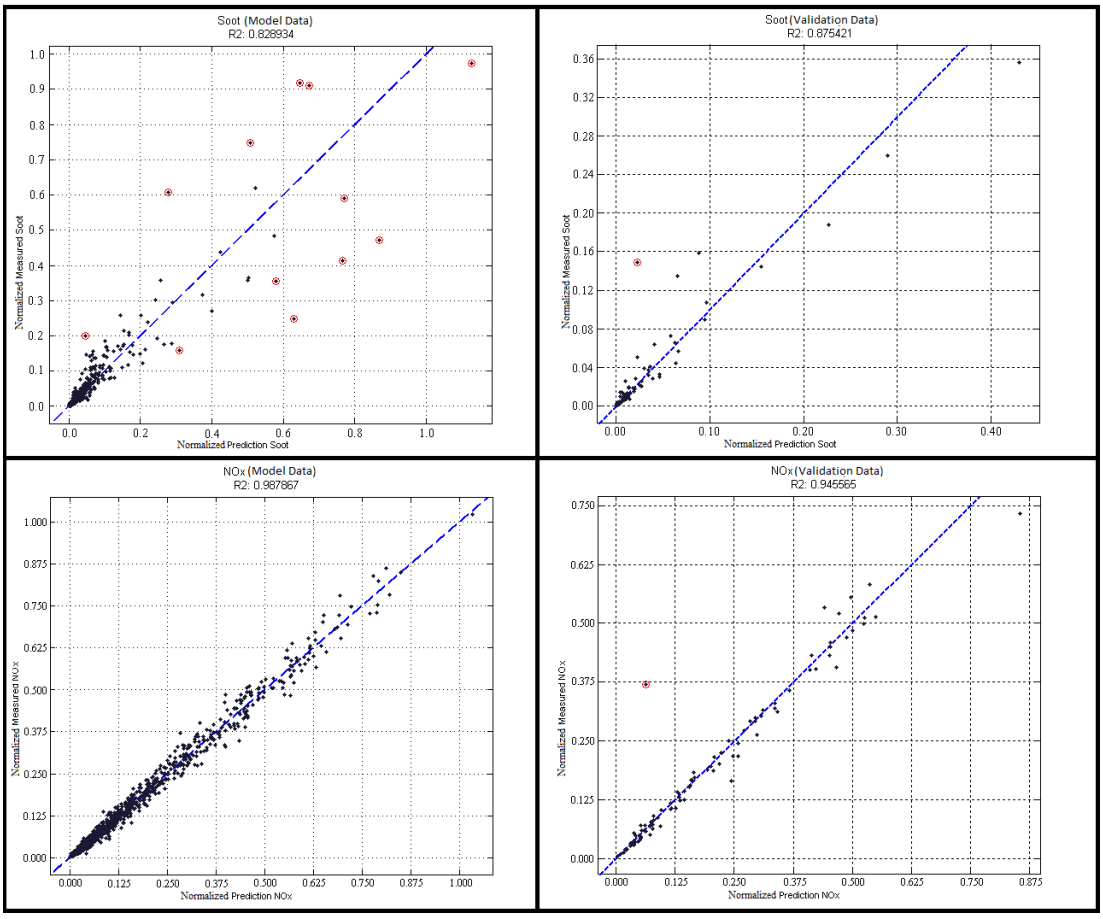

Figure 6.5: Soot and NOx results of 31st model.

It can be concluded that soot and NOx emissions can be modeled mathematically with 8 parameters and low error rates. It was also observed that the high soot emissions can not be predicted well, and higher errors were obtained for higher soot values.

EGR rate and pilot injection quantity were investigated separately to explain why these parameters are not affective for emission predictions.

- EGR rate

Volumetric efficiency is required to calculate total flow into the engine (i.e. egr and fresh air). The efficiency mentioned here is the ratio of air mass in the cylinder to the ideal gas mass when cylinder is filled with gas at intake manifold pressure and temperature. Volumetric Efficiency is used for EGR flow predictions and determining possible maximum flow quantities. The formula is given;

$$\lambda_a = \frac{\dot{m}_{L,actual}}{\dot{m}_{L,theoretical}} \tag{6.2}$$

where $\dot{m}_{L,actual}$ is actual air mass flow into the engine (HFM), and $\dot{m}_{L,theoretical}$ is theoretically possible air mass flow into the engine.

$$\dot{m}_{L,theoretical} = \frac{p_2 * V_H * N}{T_{21} * R_{air} * 2} \tag{6.3}$$

where p_2 is boost pressure in hPa; $V_H=V_{Eng}$ is engine displacement (l); N is engine speed (1/min); T_{21} is charge-air temperature in K; R_{air} is gas constant for air, and $m_{22}=m_{L,actual}$.

$$\lambda_a = 95.67 \frac{m_{22} * T_{21} + 273.15}{n * V_{Eng} * p_2} \tag{6.4}$$

where 95.67 is a calculated constant from 2. R_{air} and transforming the units (l), (1/min), (J) and (hPa) into comparable units.

Then, EGR rate is calculated by using given equation below:

$$EGR\ Rate = \frac{Total\ Air\ Flow - Mass\ Air\ Flow}{Total\ Air\ Flow} \tag{6.5}$$

The equations show that EGR rate is a function of intake manifold temperature, intake manifold pressure, mass air flow and engine speed. Thus, this parameter is not a independent variable, and other parameters include this term inside.

- Pilot Injection Quantity

All test points include pilot injection as the engine always operates with pilot injection due to NVH problems. Thus, effect of pilot injection quantity couldn't be seen clearly.

Pilot injection precision is around 2 mg for the injectors. Effect of pilot quantity on total quantity measurement is shown in Figure 6.6.

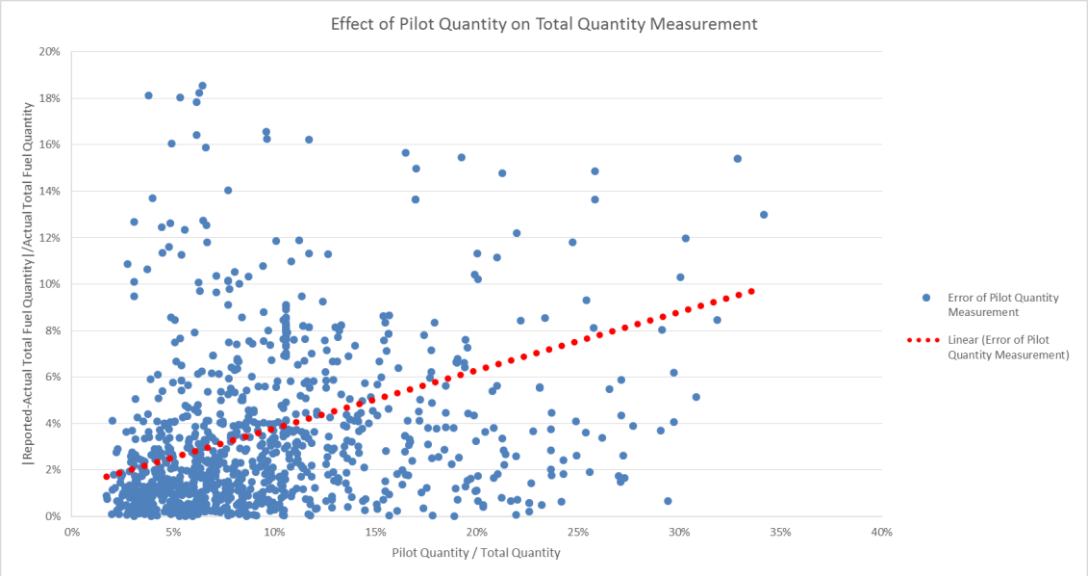

Figure 6.6: Effect of pilot quantity on total quantity measurement.

It's observed that total injection error increases with increasing pilot / total quantity ratio. This situation causes to see no effect of pilot injection quantity on soot and NOx emissions.

6.1.2 Modeling improvement with combustion output parameters

In this section, it is aimed to increase soot model accuracy by adding combustion output parameters that can be measured on dynamometer since NOx model already has high accuracy. The combustion output parameters used for the models are listed below:

- Turbine inlet temperature
- Turbine inlet pressure
- Maximum cylinder pressure

Parameters of the model, which was obtained in previous section, were kept constant. These parameters are listed below:

- Engine speed
- Fuel rail pressure
- Total fuel quantity
- Start of main injection
- Start of pilot injection
- Mass air flow
- Intake manifold temperature

- Intake manifold pressure

The combustion output parameters were added into these parameters as variables. Models that have 9, 10, 11 input parameters respectively were created and investigated by considering soot and NOx predictions. The results obtained from the models are shown in Table 6.2.

Table 6.2: All results obtained from the models (2nd step).

Model No	No of Param.	ES	RFP	TFQ	SOMI	SOPI	MAF	IMT	IMP	TIT	TIP	MCP	R2 of Soot Model Data	R2 of Soot Valid. Data	R2 of NOx Model Data	R2 of NOx Valid. Data
1	8	+	+	+	+	+	+	+	+	-	-	-	82.89%	87.54%	98.79%	94.56%
2	9	+	+	+	+	+	+	+	+	+	-	-	93.40%	77.35%	98.26%	95.13%
3	9	+	+	+	+	+	+	+	+	-	+	-	76.55%	87.17%	98.18%	95.20%
4	9	+	+	+	+	+	+	+	+	-	-	+	84.44%	86.07%	98.60%	95.00%
5	10	+	+	+	+	+	+	+	+	+	+	-	92.99%	80.11%	98.23%	95.11%
6	10	+	+	+	+	+	+	+	+	+	-	+	91.74%	76.89%	98.68%	95.14%
7	10	+	+	+	+	+	+	+	+	-	+	+	83.78%	89.65%	98.62%	95.05%
8	11	+	+	+	+	+	+	+	+	+	+	+	91.80%	78.20%	98.74%	95.21%

In addition to reference model coming from previous section, 7 more models were built and checked in terms of soot and NOx predictions. Effects of three combustion output parameters were analyzed. It is observed that only turbine inlet temperature affects soot and NOx modeling predictions. Also, effects of turbine inlet temperature on soot and NOx emissions can be obviously seen when the measurement results are checked linearly.

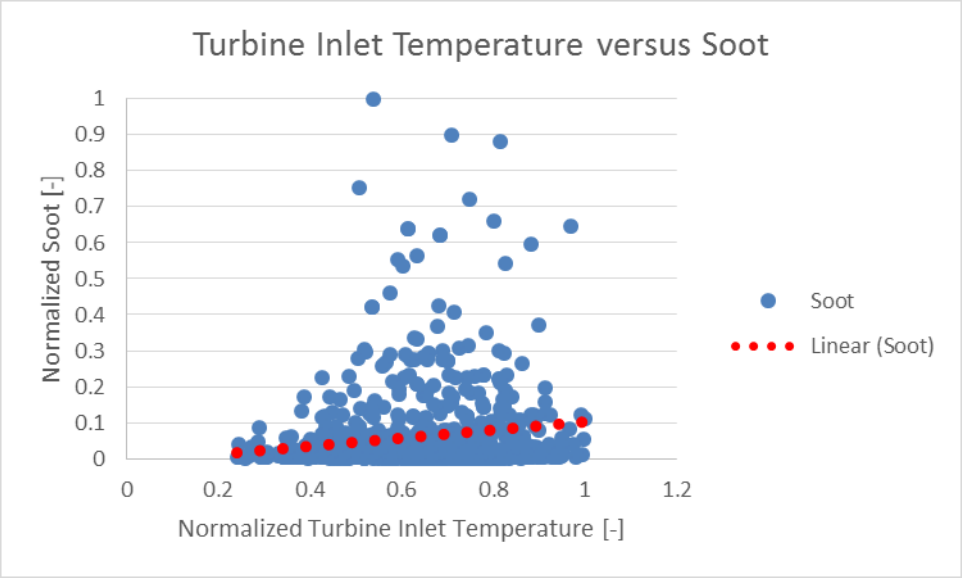

Figure 6.7: The effect of turbine inlet temperature on soot emissions.

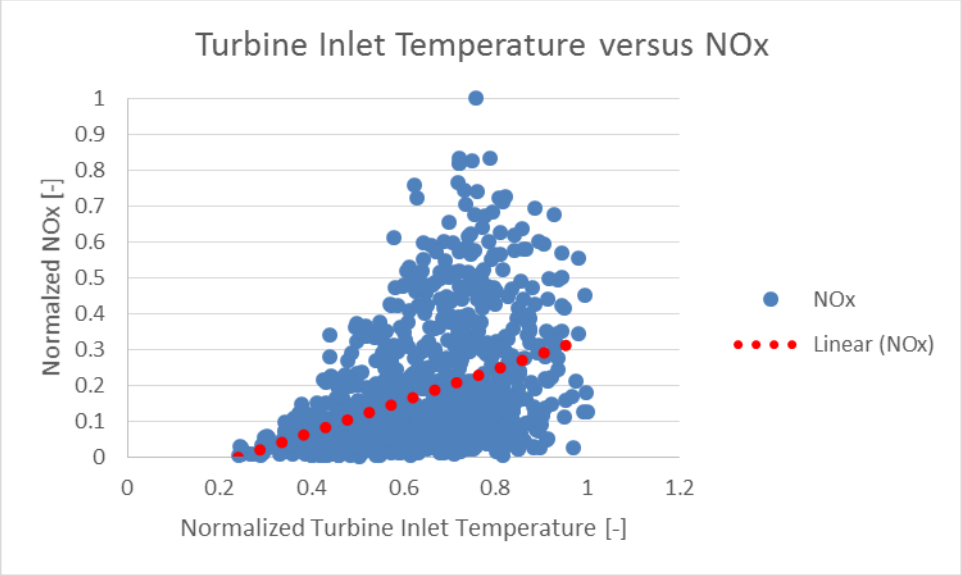

Figure 6.8: The effect of turbine inlet pressure on NOx emissions.

Turbine inlet temperature and turbine inlet pressure are fundamentally coupled parameters, but the effect of turbine inlet pressure on emission prediction cannot be observed.

6.1.3 Effects of parameters by 1D engine modeling

In this section, it's aimed to observe effects of other combustion parameters on soot and NOx predictions. These parameters can not be measured on a dynamometer, and 1D engine model (GT Suite) were used to obtain values of the parameters. Parameters of the model, which was obtained in section 6.1.1, were kept constant The parameters are listed below:

- Engine speed
- Fuel rail pressure
- Total fuel quantity
- Start of main injection
- Start of pilot injection
- Mass air flow
- Intake manifold temperature
- Intake manifold pressure

The combustion output parameters and other parameters by 1D engine modeling were added into these parameters as variables. The parameters are listed below:

- Turbine inlet pressure
- Turbine inlet temperature
- Maximum cylinder pressure
- Maximum cylinder temperature
- Burn duration 0-50%

Burn duration 0-50% is duration in crank angle degrees from the 0% burned point to the 50% burned point, taking into account the total fuel in the cylinder.

- Burn duration 10-90%

Burn duration 10-90% is duration in crank angle degrees from the 10% burned point to the 90% burned point, taking into account the total fuel in the cylinder.

- Burn duration 0-90%

Burn duration 0-90% is duration in crank angle degrees from the 0% burned point to the 90% burned point, taking into account the total fuel in the cylinder.

Models that have 9, 10, 11, 12, 13, 14, 15 input parameters respectively were created and investigated by considering soot and NOx predictions. The highest results obtained from the models are shown in Table 6.3. Also, all results can be seen in Appendix B.1.

Table 6.3: Highest results obtained from the models (3rd step).

Model No	No of Param.	ES	RFP	TFQ	SOMI	SOPI	MAF	IMT	IMP	TIT	TIP	BD 0-50%	BD 10-90%	BD 0-90%	MCP	MCT	R2 of Soot Model Data	R2 of Soot Valid. Data	R2 of NOx Model Data	R2 of NOx Valid. Data
37	11	+	+	+	+	+	+	+	+	+	-	+	-	-	+	-	91.61%	81.57%	98.23%	95.12%
42	11	+	+	+	+	+	+	+	+	+	-	-	-	+	+	-	91.42%	81.33%	98.77%	95.19%
83	12	+	+	+	+	+	+	+	+	+	-	-	+	+	+	-	91.54%	82.94%	98.75%	95.18%
86	12	+	+	+	+	+	+	+	+	+	-	+	-	+	+	-	91.65%	81.73%	98.74%	95.17%
88	12	+	+	+	+	+	+	+	+	+	-	+	+	-	+	-	91.46%	82.77%	98.75%	95.10%
110	13	+	+	+	+	+	+	+	+	+	-	+	+	+	+	-	91.55%	81.98%	98.76%	95.14%
114	13	+	+	+	+	+	+	+	+	+	+	-	+	+	+	-	91.34%	82.03%	98.73%	95.11%
117	13	+	+	+	+	+	+	+	+	+	+	+	-	+	+	-	91.81%	82.29%	98.70%	95.17%
119	13	+	+	+	+	+	+	+	+	+	+	+	+	-	+	-	91.73%	82.24%	98.74%	95.17%
127	14	+	+	+	+	+	+	+	+	+	+	+	+	+	+	-	91.84%	83.21%	98.73%	95.17%

The results show that models which have high R^2 values both for soot and NOx predictions include commonly turbine inlet temperature and maximum cylinder pressure variables. However, only maximum cylinder pressure is not enough to improve validation results of the model and another combustion parameter must be involved to obtain higher accuracy. In addition, effects of other combustion parameters could not be observed clearly. Almost same results were obtained by using only turbine inlet temperature in section 6.1.2.

Effects of maximum cylinder pressure on soot and NOx emissions can be obviously seen when the measurement results are checked linearly. Soot emission decreases with increasing maximum cylinder pressure whereas NOx emission increases with increasing maximum cylinder pressure.

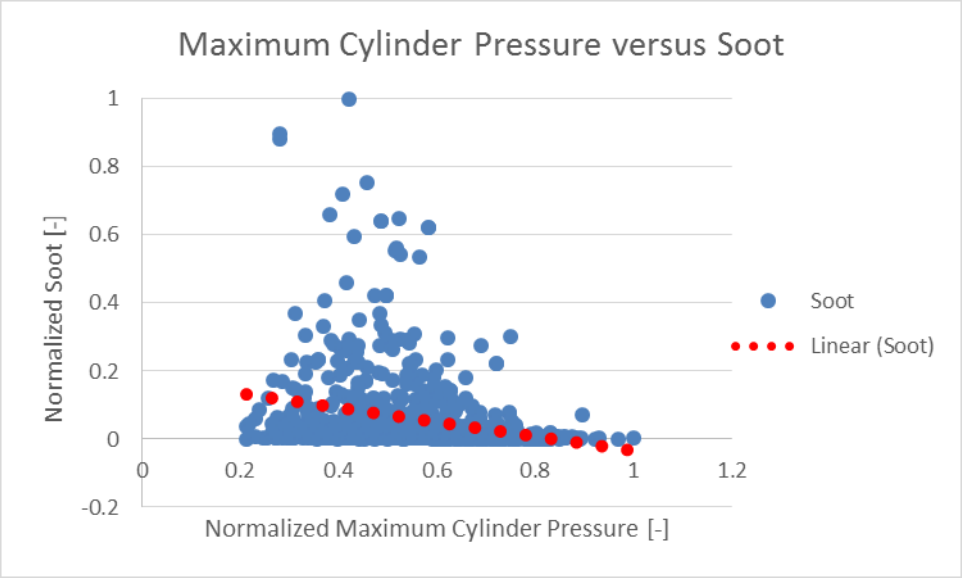

Figure 6.9: The effect of maximum cylinder pressure on soot emissions.

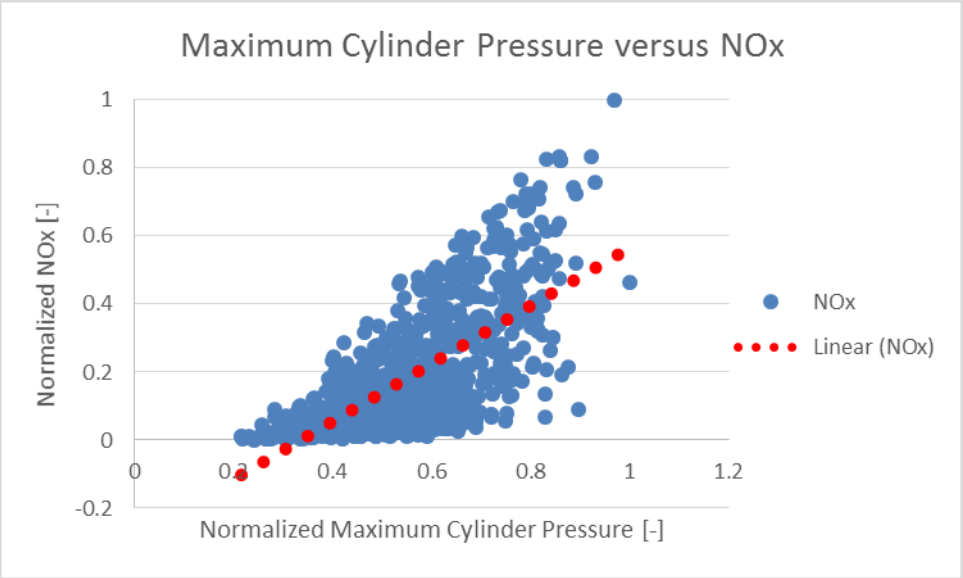

Figure 6.10: The effect of maximum cylinder pressure on NOx emissions.

6.1.4 Coupled mathematical model with 1D engine model

1D engine modeling tools are more commonly used than other engine simulation programs in the automotive industry due to providing fast and practical solutions. These tools help engineers to specify hardware limits and performance metrics and make component selections in early stages of engine design. A significant shortcoming of these tools is that the tools are not good enough to provide solutions about emissions modeling as models are run in one dimension. For this reason, it' s aimed to model emissions mathematically by using only outputs of the 1D engine model and to show its feasibility. Thus, optimum design of an engine may be obtained by using a coupled model of 1D engine model with a mathematical emission model. All DoE points were implemented into the model separately run in GT Suite, and its results are exported. Mathematical models were built by using ASCMO tool, in which the results are imported.

Combustion is modeled in GT Suite via maximum cylinder pressure and heat release rate. For this reason, fuel rail pressure, start of main injection and start of pilot injection parameters cannot be obtained from 1D engine model. Start of injection parameter was used instead of injection parameters. However, there is no parameter, which can be replaceable for fuel rail pressure. The constant parameters are listed below:

- Engine speed

- Total fuel quantity
- Start of injection
- Mass air flow
- Intake manifold temperature
- Intake manifold pressure

The combustion output parameters by 1D engine modeling were added into these parameters as variables. The parameters are listed below:

- Turbine inlet pressure
- Turbine inlet temperature
- Maximum cylinder pressure
- Maximum cylinder temperature
- Burn duration 0-50%
- Burn duration 10-90%
- Burn duration 0-90%

Models that have 6, 7, 8, 9, 10, 11, 12, 13 input parameters respectively were created and investigated by considering soot and NOx predictions. The highest results obtained from the models are shown in Table 6.4. Also, all results can be seen in Appendix C.1.

Table 6.4: Highest results obtained from the models (4th step)

Model No	No of Param.	ES	TFQ	MAF	IMP	IMT	SOI	TIT	TIP	BD 0-50%	BD 10-90%	BD 0-90%	MCP	MCT	R2 of Soot Model Data	R2 of Soot Valid. Data	R2 of NOx Model Data	R2 of NOx Valid. Data
33	9	+	+	+	+	+	+	+	+	-	-	-	+	-	49.98%	48.54%	87.65%	85.98%
40	9	+	+	+	+	+	+	+	-	-	+	-	+	-	49.32%	52.74%	87.47%	84.05%
41	9	+	+	+	+	+	+	+	-	-	+	-	-	+	49.73%	46.67%	88.40%	83.52%
42	9	+	+	+	+	+	+	+	-	-	-	+	+	-	49.22%	46.36%	87.65%	84.38%
81	10	+	+	+	+	+	+	+	-	-	+	-	+	+	49.65%	45.30%	88.30%	83.79%
82	10	+	+	+	+	+	+	+	-	-	+	+	-	+	49.91%	45.49%	88.35%	83.36%
83	10	+	+	+	+	+	+	+	-	-	+	+	+	-	51.17%	47.83%	87.65%	84.49%
87	10	+	+	+	+	+	+	+	-	+	+	-	-	+	49.11%	49.12%	88.33%	83.37%
92	10	+	+	+	+	+	+	+	+	-	-	+	+	-	49.02%	47.56%	87.78%	85.46%
94	10	+	+	+	+	+	+	+	+	-	+	-	+	-	49.24%	47.91%	87.45%	84.87%
99	10	+	+	+	+	+	+	+	+	+	+	-	-	-	49.06%	49.87%	87.38%	84.43%
110	11	+	+	+	+	+	+	+	-	+	+	+	+	-	49.27%	47.87%	87.37%	83.56%
119	11	+	+	+	+	+	+	+	+	+	+	-	+	-	49.35%	48.53%	87.02%	84.25%
126	12	+	+	+	+	+	+	+	+	+	+	+	-	+	49.30%	45.71%	88.11%	83.35%
127	12	+	+	+	+	+	+	+	+	+	+	+	+	-	49.10%	47.88%	87.47%	84.63%

Fuel rail pressure, start of pilot injection and pilot injection quantity are not input parameters for 1D engine model. Thus, it is not possible to model soot emissions without these parameters. Maximum R^2 of around 88% for NOx prediction and R^2 of around 50% for soot prediction could be obtained. These results show that effect of NOx may be assessed during design optimization but the same thing cannot be said for soot emissions, and further improvements are needed.

6.2 Transient Conditions

The results of steady state conditions are shared in previous sections. It was shown that soot and NOx emissions can be modeled mathematically with high accuracy for steady state conditions. Within next sections, the results of mathematical emissions models will be shared for transient conditions.

6.2.1 World harmonized transient cycle (WHTC)

The World Harmonized Transient Cycle test is a transient engine dynamometer schedule defined by European Union Regulations. WHTC testing requirements must be met by heavy duty engines, which have Euro VI emissions standards. The WHTC is a transient test lasting 1800 seconds. Normalized torque and engine speed values defined for WHTC cycle can be seen in Figure 6.11.

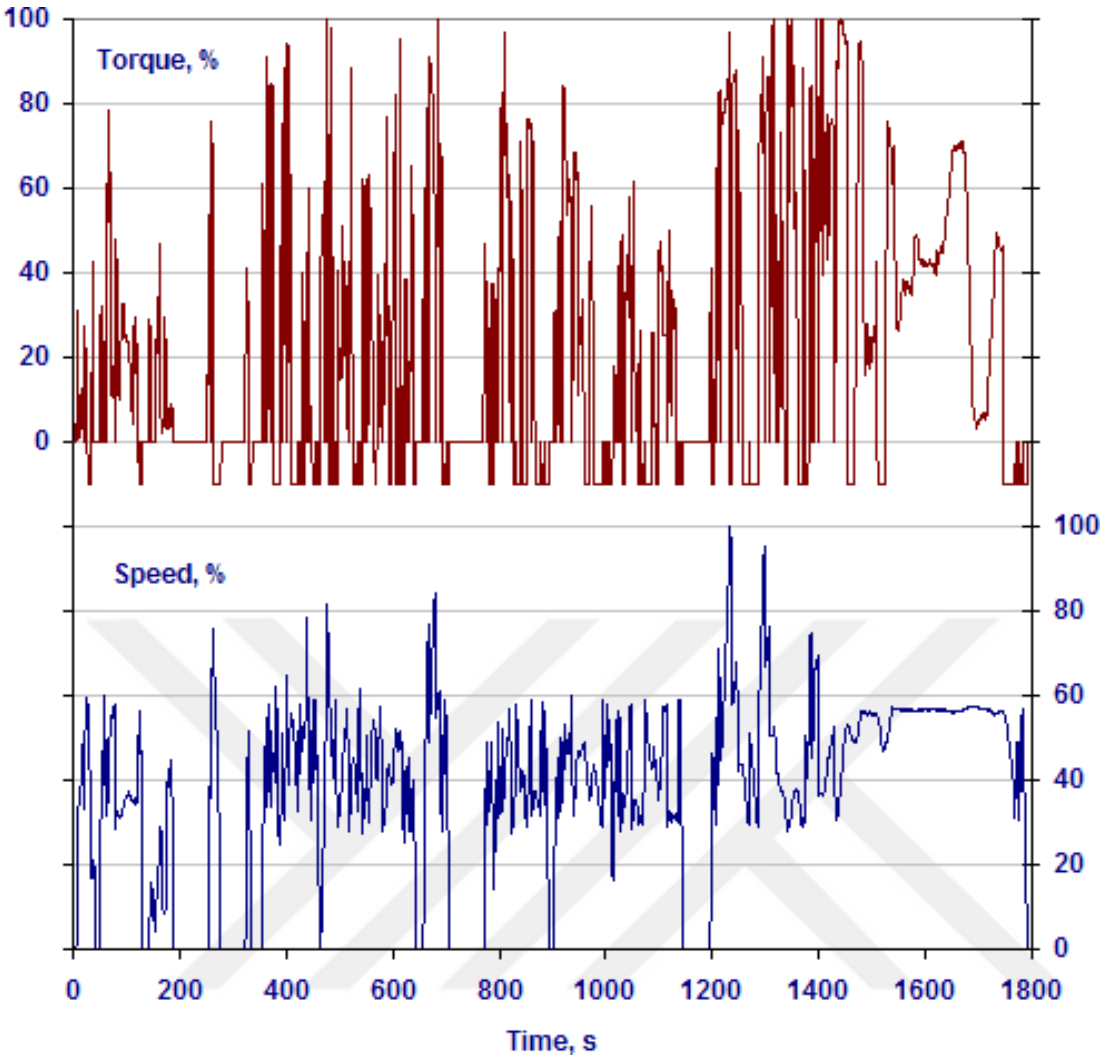

Figure 6.11: Speed and torque traces of the World Harmonized Transient Cycle [41].

6.2.2 Matlab models for the WHTC

The WTHC was used to evaluate the model quality for transient conditions. The engine was tested over the WHTC and all ECU signals were collected via INCA during the tests. Other temperature and pressure measurements, which can be measured on a dynamometer, were also taken. Soot and NOx emissions were measured second-by-second with AVL Microsoot and AMA i60 devices while running the tests. Then, all these measurements were converted into MATLAB format.

ASCMO tool also enables users to export a model in MATLAB and Simulink formats. The emission models in section 6.1.2 were exported, and one of the models is shown in Figure 6.12.

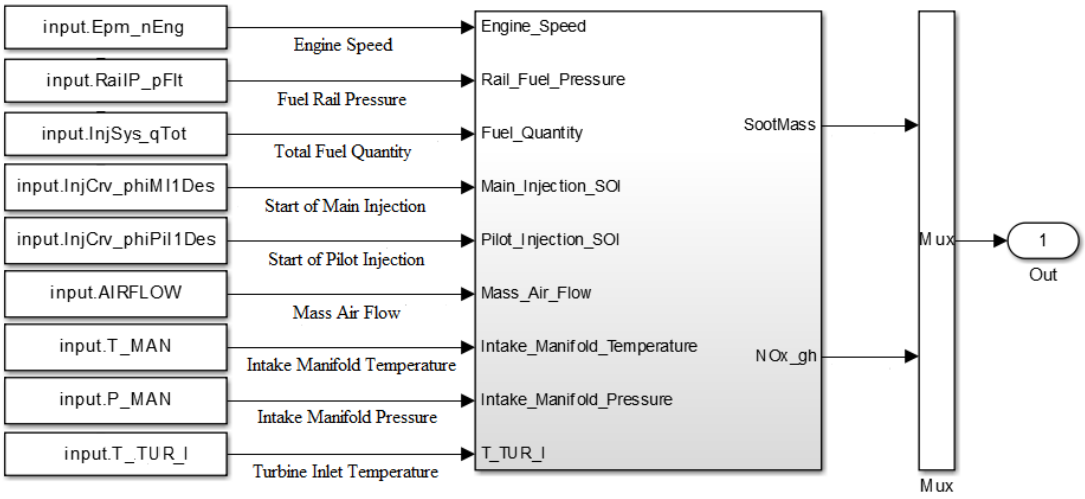

Figure 6.12: Simulink diagram of a mathematical emission model.

Eight models were totally exported with same way, and their simulations were run in Simulink. Results of the models were analyzed separately. The percentage error formulas were used to identify model quality during assessments. The formulas are given below.

$$NOx_{error} = 100 * \frac{|NOx_{max,pred} - NOx_{max,meas}|}{NOx_{max,meas}} \quad (6.6)$$

$$Soot_{error} = 100 * \frac{|Soot_{max,pred} - Soot_{max,meas}|}{Soot_{max,meas}} \quad (6.7)$$

where $NOx_{max,pred}$ is a predicted NOx value of a cumulative model result, $NOx_{max,meas}$ is a measured NOx value of a cumulative dyno result, $Soot_{max,pred}$ is a predicted soot value of a cumulative model result, $Soot_{max,meas}$ is a measured soot value of a cumulative dyno result.

6.2.2.1 Model 1

The 1st model consists of parameters listed below. Steady state results of the model are shown in section 6.1.2. Accordingly, R^2 value of soot model data is 82.89%, R^2 value of soot validation data 87.54%, R^2 value of NOx model data is 98.79%, and R^2 value of NOx validation data is 94.56%.

- Engine speed
- Rail fuel pressure

- Total fuel quantity
- Start of main injection
- Start of pilot injection
- Mass air flow
- Intake manifold temperature
- Intake manifold pressure

The model including the parameters listed above were run in MATLAB Simulink. Second by second and cumulative results were plotted both for soot and NOx emissions.

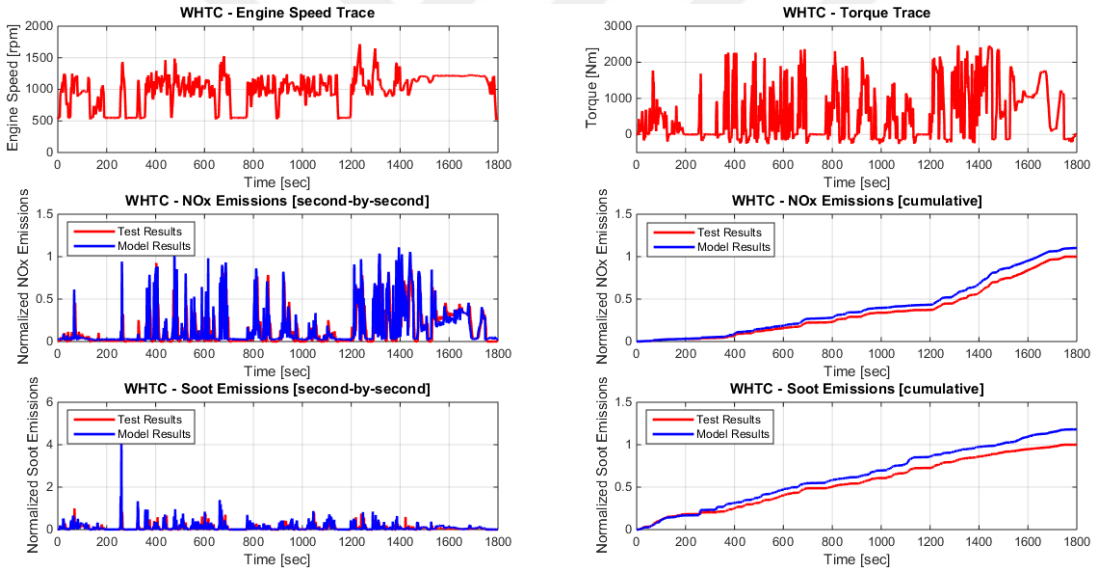

Figure 6.13: Transient cycle results of model 1.

Percentage error of cumulative results is calculated both for soot and NOx emissions by using equation 6.6 and 6.7. The percent error of NOx results is 10.28%, and the percent error of soot results is 18.13%.

6.2.2.2 Model 2

The 2nd model consists of parameters listed below. Steady state results of the model are shown in section 6.1.2. Accordingly, R^2 value of soot model data is 93.40%, R^2

value of soot validation data 77.35%, R^2 value of NOx model data is 98.26%, and R^2 value of NOx validation data is 95.13%.

- Engine speed
- Rail fuel pressure
- Total fuel quantity
- Start of main injection
- Start of pilot injection
- Mass air flow
- Intake manifold temperature
- Intake manifold pressure
- Turbine inlet temperature

The model including the parameters listed above were run in MATLAB Simulink. Second by second and cumulative results were plotted both for soot and NOx emissions.

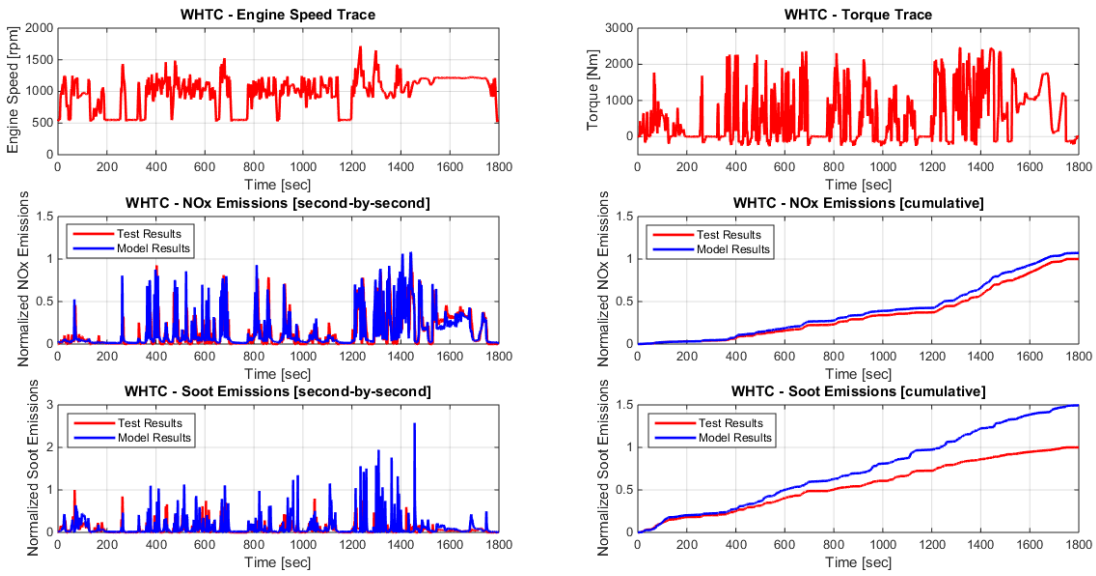

Figure 6.14: Transient cycle results of model 2.

Percentage error of cumulative results is calculated both for soot and NOx emissions by using equation 6.6 and 6.7. The percent error of NOx results is 7.13%, and the percent error of soot results is 49.54%.

6.2.2.3 Model 3

The 3rd model consists of parameters listed below. Steady state results of the model are shown in section 6.1.2. Accordingly, R^2 value of soot model data is 76.55%, R^2 value of soot validation data 87.17%, R^2 value of NOx model data is 98.18%, and R^2 value of NOx validation data is 95.20%.

- Engine speed
- Rail fuel pressure
- Total fuel quantity
- Start of main injection
- Start of pilot injection
- Mass air flow
- Intake manifold temperature
- Intake manifold pressure
- Turbine inlet pressure

The model including the parameters listed above were run in MATLAB Simulink. Second by second and cumulative results were plotted both for soot and NOx emissions.

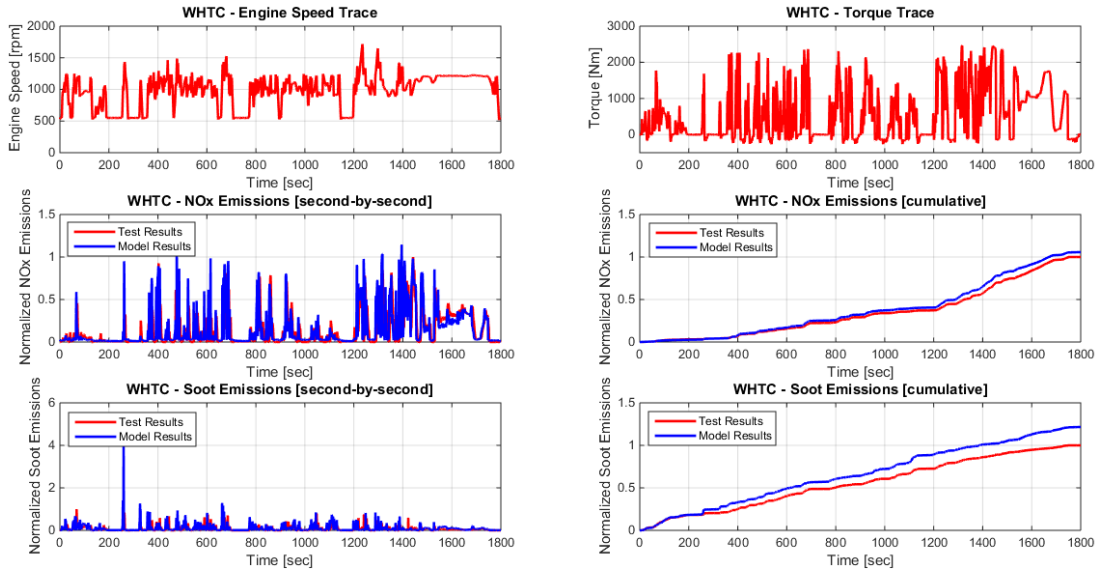

Figure 6.15: Transient cycle results of model 3.

Percentage error of cumulative results is calculated both for soot and NOx emissions by using equation 6.6 and 6.7. The percent error of NOx results is 5.73%, and the percent error of soot results is 21.62%.

6.2.2.4 Model 4

The 4th model consists of parameters listed below. Steady state results of the model are shown in section 6.1.2. Accordingly, R^2 value of soot model data is 84.44%, R^2 value of soot validation data 86.07%, R^2 value of NOx model data is 98.60%, and R^2 value of NOx validation data is 95.00%.

- Engine speed
- Rail fuel pressure
- Total fuel quantity
- Start of main injection
- Start of pilot injection
- Mass air flow
- Intake manifold temperature

- Intake manifold pressure
- Maximum cylinder pressure

The model including the parameters listed above were run in MATLAB Simulink. Second by second and cumulative results were plotted both for soot and NOx emissions.

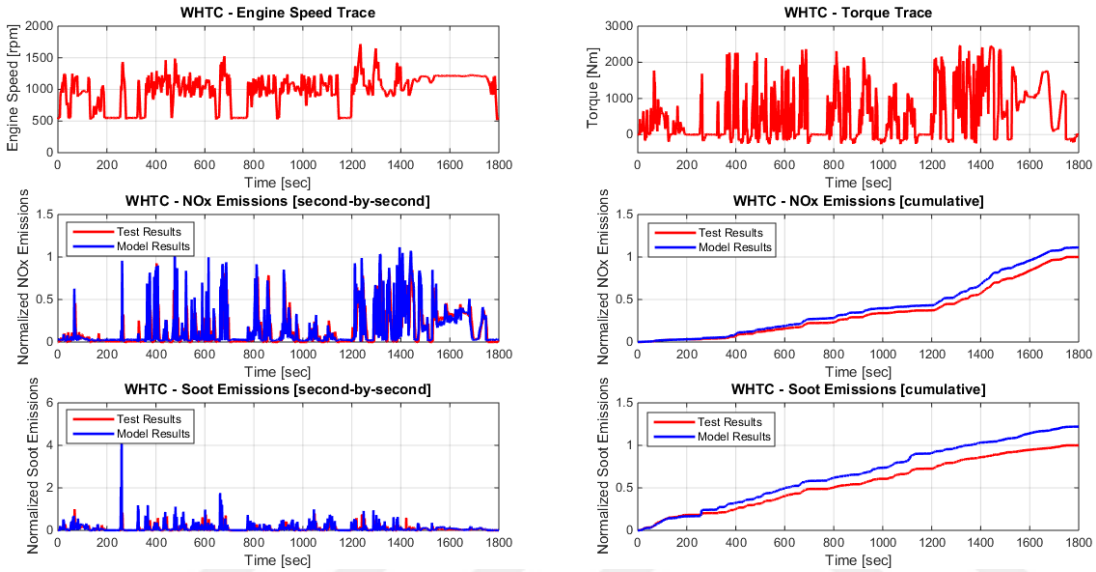

Figure 6.16: Transient cycle results of model 4.

Percentage error of cumulative results is calculated both for soot and NOx emissions by using equation 6.6 and 6.7. The percent error of NOx results is 11.29%, and the percent error of soot results is 22.09%.

6.2.2.5 Model 5

The 5th model consists of parameters listed below. Steady state results of the model are shown in section 6.1.2. Accordingly, R^2 value of soot model data is 92.99%, R^2 value of soot validation data 80.11%, R^2 value of NOx model data is 98.23%, and R^2 value of NOx validation data is 95.11%.

- Engine speed
- Rail fuel pressure
- Total fuel quantity

- Start of main injection
- Start of pilot injection
- Mass air flow
- Intake manifold temperature
- Intake manifold pressure
- Turbine inlet temperature
- Turbine inlet pressure

The model including the parameters listed above were run in MATLAB Simulink. Second by second and cumulative results were plotted both for soot and NOx emissions.

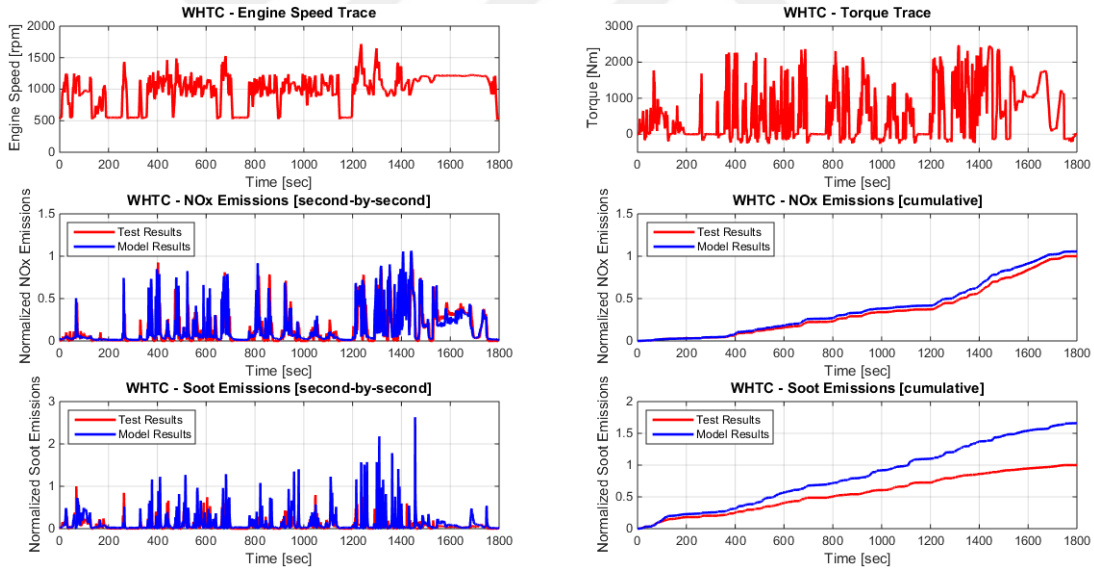

Figure 6.17: Transient cycle results of model 5.

Percentage error of cumulative results is calculated both for soot and NOx emissions by using equation 6.6 and 6.7. The percent error of NOx results is 5.63%, and the percent error of soot results is 66.04%.

6.2.2.6 Model 6

The 6th model consists of parameters listed below. Steady state results of the model are shown in section 6.1.2. Accordingly, R^2 value of soot model data is 91.74%, R^2 value of soot validation data 76.89%, R^2 value of NOx model data is 98.68%, and R^2 value of NOx validation data is 95.14%.

- Engine speed
- Rail fuel pressure
- Total fuel quantity
- Start of main injection
- Start of pilot injection
- Mass air flow
- Intake manifold temperature
- Intake manifold pressure
- Turbine inlet temperature
- Maximum cylinder pressure

The model including the parameters listed above were run in MATLAB Simulink. Second by second and cumulative results were plotted both for soot and NOx emissions.

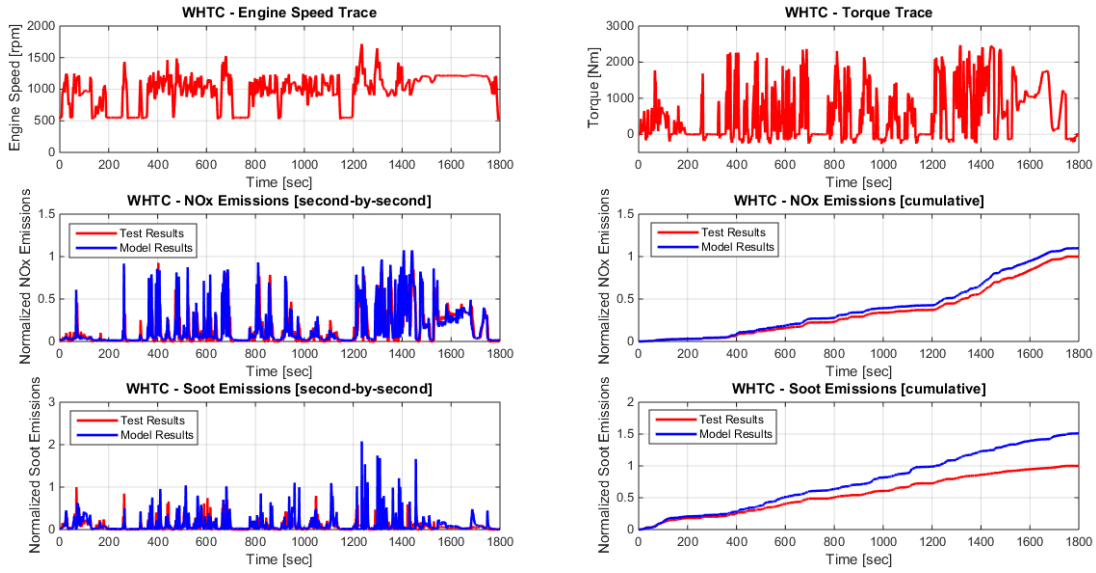

Figure 6.18: Transient cycle results of model 6.

Percentage error of cumulative results is calculated both for soot and NOx emissions by using equation 6.6 and 6.7. The percent error of NOx results is 9.89%, and the percent error of soot results is 51.02%.

6.2.2.7 Model 7

The 7th model consists of parameters listed below. Steady state results of the model are shown in section 6.1.2. Accordingly, R^2 value of soot model data is 83.78%, R^2 value of soot validation data 89.65%, R^2 value of NOx model data is 98.62%, and R^2 value of NOx validation data is 95.05%.

- Engine speed
- Rail fuel pressure
- Total fuel quantity
- Start of main injection
- Start of pilot injection
- Mass air flow
- Intake manifold temperature

- Intake manifold pressure
- Turbine inlet pressure
- Maximum cylinder pressure

The model including the parameters listed above were run in MATLAB Simulink. Second by second and cumulative results were plotted both for soot and NOx emissions.

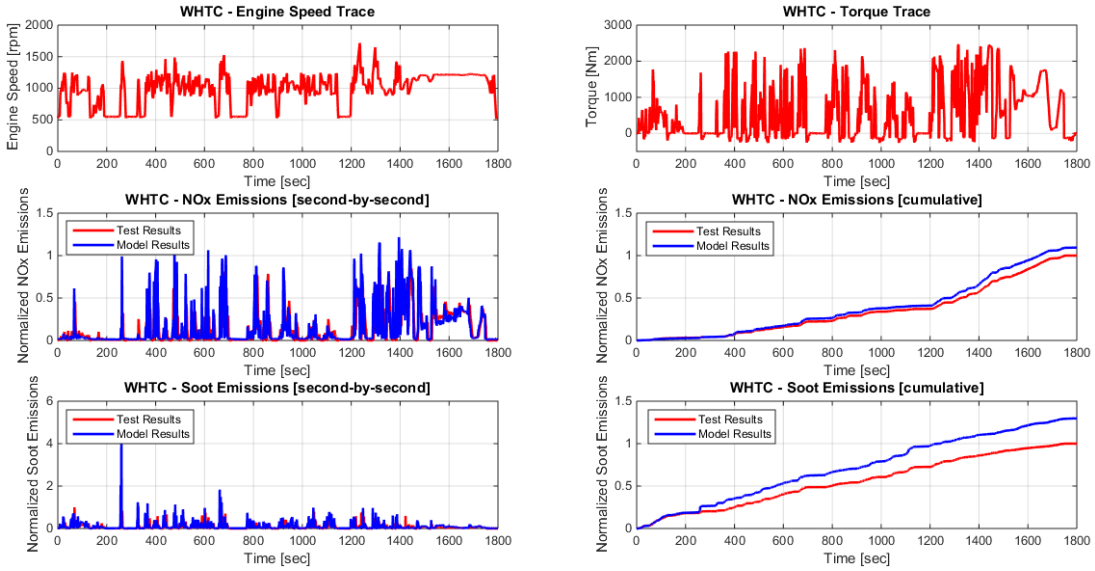

Figure 6.19: Transient cycle results of model 7.

Percentage error of cumulative results is calculated both for soot and NOx emissions by using equation 6.6 and 6.7. The percent error of NOx results is 9.43%, and the percent error of soot results is 29.78%.

6.2.2.8 Model 8

The 8th model consists of parameters listed below. Steady state results of the model are shown in section 6.1.2. Accordingly, R^2 value of soot model data is 91.80%, R^2 value of soot validation data 78.20%, R^2 value of NOx model data is 98.74%, and R^2 value of NOx validation data is 95.21%.

- Engine speed
- Rail fuel pressure
- Total fuel quantity

- Start of main injection
- Start of pilot injection
- Mass air flow
- Intake manifold temperature
- Intake manifold pressure
- Turbine inlet temperature
- Turbine inlet pressure
- Maximum cylinder pressure

The model including the parameters listed above were run in MATLAB Simulink. Second by second and cumulative results were plotted both for soot and NOx emissions.

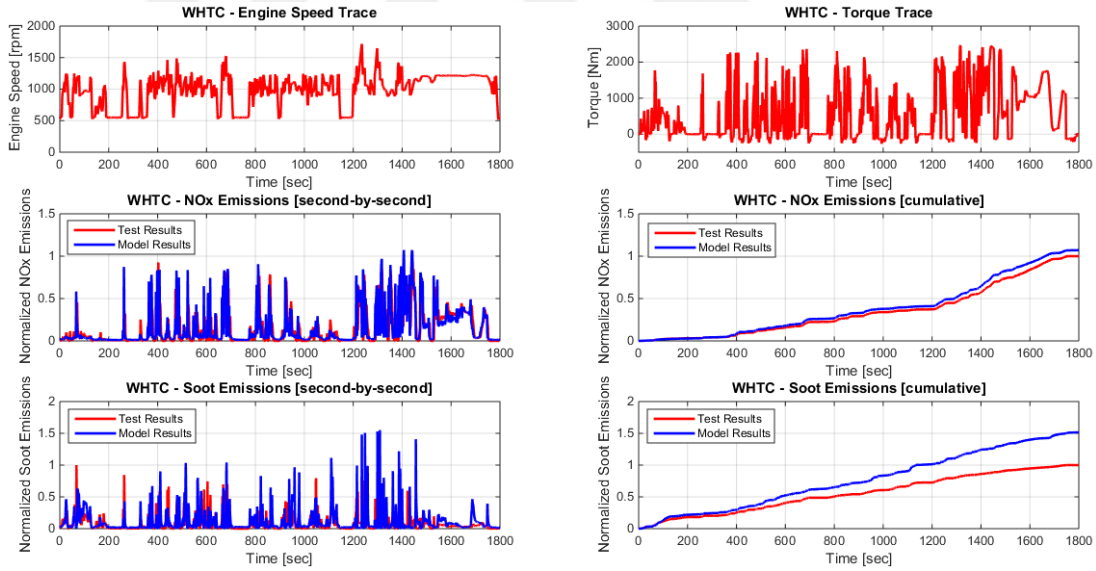

Figure 6.20: Transient cycle results of model 8.

Percentage error of cumulative results is calculated both for soot and NOx emissions by using equation 6.6 and 6.7. The percent error of NOx results is 7.08%, and the percent error of soot results is 51.24%.

6.2.2.9 Comparison of the models

8 models were totally run to see capabilities of mathematical emission models, which were created by using Gaussian Regression Method. Results of the models show that

the mathematical models are capable of predicting NOx and soot emissions with high accuracy. The overview of the results is shown in Table 6.5.

Table 6.5: Comparison of the model results

Model No	Percent Error(NOx)	Percent Error(Soot)
1	10.28%	18.13%
2	7.13%	49.54%
3	5.73%	21.62%
4	11.29%	22.09%
5	5.63%	66.04%
6	9.89%	51.02%
7	9.43%	29.78%
8	7.08%	51.24%

All models showed different results for soot emissions, and the models can predict soot emissions with at least 18.13% error. 1st model, which consists of only combustion input parameters, has the lowest error for soot prediction. Models including turbine inlet temperature cannot predict soot emissions well for transient cycles although the models have the highest accuracy for steady state conditions. For NOx prediction, all models have almost same capabilities, and the models can predict NOx emissions with maximum 11.29% error. 5th model, which includes turbine inlet pressure, has the lowest error for NOx prediction. Moreover, it can be stated models that have at least one of combustion output parameters are better to predict NOx for transient cycles. As a results, 1st and 3rd models can be used to predict NOx and soot emissions at the same time. However, due to the fact that turbine inlet pressure is a combustion output parameters, 1st model is more suitable to be used by ECU while calibrating the engine.

There are some problems observed during analysis of results of the models. These problems are overestimation of soot emissions and time delay between model and test results. Overestimation of soot emissions can be seen in Figure 6.21.

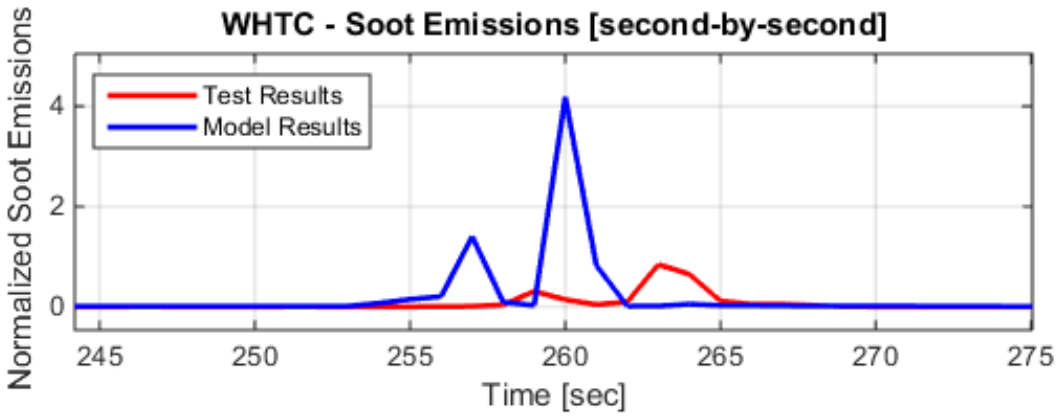

Figure 6.21: Overestimation of soot emissions.

Models created by using Gaussian Regression Method are better at extrapolation beyond the range of the training data compared to models created by using Neural Networks. Data used for model training does not contain the point showed in Figure 6.21. This situation causes overshooting of soot predictions.

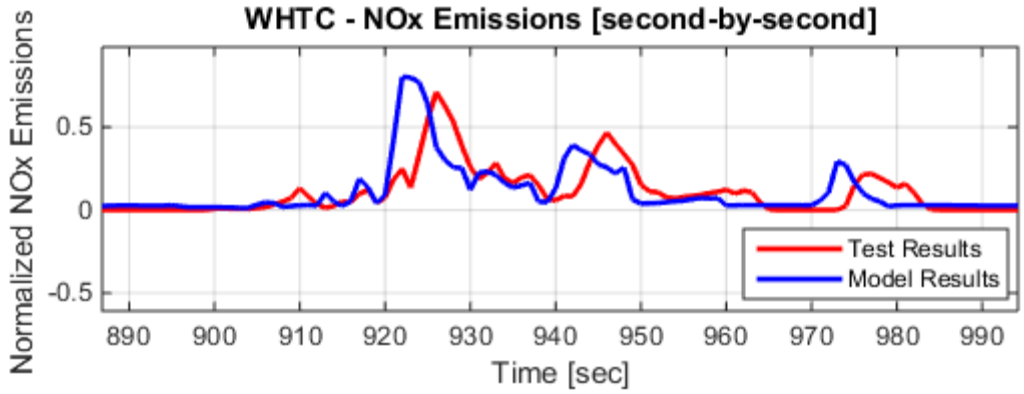

Figure 6.22: Time delay between model and test results.

Setpoints of combustion variables are specified at the beginning of combustion by ECU, however , soot and NOx emissions are measured at engine outlet. This situation causes a delay between test and model results for transient cycles although it is not a problem for steady state conditions. Due to this, second-by-second analysis of the results cannot be made. Results of emission measurements must be drifted in time domain to make better evaluations.

.

7. CONCLUSIONS

In this study, it is shown that both soot and NOx emissions in the diesel engine can be predicted with high accuracy by using the mathematical method, which is based on Gaussian Regression Method.

Models used for emission predictions are created by using input parameters, which is directly or indirectly controlled by ECU. Optimization of the input parameters are performed to obtain highest results, and the model comprising of eight parameters are sufficient to predict soot and NOx emissions. Suggested model includes the parameters: engine speed, fuel rail pressure, total fuel quantity, start of main injection, start of pilot injection, mass air flow, intake manifold temperature and intake manifold pressure. Due to dependency of EGR rate to other model parameters, it is not required to add EGR rate parameter into the models. Controlling of pilot injection quantity have high errors, and thus its effect on modeling quality could not be observed.

Effects of some combustion output parameters are also investigated in this thesis. Modeling improvement are aimed by using these parameters. Studies show that adding turbine inlet temperature into the models increases modeling quality of soot emissions. Also, it is obtained that using maximum cylinder pressure in the models increases the accuracy of validation data for steady state conditions, but it requires to use other combustion parameters such as turbine inlet pressure, burn duration 0-50%, burn duration 0-90% and burn duration 10-90%.

It is also aimed to model emissions mathematically by using only outputs of the 1D engine model and to show its feasibility. Thus, optimum design of an engine can be obtained by using a coupled model of 1D engine model with a mathematical emission model. However, the results show that NOx emissions can be assessed during design optimization process but the same thing cannot be stated for soot emissions, and further improvements are needed.

The models including combustion input and output parameters are run in MATLAB to evaluate the model quality for transient conditions. World harmonized transient cycle (WHTC) is used for comparison of model and test data. The results show that

mathematical emission models are capable of predicting transient results of emissions. The same model suggested for steady state conditions can be also used for transient conditions. However, there are some problems observed during analysis of transient results of the models. These problems are overestimation of soot emissions and time delay between model and test results. One of transient cycle points is out of range for training data of the models, and it results in overshooting of soot emissions. Setpoints of combustion variables are specified at the beginning of combustion by ECU, however , soot and NOx emissions are measured at engine outlet. This situation causes a delay between test and model results. The delay should be removed to make better evaluations. Also, it is proved that space filling DoE is good enough to describe system behaviors of the engine. For this thesis, experimental design having 1000 measurement points is created. Mathematical models using less measurement points can be investigated to decrease cost and time for future works.

REFERENCES

[1] Alfieri, E. (2009). *Emissions-controlled diesel engine* (Doctoral Thesis). Swiss Federal Institute of Technology Zurich, Zurich.

[2] Arsie, I., Pianese, C., and G. Rizzo (1998). Enhancement of control oriented engine models using neural network. *6th IEEE Mediterranean Conference on Control Systems*, Alghero, Italy.

[3] Barba, C., Burkhardt, C., Boulouchos, K., and Bargende, M. (2000). A Phenomenological Combustion Model For Heat Release Rate Prediction In High-Speed DI Diesel Engines With Common Rail Injection. *SAE Technical Paper*, Paper no: 2000-01-2933, https://doi.org/10.4271/2000-01-2933.

[4] Belardini, P., Bertoli, C., Ciajolo, A., D'Anna, A., and Del Giacomo, N. (1992). Three Dimensional Calculations of DI Diesel Engine Combustion and Comparison whit In Cylinder Sampling Valve Data. *SAE Technical*, Paper no: 922225, Retrieved from https://doi.org/10.4271/922225.

[5] Benz, M. (2009). Model-Based Optimal Emission Control of Diesel Engines (Doctoral Thesis). ETH Zurich, Mechanical Engineering, Zurich.

[6] Choi, M. Y., Hamins, A., Mulholland, and G.W., Kashiwagi, T. (1994). Simultaneous Optical Measurement of Soot Volume Fraction and Temperature in Premixed Flames," *Combust Flame*, 99, 174-186.

[7] Christen, U., Vantine, K., and Collings, N. (2001). Event-based mean-value modeling of DI diesel engines for controller design. *SAE Technical Paper*, Paper no: 2001-01-1242, Retrieved from https://doi.org/10.4271/2001-01-1242.

[8] Colin, O., Benkenida, A. and Angelberger, C. (2003). 3D Modeling of Mixing, Ignition and Combustion Phenomena in Highly Stratified Gasoline Engines. *Oil Gas Sci. Technol*., 58(1), 47-62.

[9] Dec, J. (1997). A Conceptual Model of DI Diesel Combustion Based on Laser-Sheet Imaging. *SAE Technical Paper*, Paper no: 970873, Retrieved from https://doi.org/10.4271/970873.

[10] Delphi (2012). Worldwide emissions standards—heavy duty and offhighway vehicles. *Delphi*, Michigan.

[11] Englert, N. (2004). Fine particles and human health—a review of epidemiological studies. *Toxicol Lett.*, 149, 235–242.

[12] Fenimore, C. P. (1970). Formation of Nitric Oxide in Premixed Hydrocarbon Flames. *Thirteenth Symposium (International) on Combustion*, The Combustion Institute, Pittsburgh, PA, 373-380.

[13] Grewe, V., Dahlmann, K., Matthes, S., and Steinbrecht, W. (2012). Attributing ozone to NOx emissions: implications for climate mitigation measures. *Atmos. Environ.*, 59, 102–107.

[14] Gutjahr, T. (2012). Dynamic System Identification with Gaussian Processes in Model-Based Engine Development (Doctoral Thesis). Universität Ilmenau, Ilmenau, Thuringia.

[15] Heywood, J.B., (2011). *Construction of a Diesel Engine Test Stand and a Crank Angle Based Heat Release Model* (Master Thesis). Auburn University, Mechanical Engineering, Auburn Alabama.

[16] Hiroyasu, H. and Kadota, T. (1976). Models for Combustion and Formation of Nitric Oxide and Soot in Direct Injection Diesel Engines. *SAE Technical Paper*, Paper No: 760129, Retrieved from https://doi.org/10.4271/760129.

[17] Kee, R. J., Coltrin, M.E., and Glarborg, P. (2003). Chemically Reacting Flow, *Wiley-Interscience*.

[18] Kirchen, P. (2008). Steady-State and Transient Diesel Soot Emissions: Development of a Mean Soot Model and Exhaust-Stream and In-Cylinder Measurements (Doctoral Thesis). *ETH Zurich*, Switzerland.

[19] Kruse, T., Ulmer, H., and Schulmeister, U. (2007). Use of Advanced Modelling and Optimization for Diesel- and Gasoline Engine Calibration. In K. Röpke, editor, *Design of Experiments (DoE) in Engine Development*, 4, 91-102.

[20] Lee, T., Park, J., Kwon, S., Lee, J., and Kim, J. (2013). Variability in operation based NOx emission factors with different test routes, and its effects on the real-driving emissions of light diesel vehicles. *Sci Total Environ*, 461–462, 377–385.

[21] Majewski, W. A., and Khair, M. K. (2006). Comparing neural network and autoregressive moving average techniques for the provision of continuous river flow forecasts in two contrasting catchments, *Diesel Emissions and Their Control,* 14, 2157–2172.

[22] Miller, J. A., and Bowman, C. T., (1989). Mechanism and Modeling of Nitrogen Chemistry in Combustion. *Prog. Energy Combust. Sci*, 15,287-338.

[23] Nagle, J., and Strickland-Constable, R. F. (1962). Oxidation of Carbon between 1000-2000 C. *Proc. of the Fifth Carbon Conf.*, Volume 1, Pergammon Press, p. 154.

[24] Narendra, K. S., and Parthasarathy, K. (1990). Identification and Control of Dynamical Systems Using Neural Networks. *IEEE Transactions on Neural Networks*. Vol.1 No.1.

[25] Nelles, O. (2001). "Nonlinear System Identification", Springer-Verlag Berlin Heidelberg New York.

[26] Payri, F., Olmeda, P., Martin, J., and Garcia, A. (2011). A complete 0D thermodynamic predictive model for direct injection diesel engines. *Appl. Energy*, 88(12), 4632-4641.

[27] Prasad, R., and Bella, V. R. (2010). A review on diesel soot emission, its effect and control. *Bull Chem React Eng Catal*, *5*(2), 69–86.

[28] Quérel, C., Grondin, O., and Letellier, C. (2012). State of the Art and Analysis of Control Oriented NOx Models. *SAE Technical Paper*, Paper no: 2012-01-0723, Retrieved from https://doi.org/10.4271/2012-01-0723.

[29] Rakopoulos, C. and Hountalas, D. (1998). Development and Validation of a 3-D Multi-Zone Combustion Model for the Prediction of DI Diesel Engines Performance and Pollutants Emissions. *SAE Technical Paper* Paper No:981021, Retrieved from doi: 10.4271/981021.

[30] Rasmussen, C. E., and Williams, C. K. I. (2006). Gaussian Processes for Machine Learning. The MIT Press.

[31] Resitoglu, A. R., Altinisik, K., and Keskin, A. (2015). The pollutant emissions from disel-engine vehicles and exhaust after treatment systems. *Clean Techn Environ Policy, 17*, 15-27. Retrieved from DOI 10.1007/s10098-014-0793-9.

[32] Robert Bosch GmbH (2003) Electronic Diesel Control EDC: Bosch Technical Instruction. Bently Publishers.

[33] Schmitt, J-C., Fremovici, M., Grondin, O., and Le Berr, F. (2009).Compression ignition engine model supporting powertrain development. *In Proc. of the E-COSM'09 - IFAC Workshop on Engine and Powertrain Control, Simulation and Modeling*, 75-82, Rueil-Malmaison, France.

[34] Thames, M. B. (2013). *Experimentation and modeling of NOx formation in a small urbo-charged diesel engine* (Master's Thesis). Auburn University, Mechanical Engineering, Auburn, Alabama.

[35] Tietze, N. (2015). *Model-based Calibration of Engine Control Units Using Gaussian Process Regression* (Doctoral Thesis). The Technische Universität Darmstadt, Control Systems and Mechatronics, Germany.

[36] Tree, D. R., and Svensson, K. I. (2007). Soot processes in compression ignition engines. *Prog. Energy Combust. Sci*, 33 (3), 272–309.

[37] Wingo, T. J., (2011). Construction of a Diesel Engine Test Stand and a Crank Angle Based Heat Release Model (Master Thesis). Auburn University, Mechanical Engineering, Auburn, Alabama.

[38] Wingo, T. J., Benz, M., Hehn, M., Onder, C.H., and Guzzella, L. (2011)**.** Model- Based Actuator Trajectories Optimization for a Diesel Engine Using a Direct Method. *J. Eng. Gas Turbines* Power, 133(3), doi: 10.1115/1.4001807.

[39] ETAS GmbH, *ETAS ASCMO User's Guide*, Program version 4.8, 2015.

[40] Gamma Technologies, *GT-Power User's Manuel*, GT Suite Version 2016, 2016.

[41] Url-1 <*https://www.dieselnet.com/standards/cycles/whtc.php*>, data retrieved 01.11.2017

APPENDICES

APPENDIX A

Table A.1: All results obtained from the models (1st step)

Model No	No of Param.	ES	RFP	TFQ	SOMI	PIQ	SOPI	MAF	EGR Rate	IMT	IMP	R2 of Soot Model Data	R2 of Soot Valid. Data	R2 of NOx Model Data	R2 of NOx Valid. Data
1	10	+	+	+	+	+	+	+	+	+	+	87.37%	75.33%	98.91%	95.78%
2	9	+	+	+	+	+	+	+	+	+	-	81.76%	79.45%	98.18%	96.87%
3	9	+	+	+	+	+	+	+	+	-	+	82.71%	56.77%	98.84%	95.96%
4	9	+	+	+	+	+	+	+	-	+	+	83.00%	81.40%	98.62%	94.93%
5	9	+	+	+	+	+	+	-	+	+	+	86.19%	65.10%	98.32%	97.33%
6	9	+	+	+	+	+	-	+	+	+	+	82.84%	52.66%	98.96%	95.91%
7	9	+	+	+	+	-	+	+	+	+	+	85.50%	76.20%	98.86%	95.95%
8	9	+	+	+	-	+	+	+	+	+	+	82.51%	83.34%	80.57%	78.54%
9	9	+	+	-	+	+	+	+	+	+	+	77.01%	66.41%	95.88%	93.64%
10	9	+	-	+	+	+	+	+	+	+	+	62.17%	39.66%	68.22%	67.09%
11	9	-	+	+	+	+	+	+	+	+	+	84.37%	39.13%	97.47%	97.01%
12	8	+	+	+	+	+	+	+	+	-	-	82.92%	32.06%	97.86%	96.13%

13	8	+	+	+	+	+	+	+	-	+	-	77.70%	80.27%	95.27%	94.13%
14	8	+	+	+	+	+	+	-	+	+	-	67.23%	80.13%	94.83%	93.53%
15	8	+	+	+	+	+	-	+	+	+	-	85.06%	51.19%	97.97%	96.78%
16	8	+	+	+	+	-	+	+	+	+	-	70.42%	75.21%	97.97%	96.83%
17	8	+	+	+	-	+	+	+	+	+	-	82.93%	74.76%	80.36%	78.04%
18	8	+	+	-	+	+	+	+	+	+	-	76.67%	58.71%	95.71%	93.96%
19	8	+	-	+	+	+	+	+	+	+	-	38.75%	46.91%	68.09%	66.27%
20	8	-	+	+	+	+	+	+	+	+	-	45.37%	52.11%	89.74%	86.00%
21	8	+	+	+	+	+	+	+	-	-	+	80.33%	24.63%	98.70%	94.02%
22	8	+	+	+	+	+	+	-	+	-	+	77.60%	10.10%	97.93%	96.08%
23	8	+	+	+	+	+	-	+	+	-	+	87.34%	24.78%	98.67%	96.03%
24	8	+	+	+	+	-	+	+	+	-	+	84.51%	66.54%	98.81%	96.17%
25	8	+	+	+	-	+	+	+	+	-	+	86.48%	75.48%	80.21%	74.74%
26	8	+	+	-	+	+	+	+	+	-	+	63.88%	46.55%	96.13%	92.98%
27	8	+	-	+	+	+	+	+	+	-	+	36.03%	33.75%	68.03%	65.69%
28	8	-	+	+	+	+	+	+	+	-	+	73.78%	18.39%	96.73%	95.97%
29	8	+	+	+	+	+	+	-	-	+	+	76.21%	85.14%	92.45%	93.33%
30	8	+	+	+	+	+	-	+	-	+	+	80.66%	62.94%	98.59%	94.79%
31	8	+	+	+	+	-	+	+	-	+	+	82.89%	87.54%	98.79%	94.56%
32	8	+	+	+	-	+	+	+	-	+	+	84.37%	83.62%	79.43%	77.61%
33	8	+	+	-	+	+	+	+	-	+	+	73.17%	70.29%	94.06%	80.01%
34	8	+	-	+	+	+	+	+	-	+	+	61.79%	41.13%	66.82%	65.66%
35	8	-	+	+	+	+	+	+	-	+	+	82.94%	84.91%	91.56%	93.28%
36	8	+	+	+	+	+	-	-	+	+	+	81.14%	46.44%	97.93%	97.52%
37	8	+	+	+	+	-	+	-	+	+	+	80.84%	71.19%	98.02%	97.36%

38	8	+	+	+	-	+	+	-	+	+	+	77.83%	84.32%	80.21%	79.20%
39	8	+	+	-	+	+	+	-	+	+	+	81.26%	66.34%	95.15%	95.46%
40	8	+	-	+	+	+	+	-	+	+	+	41.30%	50.32%	68.54%	67.05%
41	8	-	+	+	+	+	+	-	+	+	+	81.00%	73.75%	95.23%	93.13%
42	8	+	+	+	+	-	-	+	+	+	+	80.59%	50.76%	98.72%	95.59%
43	8	+	+	+	-	+	-	+	+	+	+	83.91%	66.59%	74.42%	76.12%
44	8	+	+		+	+	-	+	+	+	+	81.16%	65.42%	95.81%	93.26%
45	8	+	-	+	+	+	-	+	+	+	+	38.23%	47.40%	68.07%	67.28%
46	8	-	+	+	+	+	-	+	+	+	+	86.15%	0.00%	96.89%	97.10%
47	8	+	+	+	-	-	+	+	+	+	+	82.97%	83.19%	80.70%	77.73%
48	8	+	+	-	+	-	+	+	+	+	+	68.30%	63.83%	95.63%	93.67%
49	8	+	-	+	+	-	+	+	+	+	+	43.39%	51.64%	67.39%	68.99%
50	8		+	+	+	-	+	+	+	+	+	85.97%	27.91%	97.32%	97.14%
51	8	+	+	-	-	+	+	+	+	+	+	77.13%	60.20%	79.08%	76.93%
52	8	+	-	+	-	+	+	+	+	+	+	43.15%	44.33%	56.31%	59.45%
53	8	-	+	+	-	+	+	+	+	+	+	77.83%	84.82%	79.78%	79.24%
54	8	+	-	-	+	+	+	+	+	+	+	35.47%	53.62%	62.93%	62.78%
55	8	-	+	-	+	+	+	+	+	+	+	61.93%	63.52%	94.36%	95.30%
56	8	-	-	+	+	+	+	+	+	+	+	24.20%	28.98%	68.14%	67.59%
57	8	+	+	+	+	+	+	+	-	-	-	77.79%	84.39%	83.77%	78.08%
58	8	+	+	+	+	+	+	-	+	-	-	60.96%	78.41%	94.73%	92.12%
59	8	+	+	+	+	+	-	+	+	-	-	84.24%	0.00%	97.76%	96.44%
60	8	+	+	+	+	-	+	+	+	-	-	75.31%	0.00%	97.71%	96.34%
61	8	+	+	+	-	+	+	+	+	-	-	84.83%	71.06%	79.53%	76.99%
62	8	+	+	-	+	+	+	+	+	-	-	43.21%	36.29%	95.32%	93.70%

63	8	+	-	+	+	+	+	+	+	-	-	37.73%	38.09%	68.50%	65.84%
64	8	-	+	+	+	+	+	+	+	-	-	30.34%	45.90%	88.17%	83.83%
65	8	+	+	+	+	+	+	-	-	+	-	70.29%	80.22%	89.00%	88.72%
66	8	+	+	+	+	+	-	+	-	+	-	83.34%	60.72%	96.41%	93.15%
67	8	+	+	+	+	-	+	+	-	+	-	77.49%	79.60%	95.11%	94.34%
68	8	+	+	+	-	+	+	+	-	+	-	81.27%	83.37%	78.51%	78.38%
69	8	+	+	-	+	+	+	+	-	+	-	53.66%	61.83%	91.40%	88.80%
70	8	+	-	+	+	+	+	+	-	+	-	35.38%	46.20%	66.63%	66.78%
71	8	-	+	+	+	+	+	+	-	+	-	55.53%	51.17%	86.80%	85.53%
72	8	+	+	+	+	+	-	-	+	+	-	68.57%	80.22%	94.83%	93.86%
73	8	+	+	+	+	-	+	-	+	+	-	68.30%	78.29%	94.79%	93.72%
74	8	+	+	+	-	+	+	-	+	+	-	72.46%	72.58%	78.38%	74.07%
75	8	+	+	-	+	+	+	-	+	+	-	60.77%	67.79%	91.25%	91.79%
76	8	+	-	+	+	+	+	-	+	+	-	16.64%	32.91%	68.15%	62.90%
77	8	-	+	+	+	+	+	-	+	+	-	47.50%	52.22%	87.72%	83.04%
78	8	+	+	+	+	-	-	+	+	+	-	84.93%	58.14%	97.85%	96.48%
79	8	+	+	+	-	+	-	+	+	+	-	84.92%	50.08%	73.27%	73.61%
80	8	+	+	-	+	+	-	+	+	+	-	72.37%	58.10%	95.86%	94.35%
81	8	+	-	+	+	+	-	+	+	+	-	36.11%	47.63%	68.51%	66.21%
82	8	-	+	+	+	+	-	+	+	+	-	55.29%	51.05%	89.85%	86.46%
83	8	+	+	+	-	-	+	+	+	+	-	81.06%	81.31%	80.58%	77.64%
84	8	+	+	-	+	-	+	+	+	+	-	82.43%	61.04%	95.65%	94.61%
85	8	+	-	+	+	-	+	+	+	+	-	34.68%	46.54%	67.26%	68.01%
86	8	-	+	+	+	-	+	+	+	+	-	57.54%	53.25%	89.87%	86.94%
87	8	+	+	-	-	+	+	+	+	+	-	84.60%	55.98%	79.11%	78.95%

88	8	+	-	+	-	+	+	+	+	+	-	36.57%	39.31%	55.61%	57.56%
89	8	-	+	+	-	+	+	+	+	+	-	47.73%	48.50%	75.97%	73.01%
90	8	+	-	-	+	+	+	+	+	+	-	32.36%	47.04%	62.71%	64.03%
91	8	-	+	-	+	+	+	+	+	+	-	40.54%	51.53%	78.52%	77.84%
92	8	-	-	+	+	+	+	+	+	+	-	59.48%	41.57%	66.98%	61.06%
93	7	+	+	+	+	+	+	-	-	-	+	35.90%	40.03%	80.38%	80.87%
94	7	+	+	+	+	+	-	+	-	-	+	84.29%	3.31%	98.67%	94.11%
95	7	+	+	+	+	-	+	+	-	-	+	82.61%	33.52%	98.54%	93.68%
96	7	+	+	+	-	+	+	+	-	-	+	84.77%	61.69%	79.07%	75.06%
97	7	+	+	-	+	+	+	+	-	-	+	42.79%	45.49%	94.80%	82.50%
98	7	+	-	+	+	+	+	+	-	-	+	62.96%	39.20%	66.79%	61.46%
99	7	-	+	+	+	+	+	+	-	-	+	60.12%	39.23%	63.40%	64.32%
100	7	+	+	+	+	+	-	-	+	-	+	79.92%	0.00%	97.71%	96.25%
101	7	+	+	+	+	-	+	-	+	-	+	80.63%	27.01%	97.79%	96.16%
102	7	+	+	+	-	+	+	-	+	-	+	76.55%	73.00%	79.80%	76.96%
103	7	+	+	-	+	+	+	-	+	-	+	52.99%	39.37%	94.90%	93.99%
104	7	+	-	+	+	+	+	-	+	-	+	28.02%	18.65%	68.31%	65.93%
105	7	-	+	+	+	+	+	-	+	-	+	25.75%	41.65%	86.93%	83.02%
106	7	+	+	+	+	-	-	+	+	-	+	83.23%	38.57%	98.76%	96.16%
107	7	+	+	+	-	+	-	+	+	-	+	84.28%	65.19%	75.06%	74.73%
108	7	+	+	-	+	+	-	+	+	-	+	59.24%	48.00%	96.10%	93.02%
109	7	+	-	+	+	+	-	+	+	-	+	34.36%	28.26%	68.49%	65.23%
110	7	-	+	+	+	+	-	+	+	-	+	83.22%	5.82%	96.40%	96.39%
111	7	+	+	+	-	-	+	+	+	-	+	84.15%	74.50%	80.15%	74.20%
112	7	+	+	-	+	-	+	+	+	-	+	60.25%	44.21%	96.30%	94.47%

113	7	+	-	+	+	-	+	+	+	-	+	37.62%	37.07%	67.33%	67.41%
114	7	-	+	+	+	-	+	+	+	-	+	72.43%	21.69%	96.54%	96.12%
115	7	+	+	-	-	+	+	+	+	-	+	45.91%	40.30%	79.59%	75.71%
116	7	+	-	+	-	+	+	+	+	-	+	38.31%	23.57%	55.65%	58.73%
117	7	-	+	+	-	+	+	+	+	-	+	78.15%	65.06%	79.25%	74.52%
118	7	+	-	-	+	+	+	+	+	-	+	11.27%	14.87%	62.17%	61.16%
119	7	-	+	-	+	+	+	+	+	-	+	52.16%	38.05%	93.81%	93.73%
120	7	-	-	+	+	+	+	+	+	-	+	23.21%	24.50%	67.83%	66.07%
121	7	+	+	+	+	+	-	-	-	+	+	76.54%	80.09%	93.19%	92.80%
122	7	+	+	+	+	-	+	-	-	+	+	74.70%	85.64%	93.08%	93.42%
123	7	+	+	+	-	+	+	-	-	+	+	70.74%	80.87%	77.10%	76.77%
124	7	+	+	-	+	+	+	-	-	+	+	50.27%	55.27%	82.32%	85.10%
125	7	+	-	+	+	+	+	-	-	+	+	39.99%	48.05%	66.05%	65.93%
126	7	-	+	+	+	+	+	-	-	+	+	77.55%	82.71%	89.63%	88.85%
127	7	+	+	+	+	-	-	+	-	+	+	78.55%	66.60%	98.73%	94.59%
128	7	+	+	+	-	+	-	+	-	+	+	84.08%	61.45%	74.17%	75.25%
129	7	+	+	-	+	+	-	+	-	+	+	69.81%	74.02%	95.04%	83.54%
130	7	+	-	+	+	+	-	+	-	+	+	41.30%	48.63%	67.24%	65.34%
131	7	-	+	+	+	+	-	+	-	+	+	77.32%	81.71%	91.63%	93.28%
132	7	+	+	+	-	-	+	+	-	+	+	84.82%	83.72%	79.42%	76.27%
133	7	+	+	-	+	-	+	+	-	+	+	75.72%	73.13%	94.94%	88.64%
134	7	+	-	+	+	-	+	+	-	+	+	42.95%	50.89%	66.43%	66.93%
135	7	-	+	+	+	-	+	+	-	+	+	83.66%	84.87%	91.42%	93.21%
136	7	+	+	-	-	+	+	+	-	+	+	72.33%	65.23%	76.40%	72.92%
137	7	+	-	+	-	+	+	+	-	+	+	42.46%	44.73%	54.35%	56.82%

138	7	-	+	+	-	+	+	+	-	+	+	74.19%	76.81%	76.86%	77.28%
139	7	+	-	-	+	+	+	+	-	+	+	27.70%	44.68%	59.07%	59.75%
140	7	-	+	-	+	+	+	+	-	+	+	56.77%	66.09%	80.11%	81.24%
141	7	-		+	+	+	+	+	-	+	+	37.44%	48.47%	64.97%	64.47%
142	7	+	+	+	+	-	-	-	+	+	+	83.30%	48.89%	97.66%	97.25%
143	7	+	+	+	-	+	-	-	+	+	+	81.29%	66.95%	74.72%	78.02%
144	7	+	+	-	+	+	-	-	+	+	+	81.01%	65.76%	95.05%	95.74%
145	7	+	-	+	+	+	-	-	+	+	+	38.50%	48.90%	68.49%	67.20%
146	7	-	+	+	+	+	-	-	+	+	+	76.61%	72.01%	95.07%	92.55%
147	7	+	+	+	-	-	+	-	+	+	+	67.92%	84.98%	80.60%	78.95%
148	7	+	+	-	+	-	+	-	+	+	+	67.31%	62.08%	95.06%	95.71%
149	7	+	-	+	+	-	+	-	+	+	+	41.85%	50.60%	67.58%	69.11%
150	7	-	+	+	+	-	+	-	+	+	+	80.37%	75.06%	95.04%	93.31%
151	7	+	+	-	-	+	+	-	+	+	+	84.98%	60.84%	77.83%	78.52%
152	7	+		+	-	+	+	-	+	+	+	39.42%	43.17%	55.87%	58.91%
153	7	-	+	+	-	+	+	-	+	+	+	65.64%	58.36%	78.10%	76.73%
154	7	+	-	-	+	+	+	-	+	+	+	32.00%	49.54%	63.32%	63.78%
155	7	-	+	-	+	+	+	-	+	+	+	58.58%	53.50%	89.80%	88.16%
156	7	-	-	+	+	+	+	-	+	+	+	32.84%	51.00%	68.14%	65.57%
157	7	+	+	+	-	-	-	+	+	+	+	82.13%	73.90%	74.79%	76.24%
158	7	+	+	-	+	-	-	+	+	+	+	83.33%	61.95%	95.85%	94.28%
159	7	+	-	+	+	-	-	+	+	+	+	41.44%	48.75%	67.49%	68.56%
160	7	-	+	+	+	-	-	+	+	+	+	80.00%	0.00%	96.88%	97.11%
161	7	+	+	-	-	+	-	+	+	+	+	81.12%	38.98%	73.54%	75.08%
162	7	+	-	+	-	+	-	+	+	+	+	27.53%	38.68%	52.68%	55.83%

163	7	-	+	+	-	+	-	+	+	+	+	84.09%	72.31%	74.28%	77.53%
164	7	+	-	-	+	+	-	+	+	+	+	34.83%	55.22%	63.58%	64.21%
165	7	-	+	-	+	+	-	+	+	+	+	77.05%	63.60%	94.16%	95.61%
166	7	-	-	+	+	+	-	+	+	+	+	36.34%	43.34%	68.51%	67.35%
167	7	+	+	-	-	-	+	+	+	+	+	72.15%	61.97%	79.54%	76.29%
168	7	+	-	+	-	-	+	+	+	+	+	39.11%	42.09%	54.98%	58.48%
169	7	-	+	+	-	-	+	+	+	+	+	79.95%	84.60%	79.73%	78.54%
170	7	+	-	-	+	-	+	+	+	+	+	31.22%	47.60%	61.32%	65.47%
171	7	-	+	-	+	-	+	+	+	+	+	64.32%	55.25%	94.09%	95.49%
172	7	-	-	+	+	-	+	+	+	+	+	41.25%	44.43%	67.24%	69.17%
173	7	+	-	-	-	+	+	+	+	+	+	34.19%	41.45%	48.62%	52.45%
174	7	-	+	-	-	+	+	+	+	+	+	57.48%	54.55%	77.69%	76.75%
175	7	-	-	+	-	+	+	+	+	+	+	41.05%	41.77%	55.75%	58.54%
176	7	-	-	-	+	+	+	+	+	+	+	32.23%	52.04%	61.98%	60.42%

APPENDIX B

Table B.1: All results obtained from the models (3rd step)

Model No	No of Param.	ES	RFP	TFQ	SOMI	SOPI	MAF	IMT	IMP	TIT	TIP	BD 0-50%	BD 10-90%	BD 0-90%	MCP	MCT	R2 of Soot Model Data	R2 of Soot Valid. Data	R2 of NOx Model Data	R2 of NOx Valid. Data
1	8	+	+	+	+	+	+	+	+	-	-	-	-	-	-	-	82.89%	87.54%	98.79%	94.56%
2	9	+	+	+	+	+	+	+	+	+	-	-	-	-	-	-	93.40%	77.35%	98.26%	95.13%
3	9	+	+	+	+	+	+	+	+	-	+	-	-	-	-	-	76.55%	87.17%	98.18%	95.20%
4	9	+	+	+	+	+	+	+	+	-	-	+	-	-	-	-	76.81%	82.76%	98.71%	94.60%
5	9	+	+	+	+	+	+	+	+	-	-	-	+	-	-	-	80.04%	87.14%	98.77%	94.61%
6	9	+	+	+	+	+	+	+	+	-	-	-	-	+	-	-	79.24%	83.72%	98.76%	94.59%
7	9	+	+	+	+	+	+	+	+	-	-	-	-	-	+	-	84.44%	86.07%	98.60%	95.00%
8	9	+	+	+	+	+	+	+	+	-	-	-	-	-	-	+	65.94%	78.46%	98.58%	95.46%
9	10	+	+	+	+	+	+	+	+	+	+	-	-	-	-	-	92.99%	80.11%	98.23%	95.11%
10	10	+	+	+	+	+	+	+	+	+	-	+	-	-	-	-	91.71%	81.81%	98.19%	94.97%
11	10	+	+	+	+	+	+	+	+	+	-	-	+	-	-	-	92.12%	82.29%	98.19%	94.72%
12	10	+	+	+	+	+	+	+	+	+	-	-	-	+	-	-	92.78%	82.60%	98.20%	94.90%
13	10	+	+	+	+	+	+	+	+	+	-	-	-	-	+	-	91.74%	76.89%	98.68%	95.14%
14	10	+	+	+	+	+	+	+	+	+	-	-	-	-	-	+	93.86%	70.97%	98.69%	95.49%
15	10	+	+	+	+	+	+	+	+	-	+	+	-	-	-	-	78.57%	88.91%	98.69%	94.43%
16	10	+	+	+	+	+	+	+	+	-	+	-	+	-	-	-	76.11%	87.48%	98.75%	94.63%
17	10	+	+	+	+	+	+	+	+	-	+	-	-	+	-	-	79.09%	88.56%	98.74%	94.62%
18	10	+	+	+	+	+	+	+	+	-	+	-	-	-	+	-	83.78%	89.65%	98.62%	95.05%
19	10	+	+	+	+	+	+	+	+	-	+	-	-	-	-	+	78.01%	87.96%	98.42%	95.44%

20	10	+	+	+	+	+	+	+	+	-	-	+	+	-	-	-	83.74%	83.18%	98.80%	94.80%
21	10	+	+	+	+	+	+	+	+	-	-	+	-	+	-	-	84.32%	85.12%	98.75%	94.70%
22	10	+	+	+	+	+	+	+	+	-	-	+	-	-	+	-	88.41%	87.85%	98.95%	94.79%
23	10	+	+	+	+	+	+	+	+	-	-	+	-	-	-	+	79.91%	82.39%	98.52%	95.19%
24	10	+	+	+	+	+	+	+	+	-	-	-	+	+	-	-	83.64%	87.50%	98.84%	94.72%
25	10	+	+	+	+	+	+	+	+	-	-	-	+	-	+	-	88.60%	85.51%	99.00%	94.95%
26	10	+	+	+	+	+	+	+	+	-	-	-	+	-	-	+	80.17%	83.34%	99.05%	95.60%
27	10	+	+	+	+	+	+	+	+	-	-	-	-	+	+	-	82.63%	85.52%	99.03%	95.05%
28	10	+	+	+	+	+	+	+	+	-	-	-	-	+	-	+	76.60%	83.92%	98.59%	95.30%
29	10	+	+	+	+	+	+	+	+	-	-	-	-	-	+	+	86.76%	83.74%	98.89%	95.14%
30	11	+	+	+	+	+	+	+	+	+	+	+	-	-	-	-	92.26%	79.58%	98.36%	95.02%
31	11	+	+	+	+	+	+	+	+	+	+	-	+	-	-	-	92.02%	80.09%	98.25%	95.00%
32	11	+	+	+	+	+	+	+	+	+	+	-	-	+	-	-	91.97%	80.37%	98.24%	95.03%
33	11	+	+	+	+	+	+	+	+	+	+	-	-	-	+	-	91.80%	78.20%	98.74%	95.21%
34	11	+	+	+	+	+	+	+	+	+	+	-	-	-	-	+	93.65%	75.00%	98.68%	95.48%
35	11	+	+	+	+	+	+	+	+	+	-	+	+	-	-	-	92.50%	77.21%	98.28%	95.10%
36	11	+	+	+	+	+	+	+	+	+	-	+	-	+	-	-	92.27%	79.80%	98.27%	95.04%
37	11	+	+	+	+	+	+	+	+	+	-	+	-	-	+	-	91.61%	81.57%	98.23%	95.12%
38	11	+	+	+	+	+	+	+	+	+	-	+	-	-	-	+	93.07%	75.56%	99.04%	95.72%
39	11	+	+	+	+	+	+	+	+	+	-	-	+	+	-	-	92.08%	80.42%	98.29%	95.07%
40	11	+	+	+	+	+	+	+	+	+	-	-	+	-	+	-	91.42%	80.74%	98.77%	95.20%
41	11	+	+	+	+	+	+	+	+	+	-	-	+	-	-	+	92.68%	74.24%	99.05%	95.75%
42	11	+	+	+	+	+	+	+	+	+	-	-	-	+	+	-	91.42%	81.33%	98.77%	95.19%
43	11	+	+	+	+	+	+	+	+	+	-	-	-	+	-	+	93.05%	76.56%	99.06%	95.76%
44	11	+	+	+	+	+	+	+	+	+	-	-	-	-	+	+	92.71%	77.52%	98.88%	93.40%
45	11	+	+	+	+	+	+	+	+	-	+	+	+	-	-	-	83.02%	79.29%	98.79%	94.72%

46	11	+	+	+	+	+	+	+	+	-	+	+	-	+	-	-	83.06%	79.94%	98.79%	94.70%
47	11	+	+	+	+	+	+	+	+	-	+	+	-	-	+	-	89.08%	85.80%	98.65%	95.09%
48	11	+	+	+	+	+	+	+	+	-	+	+	-	-	-	+	82.95%	78.08%	98.92%	95.46%
49	11	+	+	+	+	+	+	+	+	-	+	-	+	+	-	-	83.40%	79.86%	98.79%	94.71%
50	11	+	+	+	+	+	+	+	+	-	+	-	+	-	+	-	80.46%	85.34%	99.04%	94.99%
51	11	+	+	+	+	+	+	+	+	-	+	-	+	-	-	+	83.37%	80.42%	99.01%	95.54%
52	11	+	+	+	+	+	+	+	+	-	+	-	-	+	+	-	82.89%	85.41%	98.63%	95.11%
53	11	+	+	+	+	+	+	+	+	-	+	-	-	+	-	+	83.49%	81.64%	99.01%	95.48%
54	11	+	+	+	+	+	+	+	+	-	+	-	-	-	+	+	87.58%	84.73%	98.89%	95.12%
55	11	+	+	+	+	+	+	+	+	-	-	+	+	+	-	-	72.82%	81.10%	98.79%	94.77%
56	11	+	+	+	+	+	+	+	+	-	-	+	+	-	+	-	82.47%	86.07%	98.99%	94.98%
57	11	+	+	+	+	+	+	+	+	-	-	+	+	-	-	+	82.35%	78.98%	99.03%	95.53%
58	11	+	+	+	+	+	+	+	+	-	-	+	-	+	+	-	83.81%	86.26%	99.04%	95.01%
59	11	+	+	+	+	+	+	+	+	-	-	+	-	+	-	+	81.46%	78.33%	99.02%	95.51%
60	11	+	+	+	+	+	+	+	+	-	-	+	-	-	+	+	82.39%	84.90%	99.05%	95.11%
61	11	+	+	+	+	+	+	+	+	-	-	-	+	+	+	-	88.36%	86.10%	98.99%	94.95%
62	11	+	+	+	+	+	+	+	+	-	-	-	+	+	-	+	81.16%	79.46%	99.04%	95.57%
63	11	+	+	+	+	+	+	+	+	-	-	-	+	-	+	+	87.64%	84.38%	98.98%	95.11%
64	11	+	+	+	+	+	+	+	+	-	-	-	-	+	+	+	87.51%	84.15%	99.06%	95.15%
65	12	+	+	+	+	+	+	+	+	-	-	-	+	+	+	+	87.58%	84.82%	99.05%	95.15%
66	12	+	+	+	+	+	+	+	+	-	-	+	-	+	+	+	87.74%	83.50%	99.05%	95.16%
67	12	+	+	+	+	+	+	+	+	-	-	+	+	-	+	+	87.81%	84.41%	99.05%	95.17%
68	12	+	+	+	+	+	+	+	+	-	-	+	+	+	-	+	81.24%	77.32%	99.03%	95.56%
69	12	+	+	+	+	+	+	+	+	-	-	+	+	+	+	-	82.33%	85.70%	99.03%	94.99%
70	12	+	+	+	+	+	+	+	+	-	+	-	-	+	+	+	87.65%	83.93%	99.05%	95.15%
71	12	+	+	+	+	+	+	+	+	-	+	-	+	-	+	+	87.55%	84.25%	99.04%	95.13%

72	12	+	+	+	+	+	+	+	+	-	+	-	+	+	-	+	81.70%	78.97%	99.03%	95.58%
73	12	+	+	+	+	+	+	+	+	-	+	-	+	+	+	-	88.08%	85.72%	99.03%	94.98%
74	12	+	+	+	+	+	+	+	+	-	+	+	-	-	+	+	82.76%	84.56%	98.88%	95.13%
75	12	+	+	+	+	+	+	+	+	-	+	+	-	+	-	+	82.73%	78.71%	99.03%	95.56%
76	12	+	+	+	+	+	+	+	+	-	+	+	-	+	+	-	82.14%	86.66%	98.66%	94.99%
77	12	+	+	+	+	+	+	+	+	-	+	+	+	-	-	+	83.31%	77.74%	99.02%	95.52%
78	12	+	+	+	+	+	+	+	+	-	+	+	+	-	+	-	80.16%	84.49%	99.00%	94.98%
79	12	+	+	+	+	+	+	+	+	-	+	+	+	+	-	-	82.42%	81.55%	98.78%	94.79%
80	12	+	+	+	+	+	+	+	+	+	-	-	-	+	+	+	90.96%	77.09%	98.86%	95.39%
81	12	+	+	+	+	+	+	+	+	+	-	-	+	-	+	+	92.76%	77.93%	98.87%	95.43%
82	12	+	+	+	+	+	+	+	+	+	-	-	+	+	-	+	93.19%	76.90%	99.07%	95.78%
83	12	+	+	+	+	+	+	+	+	+	-	-	+	+	+	-	91.54%	82.94%	98.75%	95.18%
84	12	+	+	+	+	+	+	+	+	+	-	+	-	-	+	+	92.18%	78.28%	98.88%	95.43%
85	12	+	+	+	+	+	+	+	+	+	-	+	-	+	-	+	92.17%	75.16%	99.04%	95.76%
86	12	+	+	+	+	+	+	+	+	+	-	+	-	+	+	-	91.65%	81.73%	98.74%	95.17%
87	12	+	+	+	+	+	+	+	+	+	-	+	+	-	-	+	93.16%	76.00%	99.05%	95.76%
88	12	+	+	+	+	+	+	+	+	+	-	+	+	-	+	-	91.46%	82.77%	98.75%	95.10%
89	12	+	+	+	+	+	+	+	+	+	-	+	+	+	-	-	91.40%	76.68%	98.23%	94.90%
90	12	+	+	+	+	+	+	+	+	+	+	-	-	-	+	+	90.96%	77.09%	98.86%	95.39%
91	12	+	+	+	+	+	+	+	+	+	+	-	-	+	-	+	92.31%	74.70%	99.04%	95.75%
92	12	+	+	+	+	+	+	+	+	+	+	-	-	+	+	-	91.29%	80.90%	98.73%	95.19%
93	12	+	+	+	+	+	+	+	+	+	+	-	+	-	-	+	92.62%	74.77%	99.04%	95.75%
94	12	+	+	+	+	+	+	+	+	+	+	-	+	-	+	-	90.73%	80.95%	98.75%	95.19%
95	12	+	+	+	+	+	+	+	+	+	+	-	+	+	-	-	91.60%	81.59%	98.30%	94.89%
96	12	+	+	+	+	+	+	+	+	+	+	+	-	-	-	+	91.86%	75.25%	98.70%	95.41%
97	12	+	+	+	+	+	+	+	+	+	+	+	-	-	+	-	91.53%	80.80%	98.72%	95.18%

98	12	+	+	+	+	+	+	+	+	+	+	+	-	+	-	-	92.73%	80.97%	98.22%	94.98%
99	12	+	+	+	+	+	+	+	+	+	+	+	+	-	-	-	90.90%	78.57%	98.26%	95.01%
100	13	+	+	+	+	+	+	+	+	-	-	+	+	+	+	+	87.98%	85.10%	99.11%	95.26%
101	13	+	+	+	+	+	+	+	+	-	+	-	+	+	+	+	87.46%	83.61%	99.05%	95.20%
102	13	+	+	+	+	+	+	+	+	-	+	+	-	+	+	+	80.15%	83.71%	99.05%	95.19%
103	13	+	+	+	+	+	+	+	+	-	+	+	+	-	+	+	87.43%	82.83%	99.04%	95.16%
104	13	+	+	+	+	+	+	+	+	-	+	+	+	+	-	+	83.29%	78.99%	99.02%	95.58%
105	13	+	+	+	+	+	+	+	+	-	+	+	+	+	+	-	83.04%	85.68%	98.98%	94.96%
106	13	+	+	+	+	+	+	+	+	+	-	-	+	+	+	+	92.44%	80.04%	98.88%	95.44%
107	13	+	+	+	+	+	+	+	+	+	-	+	-	+	+	+	92.75%	79.71%	99.06%	95.39%
108	13	+	+	+	+	+	+	+	+	+	-	+	+	-	+	+	92.64%	78.67%	99.09%	95.40%
109	13	+	+	+	+	+	+	+	+	+	-	+	+	+	-	+	93.12%	76.28%	99.06%	95.78%
110	13	+	+	+	+	+	+	+	+	+	-	+	+	+	+	-	91.55%	81.98%	98.76%	95.14%
111	13	+	+	+	+	+	+	+	+	+	+	-	-	+	+	+	92.20%	77.56%	98.86%	95.44%
112	13	+	+	+	+	+	+	+	+	+	+	-	+	-	+	+	92.29%	78.56%	98.85%	95.41%
113	13	+	+	+	+	+	+	+	+	+	+	-	+	+	-	+	92.47%	75.29%	99.03%	95.74%
114	13	+	+	+	+	+	+	+	+	+	+	-	+	+	+	-	91.34%	82.03%	98.73%	95.11%
115	13	+	+	+	+	+	+	+	+	+	+	+	-	-	+	+	92.19%	78.93%	98.87%	95.38%
116	13	+	+	+	+	+	+	+	+	+	+	+	-	+	-	+	93.31%	75.81%	99.04%	95.73%
117	13	+	+	+	+	+	+	+	+	+	+	+	-	+	+	-	91.81%	82.29%	98.70%	95.17%
118	13	+	+	+	+	+	+	+	+	+	+	+	+	-	-	+	93.25%	77.16%	99.04%	95.75%
119	13	+	+	+	+	+	+	+	+	+	+	+	+	-	+	-	91.73%	82.24%	98.74%	95.17%
120	13	+	+	+	+	+	+	+	+	+	+	+	+	+	-	-	91.52%	79.64%	98.25%	95.01%
121	14	+	+	+	+	+	+	+	+	-	+	+	+	+	+	+	80.22%	84.12%	99.05%	95.11%
122	14	+	+	+	+	+	+	+	+	+	-	+	+	+	+	+	92.57%	79.95%	98.87%	95.45%
123	14	+	+	+	+	+	+	+	+	+	+	-	+	+	+	+	92.55%	79.59%	99.08%	95.39%

124	14	+	+	+	+	+	+	+	+	+	+	+	-	+	+	+	92.40%	79.53%	98.85%	95.38%
125	14	+	+	+	+	+	+	+	+	+	+	+	+	-	+	+	91.85%	77.91%	99.07%	95.40%
126	14	+	+	+	+	+	+	+	+	+	+	+	+	+	-	+	93.25%	78.84%	99.04%	95.79%
127	14	+	+	+	+	+	+	+	+	+	+	+	+	+	+	-	91.84%	83.21%	98.73%	95.17%
128	15	+	+	+	+	+	+	+	+	+	+	+	+	+	+	+	92.35%	79.97%	98.87%	95.37%

APPENDIX C

Table C.1: All results obtained from the models (4th step).

Model No	No of Param.	ES	TFQ	MAF	IMP	IMT	SOI	TIT	TIP	BD 0-50%	BD 10-90%	BD 0-90%	MCP	MCT	R2 of Soot Model Data	R2 of Soot Valid. Data	R2 of NOx Model Data	R2 of NOx Valid. Data
1	6	+	+	+	+	+	+	-	-	-	-	-	-	-	42.76%	51.27%	87.12%	84.21%
2	7	+	+	+	+	+	+	+	-	-	-	-	-	-	40.37%	53.92%	87.29%	83.68%
3	7	+	+	+	+	+	+	-	+	-	-	-	-	-	42.59%	50.36%	87.26%	85.17%
4	7	+	+	+	+	+	+	-	-	+	-	-	-	-	43.73%	46.12%	87.14%	85.09%
5	7	+	+	+	+	+	+	-	-	-	+	-	-	-	40.01%	49.10%	87.46%	85.12%
6	7	+	+	+	+	+	+	-	-	-	-	+	-	-	44.11%	47.11%	87.26%	85.05%
7	7	+	+	+	+	+	+	-	-	-	-	-	+	-	45.01%	44.09%	86.68%	85.50%
8	7	+	+	+	+	+	+	-	-	-	-	-	-	+	45.33%	45.57%	87.65%	85.78%
9	8	+	+	+	+	+	+	+	+	-	-	-	-	-	40.25%	53.91%	86.93%	84.53%
10	8	+	+	+	+	+	+	+	-	+	-	-	-	-	48.09%	50.04%	87.49%	83.80%
11	8	+	+	+	+	+	+	+	-	-	+	-	-	-	45.16%	49.12%	87.78%	84.03%
12	8	+	+	+	+	+	+	+	-	-	-	+	-	-	48.72%	51.84%	87.73%	84.21%
13	8	+	+	+	+	+	+	+	-	-	-	-	+	-	39.17%	49.64%	87.53%	84.70%
14	8	+	+	+	+	+	+	+	-	-	-	-	-	+	49.05%	41.83%	88.26%	83.67%
15	8	+	+	+	+	+	+	-	+	+	-	-	-	-	43.83%	44.49%	87.13%	85.88%
16	8	+	+	+	+	+	+	-	+	-	+	-	-	-	44.80%	47.30%	87.26%	85.15%
17	8	+	+	+	+	+	+	-	+	-	-	+	-	-	44.80%	47.30%	87.26%	85.15%
18	8	+	+	+	+	+	+	-	+	-	-	-	+	-	46.40%	44.12%	86.95%	86.16%
19	8	+	+	+	+	+	+	-	+	-	-	-	-	+	44.87%	45.78%	87.55%	85.60%

20	8	+	+	+	+	+	+	-	-	+	+	-	-	-	38.95%	49.36%	86.58%	84.66%
21	8	+	+	+	+	+	+	-	-	+	-	+	-	-	41.65%	42.01%	86.33%	84.56%
22	8	+	+	+	+	+	+	-	-	+	-	-	+	-	44.54%	42.28%	86.85%	85.18%
23	8	+	+	+	+	+	+	-	-	+	-	-	-	+	44.09%	47.54%	87.72%	85.46%
24	8	+	+	+	+	+	+	-	-	-	+	+	-	-	38.40%	49.94%	87.05%	84.82%
25	8	+	+	+	+	+	+	-	-	-	+	-	+	-	38.49%	43.50%	86.99%	85.42%
26	8	+	+	+	+	+	+	-	-	-	+	-	-	+	44.92%	45.33%	87.51%	85.59%
27	8	+	+	+	+	+	+	-	-	-	-	+	+	-	47.02%	45.37%	86.99%	85.35%
28	8	+	+	+	+	+	+	-	-	-	-	+	-	+	42.10%	44.31%	87.56%	85.56%
29	8	+	+	+	+	+	+	-	-	-	-	-	+	+	43.38%	43.84%	87.66%	85.63%
30	9	+	+	+	+	+	+	+	+	+	-	-	-	-	45.56%	49.90%	86.48%	83.67%
31	9	+	+	+	+	+	+	+	+	-	+	-	-	-	40.37%	50.96%	87.86%	85.17%
32	9	+	+	+	+	+	+	+	+	-	-	+	-	-	45.84%	52.12%	87.85%	85.56%
33	9	+	+	+	+	+	+	+	+	-	-	-	+	-	49.98%	48.54%	87.65%	85.98%
34	9	+	+	+	+	+	+	+	+	-	-	-	-	+	44.79%	43.30%	88.28%	84.40%
35	9	+	+	+	+	+	+	+	-	+	+	-	-	-	37.16%	49.55%	87.65%	83.93%
36	9	+	+	+	+	+	+	+	-	+	-	+	-	-	48.07%	48.34%	87.67%	84.07%
37	9	+	+	+	+	+	+	+	-	+	-	-	+	-	48.05%	49.81%	87.33%	83.90%
38	9	+	+	+	+	+	+	+	-	+	-	-	-	+	44.93%	46.72%	88.26%	83.60%
39	9	+	+	+	+	+	+	+	-	-	+	+	-	-	47.48%	49.97%	87.96%	84.58%
40	9	+	+	+	+	+	+	+	-	-	+	-	+	-	49.32%	52.74%	87.47%	84.05%
41	9	+	+	+	+	+	+	+	-	-	+	-	-	+	49.73%	46.67%	88.40%	83.52%
42	9	+	+	+	+	+	+	+	-	-	-	+	+	-	49.22%	46.36%	87.65%	84.38%
43	9	+	+	+	+	+	+	+	-	-	-	+	-	+	44.55%	48.01%	88.39%	83.61%
44	9	+	+	+	+	+	+	+	-	-	-	-	+	+	44.87%	44.37%	88.23%	84.05%
45	9	+	+	+	+	+	+	-	+	+	+	-	-	-	45.47%	49.54%	87.31%	85.58%

46	9	+	+	+	+	+	+	-	+	+	-	+	-	-	41.45%	44.29%	87.17%	85.89%
47	9	+	+	+	+	+	+	-	+	+	-	-	+	-	45.64%	43.63%	87.02%	85.86%
48	9	+	+	+	+	+	+	-	+	+	-	-	-	+	44.54%	45.32%	87.68%	85.06%
49	9	+	+	+	+	+	+	-	+	-	+	+	-	-	37.20%	48.61%	86.39%	84.21%
50	9	+	+	+	+	+	+	-	+	-	+	-	+	-	42.28%	46.63%	87.20%	85.85%
51	9	+	+	+	+	+	+	-	+	-	+	-	-	+	45.74%	40.41%	87.68%	85.85%
52	9	+	+	+	+	+	+	-	+	-	-	+	+	-	41.64%	48.96%	87.05%	85.95%
53	9	+	+	+	+	+	+	-	+	-	-	+	-	+	44.11%	43.80%	87.21%	84.97%
54	9	+	+	+	+	+	+	-	+	-	-	-	+	+	44.95%	43.19%	87.19%	85.58%
55	9	+	+	+	+	+	+	-	-	+	+	+	-	-	40.28%	51.14%	86.71%	84.76%
56	9	+	+	+	+	+	+	-	-	+	+	-	+	-	39.90%	42.02%	86.76%	85.34%
57	9	+	+	+	+	+	+	-	-	+	+	-	-	+	43.28%	43.55%	87.75%	85.52%
58	9	+	+	+	+	+	+	-	-	+	-	+	+	-	42.69%	43.00%	86.76%	85.35%
59	9	+	+	+	+	+	+	-	-	+	-	+	-	+	38.61%	45.87%	87.76%	85.24%
60	9	+	+	+	+	+	+	-	-	+	-	-	+	+	42.84%	43.75%	87.72%	85.16%
61	9	+	+	+	+	+	+	-	-	-	+	+	+	-	45.42%	45.04%	86.84%	85.22%
62	9	+	+	+	+	+	+	-	-	-	+	+	-	+	42.53%	48.78%	87.84%	85.34%
63	9	+	+	+	+	+	+	-	-	-	+	-	+	+	43.78%	44.04%	87.68%	85.39%
64	9	+	+	+	+	+	+	-	-	-	-	+	+	+	43.28%	40.41%	87.71%	85.15%
65	10	+	+	+	+	+	+	-	-	-	+	+	+	+	45.16%	44.33%	87.49%	85.39%
66	10	+	+	+	+	+	+	-	-	+	-	+	+	+	41.82%	41.91%	87.52%	85.08%
67	10	+	+	+	+	+	+	-	-	+	+	-	+	+	39.48%	45.32%	87.51%	85.40%
68	10	+	+	+	+	+	+	-	-	+	+	+	-	+	40.84%	44.32%	87.73%	85.19%
69	10	+	+	+	+	+	+	-	-	+	+	+	+	-	41.05%	47.35%	86.56%	84.72%
70	10	+	+	+	+	+	+	-	+	-	-	+	+	+	42.28%	41.21%	87.74%	85.22%
71	10	+	+	+	+	+	+	-	+	-	+	-	+	+	43.71%	45.00%	87.70%	85.53%

72	10	+	+	+	+	+	+	-	+	-	+	+	-	+	44.32%	45.97%	87.68%	85.09%
73	10	+	+	+	+	+	+	-	+	-	+	+	+	-	43.00%	47.44%	87.36%	85.60%
74	10	+	+	+	+	+	+	-	+	+	-	-	+	+	43.22%	41.46%	87.47%	85.09%
75	10	+	+	+	+	+	+	-	+	+	-	+	-	+	43.95%	43.73%	87.62%	84.85%
76	10	+	+	+	+	+	+	-	+	+	-	+	+	-	44.04%	43.60%	86.89%	84.76%
77	10	+	+	+	+	+	+	-	+	+	+	-	-	+	44.00%	44.10%	87.66%	85.19%
78	10	+	+	+	+	+	+	-	+	+	+	-	+	-	41.97%	44.05%	86.75%	85.32%
79	10	+	+	+	+	+	+	-	+	+	+	+	-	-	42.44%	48.50%	87.22%	85.06%
80	10	+	+	+	+	+	+	+	-	-	-	+	+	+	41.93%	42.11%	88.15%	83.72%
81	10	+	+	+	+	+	+	+	-	-	+	-	+	+	49.65%	45.30%	88.30%	83.79%
82	10	+	+	+	+	+	+	+	-	-	+	+	-	+	49.91%	45.49%	88.35%	83.36%
83	10	+	+	+	+	+	+	+	-	-	+	+	+	-	51.17%	47.83%	87.65%	84.49%
84	10	+	+	+	+	+	+	+	-	+	-	-	+	+	42.91%	43.75%	88.20%	83.70%
85	10	+	+	+	+	+	+	+	-	+	-	+	-	+	48.67%	41.44%	88.13%	83.25%
86	10	+	+	+	+	+	+	+	-	+	-	+	+	-	47.78%	45.88%	87.52%	84.22%
87	10	+	+	+	+	+	+	+	-	+	+	-	-	+	49.11%	49.12%	88.33%	83.37%
88	10	+	+	+	+	+	+	+	-	+	+	-	+	-	44.71%	46.71%	87.50%	84.18%
89	10	+	+	+	+	+	+	+	-	+	+	+	-	-	34.88%	49.15%	87.55%	83.92%
90	10	+	+	+	+	+	+	+	+	-	-	-	+	+	49.23%	44.76%	88.21%	85.08%
91	10	+	+	+	+	+	+	+	+	-	-	+	-	+	49.32%	43.79%	88.08%	83.68%
92	10	+	+	+	+	+	+	+	+	-	-	+	+	-	49.02%	47.56%	87.78%	85.46%
93	10	+	+	+	+	+	+	+	+	-	+	-	-	+	45.09%	43.89%	87.99%	83.45%
94	10	+	+	+	+	+	+	+	+	-	+	-	+	-	49.24%	47.91%	87.45%	84.87%
95	10	+	+	+	+	+	+	+	+	-	+	+	-	-	45.71%	48.75%	87.42%	84.50%
96	10	+	+	+	+	+	+	+	+	+	-	-	-	+	48.63%	43.45%	87.26%	83.18%
97	10	+	+	+	+	+	+	+	+	+	-	-	+	-	48.79%	49.37%	87.89%	85.73%

98	10	+	+	+	+	+	+	+	+	+	-	+	-	-	45.33%	49.61%	86.97%	83.89%
99	10	+	+	+	+	+	+	+	+	+	+	-	-	-	49.06%	49.87%	87.38%	84.43%
100	11	+	+	+	+	+	+	-	-	+	+	+	+	+	44.49%	45.16%	87.70%	85.53%
101	11	+	+	+	+	+	+	-	+	-	+	+	+	+	44.93%	41.37%	87.56%	84.96%
102	11	+	+	+	+	+	+	-	+	+	-	+	+	+	44.48%	43.68%	87.73%	85.16%
103	11	+	+	+	+	+	+	-	+	+	+	-	+	+	44.37%	43.11%	87.72%	85.18%
104	11	+	+	+	+	+	+	-	+	+	+	+	-	+	43.95%	42.28%	87.73%	85.00%
105	11	+	+	+	+	+	+	-	+	+	+	+	+	-	40.03%	43.22%	87.06%	85.29%
106	11	+	+	+	+	+	+	+	-	-	+	+	+	+	49.36%	44.90%	88.30%	83.68%
107	11	+	+	+	+	+	+	+	-	+	-	+	+	+	49.16%	43.78%	88.27%	83.71%
108	11	+	+	+	+	+	+	+	-	+	+	-	+	+	48.97%	43.15%	88.34%	83.74%
109	11	+	+	+	+	+	+	+	-	+	+	+	-	+	49.32%	43.15%	88.29%	83.25%
110	11	+	+	+	+	+	+	+	-	+	+	+	+	-	49.27%	47.87%	87.37%	83.56%
111	11	+	+	+	+	+	+	+	+	-	-	+	+	+	48.91%	44.47%	88.03%	84.67%
112	11	+	+	+	+	+	+	+	+	-	+	-	+	+	48.64%	44.59%	88.32%	84.22%
113	11	+	+	+	+	+	+	+	+	-	+	+	-	+	48.85%	44.20%	88.16%	83.49%
114	11	+	+	+	+	+	+	+	+	-	+	+	+	-	48.14%	47.45%	87.54%	84.82%
115	11	+	+	+	+	+	+	+	+	+	-	-	+	+	48.74%	44.51%	88.22%	84.17%
116	11	+	+	+	+	+	+	+	+	+	-	+	-	+	49.43%	43.06%	88.15%	83.53%
117	11	+	+	+	+	+	+	+	+	+	-	+	+	-	48.74%	48.01%	86.60%	83.64%
118	11	+	+	+	+	+	+	+	+	+	+	-	-	+	49.15%	44.70%	87.38%	82.91%
119	11	+	+	+	+	+	+	+	+	+	+	-	+	-	49.35%	48.53%	87.02%	84.25%
120	11	+	+	+	+	+	+	+	+	+	+	+	-	-	48.98%	47.21%	87.04%	83.95%
121	12	+	+	+	+	+	+	-	+	+	+	+	+	+	44.54%	43.81%	87.69%	85.00%
122	12	+	+	+	+	+	+	+	-	+	+	+	+	+	49.18%	42.72%	88.21%	83.49%
123	12	+	+	+	+	+	+	+	+	-	+	+	+	+	49.01%	44.72%	88.27%	83.83%

124	12	+	+	+	+	+	+	+	+	+	-	+	+	+	48.99%	44.00%	88.27%	83.87%
125	12	+	+	+	+	+	+	+	+	+	+	-	+	+	49.00%	43.95%	88.16%	83.72%
126	12	+	+	+	+	+	+	+	+	+	+	+	-	+	49.30%	45.71%	88.11%	83.35%
127	12	+	+	+	+	+	+	+	+	+	+	+	+	-	49.10%	47.88%	87.47%	84.63%
128	13	+	+	+	+	+	+	+	+	+	+	+	+	+	48.71%	43.50%	88.28%	83.57%

CURRICULUM VITAE

Name Surname **:** Rüştü Taylan Yarar

Place and Date of Birth **:** 08/12/1991

E-Mail **:** taylanyarar@gmail.com

EDUCATION

- **B.Sc.** **:** Istanbul Technical University - Mechanical Eng.

PROFESSIONAL EXPERIENCE AND REWARDS:

- Ford OTOSAN R&D Center / Lead Calibration Engineer (2017 - present)

  Responsibilities include leading 1.5L diesel Fiesta, Ecosport, KA, Courier calibration projects, calibration integration of the projects, making attributes signoff plans, launch support, voice of customer support and trip planning.

- Ford OTOSAN R&D Center / Calibration Engineer (2014 - 2017)

  Responsibilities include working in 1.5L diesel Fiesta, Ecosport, KA, Courier calibration projects, performance and driveability calibration, brand DNA tests, performance and driveability benchmark, start and idle calibration, performing climate tests.

- ARÇELİK R&D Center / System Development Engineer (2013 – 2014)

  Responsibilities include washer and dryer studies, patent researches, benchmark tests, washing and drying performance tests.